Evaluation of a method for the use of periphyton recruitment on artificial substrates as an indicator of watershed land use in bays of Coeur d'Alene Lake, Idaho.

A Thesis
Presented in Partial Fulfillment of the Requirements for the
Degree of Master of Science
with a
Major in Environmental Science
in the
College of Graduate Studies
University of Idaho
by
Randi N. Notte

Major Professor: Frank Wilhelm, Ph.D.
Committee Members: Craig Cooper, Ph.D.; James Moberly, Ph.D.
Department Administrator: J.D. Wulfhorst, Ph.D.

May 2019

Authorization to Submit Thesis

This thesis of Randi N. Notte, submitted for the degree of Master of Science with a Major in Environmental Science and titled "Evaluation of a method for the use of periphyton recruitment on artificial substrates as an indicator of watershed land use in bays of Coeur d'Alene Lake, Idaho," has been reviewed in final form. Permission, as indicated by the signatures and dates below, is now granted to submit final copies to the College of Graduate Studies for approval.

Major Professor: _____ Date: _____
Frank Wilhelm, Ph.D.

Committee Members: _____ Date: _____
Craig Cooper, Ph.D.

_____ Date: _____
James Moberly, Ph.D.

Department
Administrator: _____ Date: _____
J.D. Wulfhorst, Ph.D.

Abstract

The eutrophication of freshwater is a concern across the world and often occurs in areas that are in close proximity to human development. Early indicators of nutrient enrichment are generally evidenced in the littoral zones of lakes due to their proximity to incoming sources of sediment and associated nutrients. Previous studies in local lakes of northern Idaho indicated that the rapid growth of periphyton and its high biomass were directly related to human density in the sub-watersheds, making periphyton monitoring a possible tool to identify bays at risk of eutrophication. I tested the hypothesis that monitoring the growth of periphyton on artificial substrates was a tool capable to distinguish variation in watershed anthropogenic activity across bays. Seasonal nutrient loads delivered to two of the study bays were quantified to make preliminary comparisons between watersheds. The loads of total phosphorus and total residue differed between watersheds disproportionally to watershed area, indicating that some factor(s) other than watershed size, such as differences in land use, interact to cause differential nutrient loading between the bays. Despite evidence that the watersheds differed in nutrient loading indicators, periphyton response did not differ to a high degree of confidence between bays. Differential nutrient loading to bays of Coeur d'Alene Lake may be masked by different bay-specific retention regimes or other in-bay processes that lead to internal loading. These findings indicated that the approach used in this study to monitor periphyton was not a satisfactory method to detect nutrient enrichment in bays of Coeur d'Alene Lake.

Acknowledgements

Every component of this thesis research has benefited from the support and direction of the individuals, agencies, and institutions that have helped it come to pass. Foremost, I thank my advisor, Dr. Frank Wilhelm. His willingness to teach and commitment to curiosity brought this project new life time and again, and his knowledge brought clarity to the most challenging subjects. I am grateful for the guidance of Dr. James Moberly who agreed to join my committee, offering his knowledge of chemistry to help crack the chemistry conundrum that had taken hold early on in this project. Furthermore, I thank those at the Idaho Department of Environmental Quality who have inspired, shaped, funded, and energetically participated in this research. I am forever thankful to each member of the Coeur d'Alene Lake Management Plan team for their contributions to this endeavor. To Dr. Craig Cooper for his wisdom, vision, mentorship, and ever-appreciated pep talks. Craig, thank you for believing in me. I thank Glen Pettit for encouraging me by example to work hard and persistently strive for excellence. I thank Bob Witherow for his encouragement, teamwork, and for introducing us all to Big Smo the Redneck Rapper. I also thank Jamie Brunner for championing the cause of the LMP and for all the unseen support as she coordinated the details of the project. I thank Bob Steed, Kristin Larson, and Craig Nelson for their original work that sparked this study, and for their continued support throughout. I also thank Tom Herron for his support as Water Quality Manager and guidance in this project. Next, I thank Lubia Cajas de Gliniewicz, J.D. Wulfhorst, and the rest my Environmental Science Program family for including me in the community and for giving me the opportunity to develop my teaching and leadership abilities. Finally, I thank those outside of the DEQ that supported this research. I thank Darren Brandt of Advanced EcoSolutions for his critical role in making this science possible, for teaching me fluorometry methods, and then graciously allowing me to use his lab facilities. Property access allowed by the Corporation of Gonzaga University as facilitated by Joe Smith, was greatly appreciated, as well as access granted by Nick Salisbury to his property in Kidd Island Bay. Funding for this research was provided by the Idaho Department of Environmental Quality and the Environmental Science Program at the University of Idaho.

Dedication

I remember the moment this entire story sparked to life. Walking to biology lecture, I opened an email from Jamie offering me an internship for the summer with the IDEQ. This undergraduate internship powerfully changed how I saw my own future, giving me insight to my own interests and brand new goals. The LMP offered me a place on the team, a seat on the boat, and a lakeside setting to discover my love for water quality, and all the more my love for Coeur d'Alene Lake. The day I opened that email, with anticipation and excitement I said, "this is my dream." And what a dream it has been. Thank you to each member of the LMP for fostering in me passion for, and valuable experience in, the world of water quality. I thank my parents, who have given endlessly so that I can succeed, and who have answered my every insecurity during this process with reassurance. I also thank the friends I have been blessed with, both here in Moscow and scattered elsewhere, who reminded me that my world has always extended beyond the next rack of test tubes waiting to be analyzed. I thank Sarah Burnet, without whom I am fully confident I would have been utterly lost. And to Stephanie Estell, who deserves every credit due to her, for she did not only earn her own degree but this one as well. Without you, as we have always said, I do not want to know what these years would have been.

Table of Contents

List of Tables

List of Figures

Chapter 1: Introduction

Abstract

Lake littoral zones are key focus areas to predict change in lake trophic status due to their proximity to incoming sources of sediment and associated nutrients. Here, periphyton are excellent candidate indicators to evaluate nutrient loading because they are stationary and their growth reflects the arrival of nutrients to them, unlike free-floating algae that can obtain nutrients from different parts of the water column. I tested the hypothesis that the accrual of algal biomass on artificial substrates was suitable to distinguish variation in watershed anthropogenic activity across bays. I found similar growth patterns and climax densities between bays, which indicated that this method was not suitable to discern periphyton response according to known differences in watershed characteristics. Growth patterns showed some potential for differences in climax densities, but there was too much variability to distinguish between bays to a high degree of confidence. Future efforts could employ a greater number of substrates and focus more narrowly on variation in in-bay processes. These results were inconsistent with those from another local lake in which rapid periphyton growth and high climax densities were directly related to human density in the sub-watersheds. Variation in nutrient load to bays of Coeur d'Alene Lake may be masked by different bay-specific retention regimes or other in-bay processes, thereby explaining the similar periphyton responses. These findings have important implications for the suitability of periphyton monitoring as a satisfactory method to detect nutrient enrichment in Coeur d'Alene Lake.

Background information

Freshwater resources are limited globally, and as anthropogenic pressures increase the availability of clean and beneficially useful water is threatened. Therefore, it is critical to monitor and prevent its further degradation (Ansari et al. 2013). Eutrophication, a natural process that increases the biological productivity of aquatic ecosystems over time through the deposition of nutrients often associated with particulate matter, can be accelerated by anthropogenic activities, causing the rapid degradation of ecosystem health (Rosenberger et al. 2008). Shoreline development (housing and human infrastructure), the reduction of riparian zones, septic and sewer leakage, and the application of fertilizer in nearshore areas, are some anthropogenic modifications of the landscape that mobilize particulate matter and nutrients in the watershed (Woods and Beckwith 1997; Moore et al. 2003; Kuwabara et al. 2003; Lambert et al. 2008; Rosenberger et al. 2008). Natural forces including streams, wind, and landslides provide diverse transport mechanisms that subsequently move the sediment particles and associated nutrients (Roering et al. 1999).

Overwhelmingly, the dynamic movement of matter occurs as it is transported by surface runoff to streams and larger systems. The watershed approach to land management recognizes that nutrient inputs to a waterbody depend on the characteristics of the watershed. These include but are not limited to catchment size, topology, soil type and vegetation cover, and land use practices (Woods and Beckwith 1997; Lambert et al. 2008). As many of these processes, such as septic system installation and crop production as well as land clearing and development in the wildland-urban interface, are human-mediated changes to the landscape, it follows that the influence of anthropogenic activity in a watershed expedites the mobilization of nutrients to waterbodies.

Natural vs. cultural eutrophication

The natural mobilization of particulate matter by erosion and geologic weathering results in the accumulation of nutrients in waterbodies, contributing to the growth of aquatic biomass (Wetzel 2001). It is an infilling process, and occurs naturally in all lakes, resulting in a shift in trophic state (oligotrophy to eutrophy) and eventual filling in of the entire waterbody. This general process is termed eutrophication. It should be noted that other sources of nutrients, such as the aerial deposition of nutrients from dust and smoke, pollen and plant material, and human-generated pollutants contributes to eutrophication as well. In

natural systems undisturbed by humans, this process is called ‘natural’ eutrophication and acts over tens of thousands of years (Chislock et al. 2013). With the rise of the human population and our ability to greatly modify the natural landscape, this process is greatly accelerated and is termed ‘cultural’ eutrophication – shortening the timespan between changes in trophic state to less than the span of a human lifetime (Smith et al. 1999; Chislock et al. 2013). Particulate matter transport via runoff and erosion is of particular interest to resource managers because phosphorus, a major limiting macronutrient for biological productivity in aquatic ecosystems, is typically bound to soil particles as phosphate (PO_4^{3-}) or one of its protonated forms depending on pH (Strawn et al. 2015). As urbanization increases across the world, cultural eutrophication is a growing concern in the context of water quality management.

Alterations in land use from the natural state often cause a change in runoff timing and magnitude that can exacerbate nutrient loading by increasing the erosive force of streams and the loading of particles to streams (Vadeboncoeur et al. 2001; Rosenberger et al. 2008). In urban landscapes, infiltration is diminished by impervious surfaces and storm water systems become a rapid conduit for water transport to streams during rain events (Eyles and Meriano 2010). Without swales or chemical treatment, pollutants from road dust, construction, and residences are transported into natural waterways. In agricultural areas, tilled and fallow agricultural fields often lack vegetation to slow water movement and provide particulate matter for transport (Ouyang et al. 2009). These effects of land use change show that cultural eutrophication results from a variety of point and non-point sources, increasing the complexity of land management for watershed protection.

Under cultural eutrophication, the continued loading of nutrients establishes a positive feedback loop by altering the natural patterns of nutrient cycling (Vadeboncoeur et al. 2001; Rosenberger et al. 2008). Excess nutrients produce increasing amounts of biomass that after senescence or biological consumption are remineralized into bioavailable forms (Woods 1989). As a result, trophic level changes in biological productivity occur until the symptoms of eutrophication, such as low dissolved oxygen, warm water temperatures, and increased turbidity become limiting on higher trophic levels typically valued by humans (Rosenberger et al. 2008). Additionally, eutrophic water bodies suffer from reduced aesthetic, recreational, and economic value due to their high turbidity, unpleasant smell,

increased risk of harmful algae blooms and associated cyanotoxins, and inability to support a diverse community of species (Mattila and Raisanen 1998; Jacoby et al. 2000; Rosenberger et al. 2008; Wood and Beckwith 2008). Cultural eutrophication, therefore, should be avoided to protect the function of natural ecosystems and other beneficial uses of surface water.

One result of eutrophication, the potential for future changes in hypolimnetic oxygen concentrations that alter metal solubility, is of concern in the Coeur d'Alene Region of northern Idaho, due to historic mining practices and a series of biogeochemical processes that could potentially allow the resuspension of metals deposited on the lake bottom over the last hundred years (Woods 1989; Woods and Beckwith 1997). While these processes will be discussed in more detail below, it is important to recognize that nutrient loading and the watershed practices that drive it are of keen concern regionally and also in urbanizing areas around the world. Eutrophication negatively influences property values (Liao et al. 2016) and has the potential to affect the Coeur d'Alene regional economy because it is highly dependent on tourism. Moreover, Coeur d'Alene Lake is tied to the cultural identity of indigenous cultures and the general populace in the area. For these reasons, careful attention towards indications of eutrophication are a priority for lake managers.

Coeur d'Alene watershed and lake characteristics

Coeur d'Alene Lake is the second largest lake (by volume) in Idaho, and forms a significant subbasin in the 17,300 km^2 Spokane River Basin, a tributary of the Columbia River (Woods 1989). Approximately 9,600 km^2 of the Spokane River Basin drains to Coeur d'Alene Lake which is comprised of two subbasins corresponding to the lake's two main tributaries (Figure 1). The Coeur d'Alene River basin (3,830 km^2), expands north and east from the river delta to the ridgeline of the Bitterroot Mountains of the Montana border (Woods 1989; USGS 2016). To the southeast, the St. Joe River basin encompasses 4,480 km^2 and extends to the border of the northern Palouse region. While 90% of inflow to the lake is supplied by these major tributaries, smaller tributaries enter from watersheds bordering the western and northern shorelines (Woods 1989). In total, the Coeur d'Alene Lake watershed spans Kootenai, Benewah, and Shoshone counties in northern Idaho. The southern 1/3rd of the lake lies within the Coeur d'Alene Indian Reservation and is managed by the Coeur d'Alene Tribe, while the northern 2/3^{rds} are managed by the Idaho Department of Environmental Quality (IDEQ). The city of Coeur d'Alene is a rapidly expanding urban

center at the northern end of the lake. The majority of land use in the lake's subbasins is coniferous and sparse forest (80%), while <5% is agriculture, <1% mining and <1% wetlands (Table 1.1; Woods and Beckwith 1997; USGS 2016). Developed land in the drainage, depending on classification technique, ranges from 0.56-0.85% (USGS 2016, 2018).

The City of Coeur d'Alene on the north shore contributes recreational pressure as well as stormwater to the lake (Woods and Beckwith 1997). While residential and commercial shoreline development exists in most areas around the lake (80% in 1980), shorefront population density is greatest at the north end of the lake closest to the city. Between 1970-1980, development within 80 km of the lake shoreline increased 24% (Woods 1989). Since then, the population of Coeur d'Alene has doubled from 25,000 (1990) to 50,000 (2016), indicating that population growth and recreation pressure have steadily increased (U.S. Census Bureau 2017).

Lake morphological characteristics vary slightly throughout the year as the water surface elevation changes seasonally. At full summer elevation, the lake surface area is 129.5 km^2 with 1950 km of shoreline, the average depth is 21.2 m, while the maximum depth is 61 m (Woods and Beckwith 1997). In the winter, the water is drawn down to an elevation of 644 m (2128 ft.) to 646.5 m (2121 ft.) based on the seasonal changes in operation of the Post Falls Dam, a hydroelectric facility operated by Avista Utilities on the Spokane River, the lake's northern outlet river (Woods 1989). As one of the shallower regional lakes, Coeur d'Alene Lake has a relatively short average water residence time of 175-180 days, which contrasts with the 2.2 and 2.4 years of Flathead Lake, MT and Pend Oreille Lake, ID, respectively (Woods 2004).

Coeur d'Alene Lake is a warm monomictic lake, turning over in the fall after summer thermal stratification that typically lasts from late June to mid-October (Woods 1989, 2004; Wood and Beckwith 2008), with more recent observations of stratification occurring from May to November (C. Cooper, pers. comm.). Inflow patterns from the tributaries are seasonally dependent, entering as overflow in summer, underflow in winter, and interflow for periods in the spring and fall during lake turnover (Wood and Beckwith 2008). The majority of precipitation (70%) to the drainage basin falls as snow in October to January, causing the primary inflow of water, nutrients, and pollutants to arrive with the spring freshet during snowmelt (Woods 1989).

Drawing from two USGS limnological surveys of Coeur d'Alene Lake in 1991-92 and 2004-06, Wood and Beckwith (2008) concluded that the lake had a series of significant water quality gradients. Lake-wide, concentrations of inorganic nitrogen, lead, and zinc increased radially from the central pelagic station located closest to the Coeur d'Alene River inflow near Harrison, ID, while other water quality parameters varied longitudinally. Water column transparency (secchi depth) and dissolved oxygen increased from south to north while total phosphorus was highest in the southern end and lowest in the north. As the St. Joe River is a main source of phosphorus to the lake, these nutrient and related water quality indicator gradients correspond with a settling of riverine inputs as water flows downstream to the lake outlet at the Spokane River. Additionally, the southern lake is shallow, warmer, and more productive relative to the northern end, further explaining the lower dissolved oxygen concentrations and frequent periods of anoxia in the summer months.

On Coeur d'Alene Lake, local interest in the fate of contaminated lake sediments (discussed in a later section), human health, and lake beneficial use has generated nutrient-related research since the 1970's. The lake was evaluated as part of the National Eutrophication Survey in 1975 and classified as mesotrophic, a designation that was later changed to oligotrophic after a 50% reduction of nutrient inflow occurred by 1991 (Woods and Beckwith 1997). Currently Coeur d'Alene Lake is classified as meso- or oligotrophic depending on the category evaluated, falling into oligotrophy concerning chlorophyll *a* and total phosphorus and mesotrophy for secchi depth, particularly during runoff periods when high loads of particulate matter are contributed by the St. Joe and Coeur d'Alene rivers (Wood and Beckwith 2008). Lake-wide research began most notably in 1991-1992 during the USGS survey conducted to establish baseline limnological conditions for Coeur d'Alene. Later in 2004-06, the same team revisited the lake to evaluate change over time (Wood and Beckwith 2008). Key findings included the nearly uniform contamination of lakebed sediments, the significant increase in inflow P load between 1991-92 and 2004-06, and the increase in water column chlorophyll *a* over time. Finally, in a summary paper by Wood and Beckwith (2008), the USGS concluded that nearshore sites, rather than pelagic, were best to determine the effects of land-based alterations that affect water quality.

Metals interactions

Regional mining history

The Coeur d'Alene Mining District is internationally known as a top silver producer, ranking within the top one percent of producers worldwide (Balistrieri et al. 2002). Despite the region's history of resource extraction and refining, only two original mines, Galena and Lucky Friday, are in operation today. Historically, ninety mines and over 1,000 mining-related features line the mountains in the watershed (Balistrieri et al. 2002) and have produced a legacy of metal contamination that continues to affect Coeur d'Alene Lake to this day.

Metal pollution from mining activities has led to widespread ecological and human health issues including the contamination of the South Fork of the Coeur d'Alene River, its tributaries, Coeur d'Alene Lake, and the Spokane River. Studies in Coeur d'Alene Lake have concluded that metals contamination has occurred throughout the lake due to wind-generated waves, internal circulation, and dissolution during seasonal thermocline formation (Wood and Beckwith 2008). Other effects include local contamination of soil and ground water, poisoning of fish and waterfowl, and high resident blood-lead concentrations in five small towns across the basin (Woods 1989; Von Lindern et al. 2003; Blacketer 2014).

Before tailing ponds were mandated by regulation, it is estimated that 56 million metric tons of tailings entered the South Fork of the Coeur d'Alene River. Of these, 2,200 metric tons were lead and 650,000 metric tons were zinc (Balistrieri et al. 2002). At the same time, the Bunker Hill Complex's lead smelter released over 3,300 metric tons of lead into the atmosphere through a 715 ft. tall stack during its operation between 1917 and 1981.

Fate of metals buried in sediments of Coeur d'Alene Lake

The fate of sediment-associated metals currently residing at the bottom of Coeur d'Alene Lake is closely tied to the oxygen concentration of the overlying water (Horowitz et al. 1993; Harrington et al. 1998; LMP 2009; Şengör et al. 2007). Generally the metals of interest in Coeur d'Alene Lake (Pb, Cd, As, Zn, Cu and Hg) have oxygen-dependent speciation and become mobile in the upper sediment layer and water column under hypoxic and anoxic redox conditions (Horowitz et al. 1993; Boukemara et al. 2017). Hence, a major focus of the LMP (2009) is to maintain a high oxygen concentration throughout the hypolimnion of Coeur d'Alene Lake. Sufficient oxygen environments currently predominate,

but the southern end and a small region immediately adjacent to the Spokane River outlet experience hypoxia in the hypolimnion during summer stratification. Limnological studies conducted in Coeur d'Alene Lake over the past thirty years show that concentrations of phosphorus in pelagic samples and metrics of biological productivity have increased in the northern lake, indicating a trend towards eutrophy (Wood and Beckwith 2008). Despite the increase in dissolved oxygen added by primary producers during the day, respiration at night and ultimately that consumed during microbial decomposition of autotrophic biomass and organic matter delivered via river input, reduces the mass of dissolved oxygen in the water column. Thus, increased eutrophy can cause hypolimnia in lakes to become hypoxic or anoxic, a common occurrence in stratified eutrophic lakes (Wetzel 2001).

In a reduced sediment environment (defined as < 1 mg·L^{-1} dissolved oxygen, DO) phosphorus and some metals readily solubilize and transition from precipitates and surface adsorbates in the sediment into ions that can easily move into the overlying water column along a diffusion gradient (Woods 1989; Woods and Beckwith 1997). Iron (III) is a primary binding element of phosphate and metals in sediments; as such, changes in the oxidation state of Fe influence the speciation of phosphate and metals. Because iron-binding is a key factor in the solubility of phosphate and metals, the adsorption/desorption of phosphate and metal ligands is regulated by the redox state of iron minerals. Under oxic conditions, iron (III) phosphate and any sorbed ligands like metals are immobile and remain within the solid sediment fraction (Patrick et al. 1974; Strawn et al. 2015). Should this release of metals from bottom sediments occur, this could negatively affect a broad spectrum of beneficial uses.

With the limnological, human, and economic health of the region dependent on metals interactions at the sediment-water interface of Coeur d'Alene Lake, significant effort has been undertaken to understand those biogeochemical processes (Balistrieri 1998; Balistrieri et al. 2002; Kuwabara et al. 2003). Maintaining oxygenated conditions in the hypolimnion is likely the most effective management strategy to keep metals and nutrients bound to lake-bottom sediments (Woods 1989). Ultimately, nutrient management and prevention of further eutrophication regulate hypolimnetic conditions and therefore are the traditional cornerstones of modern lake management efforts.

Project objectives

The primary objective of my thesis was to test a novel periphyton monitoring method in Coeur d'Alene Lake and evaluate its suitability for use in this system. The method was rigorously evaluated concerning the spatial and temporal variability in periphyton response measured by the method and an examination of its limitations. Overall, I used this method to test the hypothesis that artificial substrates placed in bays of Coeur d'Alene Lake, ID can be used to detect trends in periphyton response in bays that differ in watershed nutrient loading potential. I placed artificial closed-cell foam substrates in multiple bays in each of two summers that were sampled repeatedly throughout each summer, collected water samples for the analysis of chemistry, and examined watershed land use using geographic information systems (GIS).

In Chapter 2, I first examined key periphyton recruitment and growth characteristics, comparing them to results garnered from a previous IDEQ study on another local lake (IDEQ 2014) that used this method to identify bays as "impacted" or "unimpacted" by human activity based on periphyton results. Second, I used geographic information systems (GIS) to analyze watershed characteristics such as dwelling density, forest clearing, and/or percent "human altered" land use designation that are shown in the literature to influence periphyton growth (Lambert et al. 2008). I then examined the strength of the relationship between the magnitude of each land use characteristic in bay watersheds and the observed periphyton growth rates and maximum biomass accrual per bay. Overall, this project contributed to the needs of the Idaho Department of Environmental Quality (IDEQ) and their implementation of the Coeur d'Alene Lake Management Plan.

In Chapter 3, I quantified stream nutrient loads in two bays, further analyzing the relationship between benthic periphyton and watershed nutrient delivery. Automated samplers and stream level loggers were placed in the tributary streams of Kidd Island and Neachen bays to aid in calculating nutrient loads. Once quantified, I examined how nutrient loads differed between watersheds with different watershed land use activities.

Finally, discrepancies in the results of lake water split samples analyzed for total phosphorus concentration between myself and third party labs contracted by the Idaho Department of Environmental Quality (IDEQ), as well as methodological differences, justified a third chapter summarizing findings, document corrective action, and describe

back-calculation methods used for 2017 water chemistry values. This summary will benefit the current thesis, as well as future students.

Literature Cited

Ansari, A. A., S. S. Gill, and F. A. Khan. 2013. Eutrophication: Threat to aquatic ecosystems, p. 143–170. *In* A.A. Ansari, G.R. Lanza, S.S. Gill, and W. Rast [eds.], Eutrophication: Causes, Consequences, and Controls in Aquatic Ecosystems. Springer.

Balistrieri, L. S. 1998. Preliminary estimates of benthic fluxes of dissolved metals in Coeur d'Alene Lake, Idaho. USGS Open-File Rep. **98**–**793**: 38.

Balistrieri, L. S., S. E. Box, A. A. Bookstrom, R. L. Hooper, and J. B. Mahoney. 2002. Impacts of historical mining in the Coeur d'Alene River Basin, *In* L.S. Balistrieri and L.L. Stillings [eds.], A synthesis of the mineral resources program's past environmental studies in the Western United States and furture research directions. Bulletin 2191. U.S. Geological Survey.

Blacketer, R. 2014. North Idaho mining history and living conditions. Personal interview.

Boukemara, L., C. Boukhalfa, S. Azzouz, L. Reinert, L. Duclaux, A. Amrane, and A. Szymczyk. 2017. Characterization of phosphorus interaction with sediments affected by acid mine drainage - relation with the sediment composition. doi:10.1016/j.ijsrc.2017.09.004

Chislock, M. F., E. Doster, R. a. Zitomer, and A. E. Wilson. 2013. Eutrophication : Causes , consequences, and controls in aquatic ecosystems, A.A. Ansari, G.R. Lanza, S.S. Gill, and W. Rast [eds.]. Springer.

Eyles, N., and M. Meriano. 2010. Road-impacted sediment and water in a Lake Ontario watershed and lagoon, City of Pickering, Ontario, Canada: An example of urban basin analysis. Sediment. Geol. doi:10.1016/j.sedgeo.2009.12.004

Harrington, J. M., M. J. LaForce, W. C. Rember, S. E. Fendorf, and R. F. Rosenzweig. 1998. Phase associations and mobilization of iron and trace elements in Coeur d'Alene Lake, Idaho. Environ. Manage. **32**: 650–656.

Horowitz, A. J., K. A. Elrick, and R. B. Cook. 1993. Effect of mining and related activities on the sediment trace element geochemistry of Lake Coeur D ' Alene, Idaho, U.S.A. Part I: Surface Sediments. Hydrol. Process. **9**: 35–54. doi:10.1002/hyp.3360070406

IDEQ. 2014. Pend Oreille Lake productivity characterization. Idaho Dep. Environ. Qual. Rep.

Jacoby, J. M., D. C. Collier, E. B. Welch, F. J. Hardy, and M. Crayton. 2000. Environmental factors associated with a toxic bloom of *Microcystis aeruginosa*. Can. J. Fish. and Aquat. Sci. **57**: 231-240, doi: 10.1139/f99-234

Kuwabara, J. S., J. L. Carter, B. R. Topping, L. S. Balistrieri, P. F. Woods, W. M. Berelson, and S. V. Fend. 2003. Importance of sediment-water interactions in Coeur d'Alene Lake, Idaho, USA: Management implications. Environ. Manage. **32**: 348–359. doi:10.1007/s00267-003-0020-7

Lambert, D., A. Cattaneo, and R. Carignan. 2008. Periphyton as an early indicator of perturbation in recreational lakes. Can. J. Fish. Aquat. Sci. **65**: 258–265. doi:10.1139/f07-168

Liao, F., F. Wilhelm, and M. Solomon. 2016. The effects of ambient water quality and Eurasian watermilfoil on lakefront property values in the Coeur d'Alene area of Northern Idaho, USA. Sustainability **8**: 44-56. doi:10.3390/su8010044

LMP. 2009. Coeur d'Alene lake management plan. Idaho Dep. Environ. Qual. Coeur d'Alene Tribe 164.

Mattila, J., and R. Raisanen. 1998. Periphyton growth as an indicator of eutrophication; an experimental approach. Hydrobiologia **377**: 15–23. doi:10.1023/A:1003265208397

Moore, J. W., D. E. Schindler, M. D. Scheuerell, D. Smith, and J. Frodge. 2003. Lake eutrophication at the urban fringe, Seattle Region, USA. R. Swedish Acad. Sci. **32**: 13–18.

Ouyang, W., A. K. Skidmore, F. Hao, and T. Wang. 2009. Soil erosion dynamics response to landscape pattern. Sci. Total Environ. **408**: 1358–1366. doi:10.1016/j.scitotenv.2009.10.062

Patrick, W. H., Jr., and R. A. Khalid. 1974. Phosphate release and sorption by soils and sediments: Effect of aerobic and anaerobic conditions. Science **186**: 53–55. doi: 10.1126/science.186.4158.53

Roering, J. J., J. W. Kirchner, and W. E. Dietrich. 1999. Evidence for nonlinear, diffusive sediment transport on hillslopes and implications for landscape morphology. Water Resour. Res. **35**: 853–870. doi:10.1029/1998WR900090

Rosenberger, E. E., S. E. Hampton, S. C. Fradkin, and B. P. Kennedy. 2008. Effects of shoreline development on the nearshore environment in large deep oligotrophic lakes. Freshw. Biol. **53**: 1673–1691. doi:10.1111/j.1365-2427.2008.01990.x

Schindler, D. E., S. I. Geib, and M. R. Williams. 2000. Patterns of fish growth along a residential development gradient in north temperate lakes. Ecosystems **3**: 229-237. doi:10.1007/s100210000022

Sevinç Şengör, S., N. F. Spycher, T. R. Ginn, R. K. Sani, and B. Peyton. 2007. Biogeochemical reactive–diffusive transport of heavy metals in Lake Coeur d'Alene sediments. Appl. Geochemistry **22**: 2569–2594. doi:10.1016/J.APGEOCHEM.2007.06.011

Smith, V. H., G. D. Tilman, and J. C. Nekola. 1999. Eutrophication: impacts of excess nutrient inputs on freshwater, marine, and terrestrial ecosystems. Environ Pollut. **100**: 179-96.

Strawn, D. G., H. L. Bohn, and G. A. O'Connor. 2015. Soil chemistry, 4th ed. Johny Wiley & Sons, Ltd.

StreamStats. 2016. Coeur d'Alene Lake watershed. US Geol. Surv. web tool.

U.S. Census Bureau. 2017. U.S. Census Bureau QuickFacts: Coeur d'Alene city, Idaho.

Vadeboncoeur, Y., D. M. Lodge, and S. R. Carpenter. 2001. Whole-lake fertilization effects on distribution of primary production between benthic and pelagic habitats. Ecology **82**: 1065-1077. doi:10.2307/2679903.

Von Lindern, I. H., S. M. Spalinger, B. N. Bero, V. Petrosyan, C. Margrit, and C. Von Braun. 2003. The influence of soil remediation on lead in house dust. Sci. Total Environ. **303**: 59–78.

Wetzel, R. G. 2001. Limnology, 3rd ed. Academic Press.

Wood, M. S., and M. A. Beckwith. 2008. Coeur d'Alene Lake, Idaho: Insights gained from limnological studies of 1991–92 and 2004–06. USGS Sci. Investig. Rep. 2008-5168 52.

Woods, P. F. 1989. Water-Resources Investigations Report 89-4032 Boise, Idaho 1989. USGS Water Resour. Investig. Rep. 89-4032.

Woods, P. F. 2004. Role of limnological processes in fate and transport of nitrogen and phosphorus loads delivered into Coeur d'Alene Lake and Lake Pend Oreille, Idaho, and Flathead Lake, Montana. US Geol. Surv. Prof. Pap.

Woods, P. F., and M. A. Beckwith. 1997. Nutrient and trace-element enrichment of Coeur d'Alene Lake, Idaho. U.S. Geol. Surv. water-supply Pap. **2485** 1–93.

Table 1.1: Classified land use for the Coeur d'Alene Lake watershed. Images classified in 1989 (Woods and Beckwith 1997).

Land use	Area (km^2)	Percent of total
Coniferous forest	5260	51.6
Sparse forest	2350	23.0
Rangeland	688	6.8
Clouds	402	3.9
Recovering clear-cut forest	385	3.8
Dryland agriculture and pasture	357	3.5
Recent clear-cut forest	227	2.2
Irrigated agriculture and pasture	196	1.9
Water	166	1.6
Dense urban or built-up land	48.9	0.48
Cloud shadows	34.6	0.34
Sparse urban or built-up land	29.1	0.29
Wetland	23.9	0.23
Barren land	15.2	0.15
Deciduous forest	7	0.07
Mined land	4.1	0.05
Total	10200	100

Chapter 2: Growth of periphyton on artificial substrates in six northern bays of Coeur d'Alene Lake, Idaho

Abstract

Lake littoral zones are key focus areas to predict change in lake trophic status due to their proximity to incoming sources of sediment and associated nutrients. Here, periphyton are excellent candidates as indicators to evaluate nutrient loading because they are stationary and their growth reflects the arrival of nutrients to them, unlike free-floating algae that can obtain nutrients from different parts of the water column. In a study in 2017-2018 of periphyton communities in six northern bays of Coeur d'Alene Lake (Idaho, USA) to test the hypothesis that their growth and density would reflect bay watershed disturbance by human activity, which also varied among the bays, I found similar growth patterns and climax densities which did not support the hypothesis. The results also were inconsistent with those from another local lake in which rapid periphyton growth and high climax densities were directly related to human density in the sub-watersheds. Periphyton biomass was regressed against indicators of anthropogenic activity in the watershed (e.g., population density) to determine if periphyton response in bays correlated with trends of anthropogenic activity indicators. No indicator variables were sufficient predictors in the models, indicating no predictive relationship between the watershed variables selected for analysis and periphyton biomass in bays of Coeur d'Alene Lake could be established. Variation in nutrient load to bays of Coeur d'Alene Lake may be masked by different bay-specific retention regimes or other in-bay processes, thereby explaining the similar periphyton responses. These findings imply that this method using artificial substrates to monitor periphyton recruitment as an indicator of watershed land use is not satisfactory to detect nutrient enrichment in Coeur d'Alene Lake.

Introduction

Eutrophication and beneficial use

With limited freshwater resources and a growing human population globally, protecting lakes from the damaging deleterious effects of eutrophication is a primary concern among regulators and water managers world-wide. Eutrophication, the nutrient enrichment of water bodies, is considered a pollution problem of aquatic ecosystems across Europe and North America (Ansari et al. 2011). "Cultural" eutrophication (Schindler and Vallentyne 2008) results from human activities on the landscape that accelerate sediment and nutrient deposition to lakes, streams, and rivers (Rosenberger et al. 2008; Vadeboncoeur et al. 2008). Disruptions and impairments to natural ecosystems occur to water bodies through eutrophication (the increase in phytoplankton and macrophyte biomass due to excess nutrients), such as habitat disruption for fish, decreased light penetration, and the development of unsightly algae blooms and surface scums that reduce or eliminate the mass of hypolimnetic oxygen and decrease the exchange of dissolved oxygen across the air/water interface (Rosenberger et al. 2008; Ansari et al. 2011; Chislock et al. 2013). Additionally, high plant biomass poses difficulties for boat navigation, decreases aesthetics causing property values to decline, and threatens human health if algal blooms produce toxins (Ansari et al. 2011). In the Coeur d'Alene region of northern Idaho, the regional economy is heavily dependent on high water quality in Coeur d'Alene Lake – known as the "Gem Lake" of Idaho for tourism and overall standard of living.

Managers use a variety of tools to monitor and detect eutrophication in lakes. These include evaluating a water body based on its ability to meet desired and designated beneficial uses. Minimally, regulators are required to address the Clean Water Act (1972), which calls for waterways to support aquatic life and recreation when possible (IDEQ 2018). Beneficial use categories range from physical, chemical, and biological characteristics to economic factors and public opinion (IDEQ 2018).

Water bodies that do not meet these standards are considered impaired and trigger the development of a Total Maximum Daily Load assessment to return the functionality of the water body (TMDL; IDAPA 58.01.02.055). TMDLs function as a prescription for the holistic treatment of a water body, rubrics for its evaluation, and as guiding documents for permitting activities that may influence water quality. Eutrophication threatens uses concerning aquatic

life and aesthetics, which are designated uses in Idaho (IDAPA 58.01.02.100). For example, lake residents and users considered excessive periphyton growth as a nuisance in Pend Oreille Lake in the 1990's (Falter 2004). Managers use indicators such as water column nutrient loads and concentrations, algal biomass, temperature, pH, and dissolved oxygen to evaluate their role and contribution to restoring beneficial uses (DEQ 2018).

Of particular interest is the role of biological indicators in water quality assessments. Existing monitoring programs often evaluate the inputs to eutrophication (nutrients) and the most easily sampled results (phytoplankton). Local lake managers in northern Idaho expressed interest in developing a new biological indicator of nutrient enrichment—the use and evaluation of periphyton. Because of its natural characteristics (described below), periphyton should be evaluated as an effective tool to monitor trends of primary productivity in the littoral regions of water bodies. My objective here is to investigate the viability of using the accrual of periphyton on artificial substrates as a means to monitor the potential nutrient enrichment in bays of Coeur d'Alene Lake.

Review of lentic periphyton studies

Periphyton, the attached algae and microfauna that develops on benthic substrates, is often underestimated in its ecological and metabolic importance in aquatic ecosystems (Wetzel 1983; Hecky and Hesslein 1995; Vadeboncoeur et al. 2008). Vadeboncoeur et al. (2008) credit periphyton as the energetic food base of lakes, particularly for grazing macroinvertebrates and fish that breed in shallow water, suggesting it is a critical link in aquatic food chains. For example, Loeb et al. (1983) concluded that periphyton contributed the majority of littoral zone primary production in steep-sided oligotrophic alpine lakes, representing 60-80% of total primary production lake-wide. In contrast, in shallow lakes the majority of lake volume is classified as littoral, thereby increasing the influence of periphyton as key primary producers. These studies demonstrate the importance of the periphyton community to overall lake trophic dynamics.

The response of periphyton communities also can be a useful early sentinel of increasing eutrophication in lakes (Jacoby et al. 1991; Havens et al. 1999; Hadwen and Bunn 2005; Rosenberger et al. 2008). Because they are limited to the littoral zone (depth of light penetration), periphyton encounter nutrients and material from external sources before nutrient dilution occurs and influences pelagic primary production (Sand-Jensen and Borum

1991; Planas et al. 2000; Lambert et al. 2008). In addition, relative to other primary producers, periphyton rapidly assimilate nutrients (Loeb et al. 1983; Goldman 1988; Jacoby et al. 1991; Hadwen and Bunn 2005; Rosenberger et al. 2008). As a result, the periphyton community can intercept and take up eutrophying nutrients resulting in significant decreases in nutrients reaching offshore waters (Rosenberger et al. 2008). Thus, by the time changes indicating the occurrence of eutrophication are seen in traditional sampling programs that concentrate on the offshore pelagic zone, potentially much damage has already occurred to a water body. Loeb et al. (1983), Kann and Falter (1989), and Lambert et al. (2008) concluded that periphyton biomass was significantly positively correlated with increasing lake recreational development. Conversely, periphyton biomass did not correlate with pelagic total phosphorus. However, pelagic phytoplankton correlated with pelagic TP but not with nearshore development (Lambert et al. 2008; Vadeboncoeur et al. 2008), meaning that it was a poor indicator of early changes occurring in the littoral zone. Thus, monitoring the littoral periphyton community as an early indicator of lake eutrophication should be a valuable tool on its own (Lavoie et al. 2006; Perrin et al. 2007; Lambert et al. 2008; Omar 2010; Scofield et al. 2011).

Motivation for the periphyton study in Coeur d'Alene Lake

In northern Idaho lakes, periphyton has been used successfully to monitor the influence of incoming nutrients to bays to evaluate localized nutrient loading and its influence on beneficial uses. For example, in Priest and Pend Oreille lakes, two meso-oligotrophic lakes with low water column total phosphorus (TP) concentrations, developed and undeveloped sites were indistinguishable with respect to water column nutrients (Rosenberger et al. 2008), but the periphyton community was more abundant and accrued more rapidly at developed vs. undeveloped sites (Rosenberger et al. 2008; IDEQ 2014). Rosenberger et al. (2008) suggested that the low water column TP hindered identifying the different watershed development classifications based solely on pelagic nutrient concentrations, while the rapid nutrient uptake by periphyton allowed the different development classifications to be distinguished and contributed to the ubiquitous low water column TP concentrations.

The success of using periphyton as an indicator of watershed development in Priest and Pend Oreille lakes was the motivation for this study in Coeur d'Alene Lake. Given the

similarities of physical geography between Pend Oreille and Coeur d'Alene lakes, I predicted that developed and undeveloped watersheds would result in significantly different periphyton responses between bays in Coeur d'Alene.

Objectives

To address the overarching hypothesis that periphyton response differed in bays with different anthropogenic activity, I monitored periphyton growth during the summer growing season, concurrently sampled water quality, and used GIS analysis of terrestrial watersheds of each of six bays in Coeur d'Alene Lake. To test the hypothesis that shallow substrates produce more biomass than deep substrates, pairs of substrates were deployed in close proximity to each other at depths of 1.8 m and 4 m during 2018. To examine the anthropogenic activity in the watersheds, I used GIS to characterize each watersheds using population density (IDEQ 2014), dwelling density (Lambert et al. 2008), percent forest and land clearing (Lambert et al. 2008), and percent urban + cropland + pasture (Dodds et al. 2002).

Methods and Materials

To test the hypothesis that periphyton response differed between bays with different watershed characteristics, I used artificial substrates (Cattaneo 1987; Kann and Falter 1989; Woods and Beckwith 1997; Falter 2004; Lambert et al. 2008; Vadeboncoeur et al. 2008, 2014; Omar 2010; DeNicola and Kelly 2014; Vadeboncoeur and Power 2017) deployed in six bays from June 22 to September 13, 2017 and May 30 to September 6, 2018.

Description of bay study sites

The six study sites were all located at the northern end of Coeur d'Alene Lake (Figure 2.1). These bays were chosen for ease of access by boat, comparable benthic contours, and a range of watershed land use and degree of shoreline development (Table 2.1; C. Cooper pers. comm.) In general, the Coeur d'Alene lake benthos is less rocky and has deeper sediment than Pend Oreille and Priest lakes where previous periphyton studies were located.

Beauty Bay

Beauty Bay (Figure 2.2) is the most highly crenulated of the bays, with approximately 4 km of shoreline and it extends 1.2 km beyond the main lake body. Its surface area is 0.55 km^2. Beauty Bay is known as an excellent bay for recreation and approximately 50% of the

land adjacent to and including the shoreline is owned and managed by the U.S. Forest Service. The steep-sided shoreline limits access despite the federal ownership. Of the 4 km of shoreline, 0.57 km has docks including 15 docks and 10 permanent houseboats. The bathymetry continues that of the steep shoreline, and water depths reach 30 m rapidly. Macrophyte growth is low compared to the other bays, with moderately dense *Potamogeton sp.* (long-leaf grass) limited to the SE arm of the bay (Word and Knowlen 2015).

Bennett Bay

Bennett Bay (Figure 2.3) is the smallest of the six study bays, at only 0.5 km long with a surface area of 0.2 km^2. Of the 1.4 km of shoreline, 0.6 km are abutted directly by the old Interstate 90 (presently Coeur d'Alene Lake Dr.). The bay has one large residence and five hillside units with 10 docks. Steep-sided terrain emphasizes the bay's sides, leaving steep bathymetry on the sides of the bay and a gentler slope to the head of the bay. Prominent macrophyte species include *Potamogeton amplifolius* and *Potamogeton robbinsii* that can grow at depths up to 7 m (Word and Knowlen 2015).

Blue Creek Bay

As the second shortest bay (0.95 km), Blue Creek Bay (Figure 2.4) exhibits one of the highest human-developed shoreline densities of the six bays. The surface area is 0.32 km^2. Of the 3.0 km of shoreline, 0.8 km is lined with homes and docks in close proximity to each other. One of the 31 docks is maintained by the Bureau of Land Management (BLM) for public access. The south shoreline of the bay is a steep mountainside of BLM land with no dwellings. Bathymetry on the south shoreline is steep, but it flattens at the wetland to the east and to the north. Macrophyte density in Blue Creek Bay is high, with *Potamogeton amplifolius, Potamogeton robbinsii,* and *Elodea sp.* beds existing out to 0.4 km from the wetland shoreline and at depths to 5.5 m (Word and Knowlen 2015).

Kidd Island Bay

Kidd Island Bay (Figure 2.5) is known by residents and lake managers for its length and shallow bathymetry towards the head of the bay, high macrophyte density, and extensive shoreline development. Kidd Island Bay is 1.6 km long with 4.4 km of shoreline and a surface area of 0.49 km^2. The entire shoreline and the 62 docks are privately owned with more gently-sloped terrain than the other bays. This causes Kidd Island's bathymetry to be extremely flat over half of the bay's length, reaching a maximum depth of just 3 m in the

shallow end of the bay. After the shelf towards the lake, the depth increases to more than 30 m in the last 0.5 km closest to the lake.

Kidd Island's unique bathymetry includes the "rabbit ears" shoreline at the head of the bay adjacent to the stream inflow. Due to flooding and homeowner support, the natural stream channel was rerouted within the last twenty years. By moving the stream to the opposite corner of the wetland, the new inflow created the second 'ear' of the bay, resulting in a 0.35 km peninsula between the former and current inflows. Kidd Island Bay also hosts two islands, one in the middle of the bay and one at the mouth near the main lake body. Macrophytes are dense in Kidd Island, with *Elodea sp.* mats and up to ten other species such as *Potamogeton amplifolius*. Maximum density occurred at 2.7 m in 2014 (Word and Knowlen 2015).

Neachen Bay

Neachen Bay (Figure 2.6) is 1.3 km long with 2.9 km of shoreline. Its 0.47 km^2 surface area is similar to Kidd Island Bay. It is well-known for boating recreation, and the bay hosts a floating gas station and a county boat launch but no public access to beaches. Almost all of the shoreline is occupied by a variety of dwellings and includes 55 docks. The head of the bay is shallow, with 5 m depth not occurring until midway into the bay. It transitions to a depth of 25 m at the mouth of the bay nearest the main lake body. The maximum density of macrophytes occurred between 2.7 and 3.7 m and consisted of *Potamogeton robbinsii,* and *Elodea sp* (Word and Knowlen 2015).

Wolf Lodge Bay

The longest of the bays (2.0 km), Wolf Lodge Bay (Figure 2.7) is also the furthest east and largest in surface area (1.14 km^2). Wolf Lodge Bay is nearly bathtub-shaped with steep sides and a deep, trough-like center. Due to the orientation and morphometry of the bay, it likely has the greatest lake influence, which is evidenced by the substantial wave action that often occurs. To the east, the wetland environment results in gentler sloping bathymetry into the center of the bay. This bay is popular for fishing and eagle watching. *Elodea sp.* is most abundant, growing in the majority of the littoral area at depths greater than 4 m. Emergent *Potamogeton amplifolius* and *Potamogeton sp*. are also abundant. The entire north shoreline is bordered by Interstate 90 while the south shoreline is steep-sided mountainous federal lands managed by the BLM. As a result, human dwellings are absent

from the near-shore environment and the only dock is the BLM Mineral Ridge boat launch. Despite the low dwelling density at the shoreline, the Wolf Lodge watershed is known for its high particulate matter transport, and probably nutrient loading, through Wolf Lodge Creek into the bay.

Design of experimental substrates

In general, each 'substrate' is an assembly (Figure 2.8) including an anchor base composed of a 0.16 m (16") × 0.16 m (16") paving stone with a central hole to accept a 1.58 cm (5/8") diam. eyebolt rod approximately 0.36 m (14") long. House cladding polystyrene (½" thick Insulfoam® Molded Expanded Polystyrene Foam R-Tech©, Tacoma, WA) was attached with the foil side down to a piece of marine plywood 0.16 m (16") × 0.16 m (16") in area and 1.9 cm (3/4") thick to serve as the substrate for periphyton growth. This polystyrene substrate material was selected based on consultation with personnel at IDEQ (IDEQ 2014). The growth substrate also had a central hole and was suspended under the eye of the bolt by means of a backing washer and nut. Elevating the growth substrate above the paver served to maintain it above the soft bottom sediments into which the paver anchor penetrated. If the growth substrate were to be attached immediately above the paver it would risk being covered by the sediment when lowered into place in the lake. A marked float (part numbers 19126, 19160, and 19151, SMI, Sumner, WA) was attached to each eyebolt with a length of 20 m polypropylene line to locate and retrieve the substrates for sampling.

Procedures for field sampling of substrates

Field sampling procedures of substrates in 2017

All 18 substrates were deployed over the course of two consecutive days into the six bays at a depth of 4 m. To avoid influences from the main lake and primarily characterize each bay, the substrates were intentionally placed as far from the mouth as possible given a bay's bathymetry. Samples for the analysis of chlorophyll *a* as an indicator of periphyton growth were collected approximately every seven days from June 2017 through September 2017. A bow and stern anchor were set to minimize boat drift from the initial substrate location. A gaff was used to retrieve each marker buoy and slowly raise the substrate to the surface. To prevent oxygen shock to the periphyton, substrates were kept underwater by attaching the substrate rope to a side cleat on the boat. Each substrate was sampled twice by randomly lowering an inverted 20 ml sample vial with a sharpened 1.7 cm diam. metal pipe

fitting embedded in its cap onto the substrate and cutting through the polystyrene foam to remove a 'plug'. Samples were labeled, wrapped in foil, and stored on dry ice until return to the lab, after which they were stored in a laboratory freezer at -20°C until analysis. Transport to Advanced Eco-Solutions, Inc. (Liberty Lake, WA) occurred within four weeks for analysis of chlorophyll *a*.

Field sampling procedures of substrates in 2018

Given that Kann and Falter (1989) reported higher periphyton biomass on substrates at a depth of 0.5 m compared to those at a depth of 1.5 m, and the US Geological Survey (USGS) placed substrates at a depth of 1.8 m during their 1991-92 USGS study on Coeur d'Alene Lake (Woods and Beckwith 1997), I placed three additional substrates at a depth of 1.8 m in each of the two bays sampled in 2018. The substrates at 1.8 m were placed in close proximity to the substrates at 4 m to reduce the need for additional samples to analyze water chemistry. All substrates deployed in 2018 were sampled in the same manner as described for 2017 above.

Collection of water samples for analysis of chemistry (2017 and 2018)

To obtain samples from the water column for the analysis of chlorophyll *a*, total phosphorus (TP), dissolved ortho-phosphorus (OP), and total nitrogen (N), a 6.2 L vertical PVC Kemmerer sampler was used to collect triplicate water samples from 4 m near the substrate. Each sample was protected from the sun and emptied into an opaque plastic churn splitter to homogenize the samples. From the churn splitter, 1.5 L of sample were filtered (GF/C- Whatman, pore size: 1.2 μm) and preserved with $MgCO_3$ for analysis of Chlorophyll *a*. Filters were placed into 15 ml polyethylene centrifuge tubes, labelled and stored in the dark on dry ice until return to the lab after which they were transferred to a freezer at -20°C until analysis. A 120 ml water sample was transferred from the churn splitter into pre-labelled pre-rinsed polyethylene bottles for the analysis of TP which were preserved with 0.25 ml of concentrated HCl. Samples for the analysis of ortho-phosphate were filtered on site within 15 minutes of removal from the lake using a pre-rinsed 0.45 um nitrocelluslose filter (SM4500-P.B; APHA 2005). Samples for analysis of TN were preserved with 0.25 ml of concentrated H_2SO_4. Samples were stored on ice until return to the lab where they were stored in a -20°C freezer until analysis, except OP which samples were analyzed within 48 h per SM 4500-P.B (Eaton et al. 2005).

Laboratory analysis of field-collected samples

Analysis of chlorophyll *a* from substrates

Cores (plugs) sampled from substrates were analyzed for periphyton biomass using chlorophyll *a* ($mg \cdot m^{-2}$), a commonly used indicator (Canfield and Bachmann 1980). Although several methods for the determination of chlorophyll *a* exist, fluorometry was used because it is more sensitive and can accommodate small sample sizes (Eaton et al. 2005). The core fluorometry methods in this study were based on SM 10200-H.3 with adjustments made by Darren Brandt of Advanced EcoSolutions (Newman Lake, WA) to accommodate the polystyrene substrate as opposed to glass fiber filters or other substrates (Eaton et al. 2005; Scofield et al. 2011). All fluorometry analyses were completed at Advanced EcoSolutions, with regular season samples analyzed by Darren and post-season QC samples analyzed by myself.

To begin analysis, samples were removed from the freezer and unwrapped from their aluminum foil coverings. Fifteen ml of 90% acetone were added to each vial as an extractant, agitated for five seconds and again after one hour, then left undisturbed in the dark between 4 and 24 hours. During this time, the polystyrene substrate partially or completely dissolved. Next, 2 ml of solution from each vial were transferred to a corresponding 2 ml optically-matched scintillation vial that was inserted into the fluorometer (Turner Trilogy, San Jose, CA). Samples were analyzed with a 430 nm excitation wavelength and 663 nm emission wavelength and converted to concentrations automatically by the fluorometer according to calibration settings.

After obtaining the first fluorescence reading, two drops (0.1 ml) of 0.1 N HCl were added to the 2 ml scintillation vial, given 90 seconds to react, and then re-analyzed to obtain a pheophytin *a* correction. Finally, the concentration of corrected chlorophyll *a* in the sample was converted to biomass per unit area ($mg\ m^{-2}$) using the following formula:

$$C_a = \frac{C_v \times V_e}{A}$$

Where:

C_a = Chlorophyll *a* biomass ($mg\ m^{-2}$)

C_v = Chlorophyll a concentration ($\mu g\ L^{-1}$)

V_e = Volume of extractant (ml)

A = Area sampled (mm^2)

Analysis of chlorophyll *a* from the water column

Water column chlorophyll *a* was analyzed using the spectrophotometric method for chlorophyll *a* determination (Sartory and Grobbelaar 1984). Chlorophyll *a* concentrations were calculated using the ethanol extraction method for spectrophotometry (SM10200-H.2; (Eaton et al. 2005). Measured volumes of sample, typically 1500 ml unless otherwise noted, were filtered through 47mm glass fiber filters (GF/C- Whatman, pore size: 1.2 µm) in the field and frozen. On the day before analysis, filters were thawed and then macerated with a stainless steel spatula in the presence of 10 mL 95% ethanol solution and replaced in the refrigerator (4°C) for 24 hours. Once thawed and centrifuged for 20 minutes at 2,600 rpm, samples were analyzed at multiple wavelengths (665, 649, and 750) on a Beckman-Coulter DU 640 spectrophotometer in 1 cm plastic cuvettes. Chlorophyll *a* was calculated using the formula:

$$Chlorophyll\ \text{a}\ \left(\mu\frac{\text{g}}{\text{L}}\right) = \frac{v\,[\,13.7(665\ -\ 750) -\ 5.76(649\ -\ 750)]}{(V)(L)}$$

Where:

v = extractant volume in ml (10 ml)

V = volume of lake water filtered in L (typically 1.5 L)

L = length of cuvette (1 cm)

And

750 is the absorbance for turbidity,

649 is the absorbance for chlorophyll *b*

665 is the absorbance for chlorophyll *a*

Analysis of TP and OP

The concentration of phosphorus in water samples collected in Coeur d'Alene Lake were analyzed according to the ascorbic acid method SM 4500-P.E (APHA 2005) with adjustments to accommodate sample preservation in some cases (discussed further in Chapter 4). For analysis of TP, 20 ml of each sample were transferred into a 16 × 125 mm Kimball screw-top borosilicate glass vial containing 0.2 g of potassium persulfate followed by digestion in an autoclave for 20 minutes at 20 kPa (30 p.s.i). This oxidized the organic and mineral material in the sample, thereby converting all forms of P into soluble reactive P. OP was not digested but was processed within 48 hours of collection.

Sample absorbance was measured with a Thermo-Scientific AquaMate VIS visible-light spectrophotometer (ThermoFisher Scientific, Whatham, MA) and 5 cm glass cuvette. Samples were poured into the cuvette from the glass vial, read for absorbance, then aspirated from the cuvette using a vacuum system. The cuvette was triple-rinsed with distilled water between each sample. Absorbance values were converted to a concentration ($\mu g \cdot L^{-1}$) using a calibration curve of phosphorus standards with known concentrations (Eaton et al. 2005).

Analysis of the periphyton community using an autotrophic index

The autotrophic index was calculated to determine the biomass of heterotrophs relative to autotrophs in the substrate samples. Two 5.08 cm^2 (2 $in.^2$) sections of each substrate were collected at the midpoint (Week 7) and endpoints (Week 13) of the experiment. To obtain ash-free dry mass (AFDM), each substrate sample was treated according to SM 10300-C.5 (Eaton et al. 2005), which included oven-drying at 105 °C for 24 hours and combustion at 500 °C for 1 hour. AFDM was compared to chlorophyll *a* which was assumed equal to that week's regular substrate core analysis.

GIS analysis of watersheds

Using the IDEQ geospatial database for Coeur d'Alene Lake, National Landcover Database Classifications (MRLC 2011), and U.S. Census Bureau data (U.S. Census Bureau 2010), I evaluated the sub-watersheds of each bay. Evaluation criteria included: land use, population and housing density, and percent forest clearing. Typically, similar studies reported use of two to three specific classifications for statistical comparison to benthic chlorophyll *a.* For example, Lambert et al. (2008) used dwelling density and percent forest clearing in a lake's watershed, while other studies have used percent watershed in

urban/cropland/pasture as a metric of human influence (e.g., Dodds et al. 2002). Similarly, Lambert et al. (2008) concluded that phosphorus export was correlated with percent land clearing. The goal of my evaluation was to predict which bays would have a higher nutrient loading potential based on these metrics and examine potential relationships to the periphyton production observed on the substrates. For further analysis, individual factors were compiled into a multiple linear regression to enhance predictions of the relationship between nutrient loading factors and periphyton response in bays (see *Statistical analysis of chapter two data*).

Delineation of watersheds in GIS

Subwatersheds of each bay were delineated using the Watershed toolbox in ArcGIS. I used a 30 m digital elevation model (DEMs; USGS 1999a) because other data layers need for analysis were available at this resolution. A 10 m DEM (USGS 1999b) was used to inform fine-scale ridgelines, particularly for shared boundaries of neighboring subwatersheds or near the bay shoreline. When necessary, I used the USGS StreamStats tool (USGS 2016) to build polygons of small stream channel watersheds within bays. I compared my delineations to the USGS Hydrologic Unit Code (HUC) level 6 subbasins to verify accuracy, however, these often did not match because the HUC-6 subbasins had misclassified pourpoints in the paleochannel of the lake resulting in erroneous inclusion of areas that were not actually in the subbasin.

Population density

Census data was acquired from the 2010 TIGER/Line Population and Housing Unit Count for population blocks (U.S. Census Bureau 2010). This was the finest spatial resolution for population data available for the area. Population density per census block was converted to a 30 m raster, then to subbasin population density using Zonal Statistics in the Spatial Analyst toolpack of ArcGIS. This tool was used to calculate the mean population density for the 30 m cells within the subbasin.

Dwelling density

The 2010 TIGER/Line Population and Housing Unit Count for population blocks (U.S. Census Bureau 2010) data set and methods of calculation methods as used for population density also were used to obtain dwelling density. I substituted the field "HOUSING10" for "POP10," which means the number of housing units per block were used

instead of population per block. In the same manner as above, dwelling density per block was converted to a raster then to mean dwelling density per subbasin.

Forest clearing

Data to represent forest clearing was obtained from the Idaho Department of Environmental Quality's Nutrient Inventory geodatabase. The layer "Forest Loss" was a 30 m raster representing cells with forest loss since the 2001 National Land Cover Database (NLCD) land use classification. However, these data only reflected land clearing since 2001, but land clearing has obviously occurred previously. To identify land cleared before 2001, cells which were classified as "scrub/clear" in the 2011 NLCD layer were used to represent areas that had been cleared before 2001. To confirm this as an acceptable approach, scrub/clear cells were compared to satellite imagery which agreed well with anthropogenic clearing, not natural scrub or other vegetation types, across all watersheds. I added these cells to the Forest Loss layer to make an overall Forest Clearing layer. Zonal Statistics were used to calculate the sum of cleared cells in the 30 m raster per subbasin, then converted to percent of cells cleared in the subbasin.

Other land use

This anthropogenic variable is the sum of cells classified as urban, cropland, and pasture in the 2011 NLCD layer (MRLC 2011), which had been simplified through reclassification by the IDEQ. I then reclassified all cells labeled "Developed," "Hay/Pasture," and "Cultivated Crops" with indicator variables of 1 for "other land use" and 0 for "otherwise." Zonal Statistics were then used to sum those cells and calculate the percent of the subbasin classified as "other land use."

Statistical analyses

Periphyton

To examine the response of periphyton mats over time, I used ordinary least squares regression to examine chlorophyll *a* biomass ($mg \cdot m^{-2}$) as a function of time (with Day 1 equal to June 29, 2017 or June 14, 2018, respectively). The date of maximum chlorophyll *a* biomass accrual was identified as the date on which the bay average biomass reached its maximum. This occurred in all bays on the date of the last sampling event in both years, on September 13, 2017 and September 6, 2018, respectively. Shallow substrates in Kidd Island reached maximum biomass during the previous sampling event (August 23, 2018), but this

was due to an outlier that was removed from further analysis. Maximum biomass was therefore considered to occur on the final week to match the other sites. Differences in the slopes between bays were analyzed using an analysis of covariance (ANCOVA) with chlorophyll *a* as the response variable, time as the independent variable, and bay as the grouping variable.

Before regression analysis the assumption of homoscedasticity of residuals and normality of data was examined. Instances that did not meet these assumptions were transformed with a Box-Cox transformation (Box and Cox 1964) of biomass using the MASS package in R (Venables and Ripley 2002). Transformed data were checked again, and then used for all analyses. After analysis, results were back-transformed for ease of interpretation. Analysis of variance (ANOVA)s was used to examine potential differences in the maximum biomass between bays (2017 and 2018) and deep and shallow substrates in 2018.

Productivity parameters as predictors of substrate biomass

Periphyton accumulation, measured as substrate chlorophyll *a* biomass as a function of trophic indicators was examined with least squares regression to determine how much of the variation in periphyton growth each could explain. These indicators included water column chlorophyll *a* ($\mu g \cdot L^{-1}$), nutrient (TP and OP) concentrations ($\mu g \cdot L^{-1}$), and cumulative nutrient concentration ($\mu g \cdot L^{-1}$). Cumulative nutrient modeling was used to relate discrete nutrient samples to periphyton biomass samples that were inherently tied to previous conditions on a continuous scale. For example, a substrate core sample collected on June 30th reflects the past nutrient and light availability over the days or weeks leading up to the sample date. Because this relationship with lag time is not well known, cumulative nutrient availability was selected because it was possible to calculate with the existing data and was a plausible description of the relationship with time. Cumulative nutrient concentrations we calculated as the number of days between sampling intervals multiplied by the nutrient concentration on the sample day.

Physical parameters also influence periphyton growth, so total light availability (hours of available sunlight per day) was included in regression models. Nutrient concentrations used for statistical analysis were bay averages, which included water samples

taken near each of the three substrates within a bay and averaged for the bay on each sampling occasion.

Step-wise multiple regression and repeated-measures ANOVA were used to identify which parameters should be included in the best model for periphyton growth (Zar 1984). Repeated measures ANOVA controls accounted for the repeated sampling of each substrate throughout the season (Potvin 2001). No multiple regression model significantly improved upon the base model that used only the explanatory variables date and time, so no further analysis was undertaken.

Similar to the *periphyton* analysis above, the assumption of homoscedasticity was violated because variation between substrates within bays increases over time. The Box-Cox transformation was applied to the subset of substrate biomass samples used in the analysis of the productivity parameters. The transformation did allow assumptions to be met for the dataset but did not alter the results of the regressions and ANOVAs described above. Therefore, the back-transformed data were described in the results and discussion for ease of interpretation.

GIS analysis of watersheds

Watershed characteristics were analyzed by calculating the population density, housing density, percent forest clearing, and percent other land use per subbasin. Ranks 1 to 6 were assigned to each subbasin with a score of 1 indicating the bay ranked lowest for that variable. With six subbasins and four variables, there were a total of 84 rank points to earn. To compare bays, a ratio was calculated as the sum of rank points earned divided by the total rank points available. The sum of the ratios equals 100%, so ratios are comparable between subbasins.

Simple linear regression was used to compare individual anthropogenic activity indicators (X) to maximum periphyton biomass (Y) in each of the bays. Models were considered significant at an α of 0.05. After simple linear regression using ordinary least squares produced models with low (<50%) predictive power, multiple linear regression (MLR) was used to test if the inclusion of multiple parameters would increase model fit. Model selection included several steps, including: 1) testing for interactions between the potentially colinear variable pairs of population and housing density, and percent other and percent forest clearing, 2) using stepwise regression (Zar 1984), to help identify

parameterizations that best balanced parsimony with model fit (Ané 2017), 3) testing for collinearity between parameters of the competing models generated in step 2, and 4) using ANOVA to compare model fit with 95% confidence intervals.

Step two was carried out using the stepAIC function in the R package MASS (Venables and Ripley 2002). This tests all parameterizations and selects the model with the lowest AIC score. Once the best models for each number of levels (1-4) were identified, parameters were checked for collinearity with variance inflation factors (VIF) using the `vif` function in the R package car (Fox and Weisberg 2011). High VIFs, typically considered >1, indicated collinearity, with <5 being acceptable (Ané 2017). Step four was used to confirm that the more complex competing models were not more informative than the single-factor percent forest clearing model. The `anova` function in R was used to compare the top full, three-factor, and two-factor models to the percent clearing model using a 95% confidence interval (Phillips 2018).

Results

Periphyton

2017 Results

Across all bays, periphyton response increased linearly with time (Figure 2.9 and 2.10), beginning with no biomass on the first sample collection day (Day 1, June 29, 2017) and reaching a maximum of 34.8 $mg \cdot m^{-2}$ in Wolf Lodge Bay on Day 77 (September 13, 2017; Table 2.2)

The maximum biomass in 2017 occurred on September 13 and ranged from 17.6 $mg \cdot m^{-2}$ in Kidd Island Bay to 34.8 $mg \cdot m^{-2}$ in Wolf Lodge Bay (Table 2.2). The means of maximum biomass did not differ (ANOVA, $F = 2.36$, d.f. = 5, $p = 0.10$) between bays (Figure 2.11).

Slope

When examining transformed chlorophyll *a* biomass as a function of the transformed day of the study using ANCOVA (Figure 2.12) the interaction term was not significant (ANCOVA, $P = 0.58$) so it was removed and the analysis re-run, which indicated that the slope of each line was significantly different than zero and Bay was significant ($p < 0.001$),

indicating that intercepts were different between bays and initial Day 1 biomass values were significantly different from one another.

2018 Results

In 2018, periphyton biomass, as indicated by chlorophyll *a* concentration, increased linearly with time at all locations, beginning on June 16, 2018 and reaching the maximum biomass during the last two sampling periods (Figures 2.13 and 2.14). On average, substrates reached maximum biomass of 62.96 $mg \cdot m^{-2}$ in Kidd Island's deep substrates and 35.98 $mg \cdot m^{-2}$ on shallow. Neachen Bay's maximum biomass was 42.64 $mg \cdot m^{-2}$ on deep substrates and 50.04 on shallow (Figure 2.14; See Table 2.3 for 2018 weekly average biomass values).

Analysis of the transformed data revealed no difference (ANOVA, F= 0.67, d.f. = 3, P = 0.59) in mean maximum biomass between the four locations (Figure 2.15). Slopes of chlorophyll a biomass as a function of time were similar (ANCOVA $F_{2,3} = 2.00$, P = 0.12) across bays but intercepts differed (ANOVA $F_{2,3}= 6.11$, $P < 0.001$; Figure 2.16). The week 7 autotrophic index (AI) ranged from 1,063 to 2,384 with a mean of 1,623 ± 201.2 (mean±SE), while the week 13 AI's ranged from 924 to 1,990 with a mean of 1,333 ± 156.9. The week 13 AI's differed (Paired *t*-test, t = 2.09, d.f. = 5, P= 0.05) from those in week 7. AIs between bays within each study week did not differ (ANOVA F = 0.90, d.f. = 5, P=0.51 for week 7 and F = 0.96, d.f. = 5, P=0.48 for week 13; Tables 2.4 and 2.5).

Productivity parameters as predictors of substrate biomass

Summary of predictor variables

A key finding was that of all predictor variables, only water column chlorophyll *a* had no temporal trend (P=0.11) in 2017, and in 2018 cumulative TP had no trend (P=0.14). All other trends were significant at α=0.05 across both years (Tables 2.8 and 2.9). OP (Figures 2.17 and 2.18) and TP (Figures 2.19 and 2.20) decreased over time in both years (all p-values <0.001). The slopes of these negative trends in nutrient concentrations ranged from -0.08 to -0.03 $\mu g \cdot L^{-1} \cdot day^{-1}$. Bay-average OP and cumulative OP concentrations were lower than TP across sample sites, with all mean concentrations in both years below 10 $\mu g \cdot L^{-1}$ (Tables 2.6 and 2.7). Trend analysis for each predictor variable revealed that all but water column chlorophyll *a* were significant. Full parameters for each regression were compiled in Table 2.8 for 2017 and Table 2.9 for 2018. In 2018, cumulative daylight hours decreased over time

due to shorter days occurring after June 21. Cumulative daylight hours, the total number of daylight hours provided to a substrate between sampling periods, decreased with a slope of -0.04 ($P<0.001$), meaning that for each additive day, the average hours of daylight per week decreased by 0.04 hours (Figure 2.21).

Single variable predictors of substrate chlorophyll *a*

In 2017, all four nutrient variables were significant predictors of TP, but adjusted R^2 measures of model fit were low, at <30% for OP and cumulative OP, and <10% for TP and cumulative TP (Table 2.10; Figure 2.22). In 2018, OP and cumulative OP (Figures 2.25a and 2.25b) had a significant effect on biomass ($P<0.001$), along with TP ($P=0.03$; Figure 2.22c) and cumulative daylight hours ($P<0.001$; Figure 2.23e). However, R^2 values for TP and cumulative TP were low (<10%; Table 2.11). The non-significant regressions (Tables 2.10 and 2.1) are shown in Figures 2.22e-f and 2.23d.

In the previous section for the analysis of periphyton response over time, the base model used two variables (Day of study and Bay) to estimate substrate chlorophyll *a* biomass over time. As described in the *statistical analysis* section, a subset (n=99) of the 198 total substrate biomass samples was used in these models. The base model using the subset dataset had an adjusted R^2 of 0.70 ($P<0.001$). When each variable (OP, cumulative OP, TP, cumulative TP, average hours, and water column chlorophyll *a*) was added as a third parameter to the base model, the best performing model included water column chlorophyll *a*, resulting in an adjusted R^2 of 0.75. Despite adding the additional parameters, these did not improve the predictive power sufficiently to justify the increase in residual error incurred. This was evaluated with an ANOVA ($F=0.0028$, d.f. = 1, $P=0.96$) that did not support the hypothesis that a three-factor model was a better predictor than the base model. Similarly, a four-factor model including day, bay, water column chlorophyll, and cumulative hours had higher predictive power than the two-factor model (adjusted $R^2 = 0.76$), but at a 95% confidence interval the ANOVA ($F=2.10$, d.f.=1, $P=0.13$) did not support the conclusion that the four-factor model improved the base model.

In 2018, the base model's adjusted R^2 was 0.66 ($P<0.001$). Only one three-factor model with cumulative TP had a higher adjusted R^2 than the base model, at $R^2 = 0.68$. As in 2017, the hypothesis that the added variable significantly improved model fit was not supported (ANOVA, $F=4.26$, d.f.=1, $P=0.05$). In stepwise regression, the next variable added

was OP, creating a four-factor model with an adjusted R^2 of 0.68 ($P<0.001$). This model also did not improve prediction of substrate chlorophyll *a* compared to the two-factor model (ANOVA, F=2.58, d.f.=1, P=0.09).

GIS analysis of watersheds

Bay watersheds varied in anthropogenic activity (Table 2.14). Population density ranged from 0.36 to 24.16 persons per km^2 with a mean of 7.14 ±3.94 (mean±SE). Dwelling density ranged from 0.44 to 10.78 housing units per km^2 with a mean of 3.98 (±3.94) $hu \cdot km^{-2}$. Percent forest clearing across watersheds ranged from 4.07% to 37.27% of total watershed area, with a mean of 22.66±13.41%. Percent of other land use was 0.72% to 16.55% across bays, with a mean of 4.68±5.98% (Table 2.14).

In three of four cases, Beauty Bay had the lowest value per indicator variable of human activity, excluding dwelling density. In the same number of cases, Bennett Bay was the highest ranked bay for indicators of human activity, excluding percent forest clearing. The rank system used to score bays based on their level of anthropogenic activity (Table 2.15) indicated that Beauty Bay ranked lowest overall, scoring 5 points, which is 6% of the total points available. Bennett Bay ranked highest with a score of 23 points, or 27% of points possible. In order from lowest to highest points earned, the bays ranked: Beauty (5), Wolf (8), Blue Creek (13), Neachen (14), Kidd Island (21), and Bennett (23).

Each anthropogenic activity indicator regressed against maximum periphyton biomass in the bays produced insignificant models for population density, dwelling density, and forest clearing, but not other land uses (Table 2.16, Figure 2.24). Although the best-performing single-factor model was percent forest clearing, with an adjusted R^2 of 0.32, the regression slope did not differ from zero ($P = 0.14$). Models generated by the MLR approach were not more informative than single variable linear regression using percent forest clearing as a predictor of maximum chlorophyll *a* biomass in bays (Table 2.17). This was ultimately confirmed by an ANOVA of model fit comparing the best performing MLR model to the single-factor model ($F = 1.64$, d.f. = 16, $p = 0.23$),

Discussion

Periphyton

Periphyton response comparisons between bays

The hypothesis for this study was that periphyton response in bays of Coeur d'Alene Lake differed between bays with different levels of anthropogenic activities in their watersheds. This was based on the findings of a similar study undertaken by IDEQ on Pend Oreille Lake, ID (IDEQ 2014). There, periphyton communities had rapid initial growth and higher maximum biomass when substrates were placed in bays with "impacted" watersheds versus those that were pristine, or without high anthropogenic influence. Thus, I was interested if this approach could be a suitable tool for application in Coeur d'Alene Lake.

Unfortunately, the accrual and final biomass of periphyton did not differ among bays with distinctly different anthropogenic activities. The addition of substrates in shallow water in 2018 also did not improve the method's ability to detect differences in periphyton response to differing watershed nutrient loading risk, meaning that this tool alone was not useful in Coeur d'Alene Lake to distinguish between impacted and unimpacted watersheds. In further sections below, add-on tests I undertook to determine if they made detection of periphyton response characteristics more robust are discussed. However, other causes for the lack of differential periphyton growth in bays should be considered. The fate of nutrients deposited from streams is unclear, particularly concerning freshet residence time during the runoff season and internal loading via the resuspension of nutrients via wave action. Another consideration is the difference in lake-bottom substrate between Coeur d'Alene Lake and Pend Oreille. Pend Oreille's rocky substrate (IDEQ 2014) may minimize the influence of sediment resuspension like that which occurs in Coeur d'Alene. Periphyton diversity in community structure and attachment type also may play a role in the different periphyton responses exhibited between lakes. Epilithic periphyton (growing on rock) in Lake Pend Oreille could characteristically differ in colonization patterns from the epipelon (on sediment) that likely dominates the sediment-rich substrate in Coeur d'Alene (Lambert et al. 2008). Some or all of these explanations could reduce the effect of differential watershed contribution of nutrients, warranting further research.

Autotrophic index

Standard interpretation of the high AI values (>500 in both weeks in all bays, Tables 2.4, 2.5) results in the conclusion that the substrates were primarily heterotrophic and indicative of organic enrichment (Falter 2004; Eaton et al. 2005; Rosenberger et al. 2008). This is somehwat surprising given the overall mesotrophic classification of Coeur d'Alene Lake with a summer TP concentration of approximately <10 $\mu g \cdot L^{-1}$ in the pelagic water column (IDEQ unpublishede data). However, given the susbstrates were placed in bays and one would expect the influence of any trends in eutrophication to be first expressed near shore, the high AI values could be indicative of a eutrophying trend and should continue to be monitord in the future.

The high AI value may also be a suprious result due to the length of the sampling interval or the deposition of detritus. For example, in studies using the AI indicator for community analysis (Barbour et al. 1999; Rosenberger et al. 2008; Omar 2010) samples were collected over shorter periods, which could reduce the amount of decayed matter contained in the samples. As well, if the substrates were left entirely undisturbed for two weeks, it is possible significant amounts of material settling to the bottom of the lake could build up on them. This would be especially true for bays in which recreational activity and thus particulate resuspension are high. Another means by which non-photosynthetic material could be deposited on the substrates is through sloughing of nearby macrophytes. These confounding issues should be examined in a future study to optimize the deployment of artificial substrates in Coeur d'Alene Lake, which appears more involved than the deployments in Pend Oreille Lake.

Productivity parameters as predictors of substrate biomass

Model fit and variable suitability

The purpose of analyzing productivity parameters, including trends in nutrients, was to characterize the bay systems and obtain basic background information on each. Nutrient concentrations in the bays were highly complex and may depend on a number of in-bay factors, such as the influx of nutrients from the watershed, the emergence, senescence, spatial distribution, species composition and density of macrophytes, the timing and succession of phytoplankton species and other anthropogenic influences such as the resuspension of

benthic sediment by recreational activities. My data serves as a start to examine these complex relationships.

My attempt to use cumulative nutrient concentrations did not improve the predictive power of relationship of the periphyton biomass over time compared to discrete nutrient concentrations (Tables 2.12 and 2.13). Based on the lack of trends with time and the weak regressions of the variables with substrate biomass, the cumulative nutrient method may not be the optimal metric to determine the temporal and biological relationship between nutrients and periphyton.

Although some variables had significant linear relationships with substrate chlorophyll *a* (Figures 2.24 and 2.25), the low R^2 values (<30%; Tables 2.12 and 2.13) indicate that they are not suitable for use as predictors of substrate biomass. Improvements to the base model should be sought in variables unaccounted for in this study, such as sloughing, wave action, and community structure, or through further study into nutrient relationships and lag time in periphyton response to nutrient availability.

Effect of light on periphyton biomass

Limiting factors other than the availability of chemical nutrients could also affect the growth of periphyton. Epiphytic communities consist of auto- and heterotrophs which could result in the heterotrophic portion of the community limiting the availability of light to the autotrophs. This could explain the lack of a relationship between substrate chlorophyll *a* biomass and cumulative daylight hours (Tables 2.8 and 2.9).

Another reason that periphyton biomass did not correlate well with available light could have be related to the timing of the experiments. Although the duration of daily sunlight is longest on June 22nd each year, this was at the beginning of substrate deployment in bays and because of the 'newness' of the substrates immediately after deployment, not much biomass had accrued on them. Thus, the lack of a relationship is not an unreasonable outcome. If modeling periphyton growth including a variable for light is needed in the future, this confounding influence between substrate deployment and peak daylight hours should be investigated further and addressed. It should be noted that cumulative light was confounded in 2017 when smoke from intense wildfires in the Pacific Northwest disrupted my sampling frequency. It is possible that cumulative daylight may have been a better predictor in 2017 for the single or linear regression models had this disruption in sampling not occurred.

GIS analysis of watersheds

The large standard deviations relative to mean size for each of the human activity indicator variables indicate that the subbasins selected for study differed greatly with respect to the anthropogenic activity occurring in each. Although statistical analyses indicated non-zero slopes, the low coefficients of determination suggested none of the relationships was sufficient to function in a predictive capacity. Perhaps none of the variables selected adequately reflected increased land-use in the subwatershed, however, I based my selection on those referenced most commonly in the literature (Dodds et al. 2002; Lambert et al. 2008; IDEQ 2014). Other variables that could be important but were not included are erosion potential, road density, and the location and age of septic systems that would cause nutrient loading. Alternatively, it could point to non-terrestrial processes that occur within the bays and/or lake-bay interactions that influence nutrient availability or limit periphyton growth that overrides any influence from terrestrial sources.

Potential in-bay factors include differential bay retention times, boat wake recirculation of sediment-bound nutrients, or sediment/nutrient load interactions with macrophyte beds within bays. Preliminary research into in-bay dynamics, such as Hale (2018), suggest that physical processes like resuspension of sediments from the benthos occur at a sufficiently high magnitude to influence water column nutrient concentrations. In this scenario, differential inputs from the watershed could be masked by resuspension of existing sediments in the bay. Additionally, complex processes like retention the bay of materials delivered during the spring freshet by streams could influence the temporal, spatial, and chemical availability of nutrients to periphyton. Finally, the results of the AI calculations for this study indicate a potential for significant detrital accumulation on substrate surfaces. This Coeur d'Alene Periphyton Study used a much longer substrate deployment period than other studies of its kind (McCormick et al. 1996; Mattila and Raisanen 1998; Vadeboncoeur et al. 2001; Liboriussen and Jeppesen 2003; Lambert et al. 2008), which could have influenced the trends, or lack thereof, in periphyton biomass.

The non-significant regression models between indicator variables and maximum chlorophyll *a* biomass (Table 2.16) in all four SLR models (population density, dwelling density, percent forest clearing, and percent land use) indicate that none were adequate

predictors of maximum periphyton biomass in this study. However, because these variables have been shown in the literature to correlate strongly with periphyton biomass, this suggests that other external or in-bay processes are confounding the relationship between watershed nutrient loading and periphyton growth. Two explanations or a combination of both, account for the insignificant (at a high degree of confidence) relationship between biomass and watershed indicators. First, the dense macrophyte beds located throughout many of the study bays, often near the stream inflows could be acting like a nutrient sponge, masking variations in watershed inputs. Second, physical limnological processes such as differential nutrient and/or inflow retention times could alter the temporal availability of nutrients and sediments throughout the year. Related to both, the spatial distribution of sediment and/or nutrient load may influence how terrestrially-sourced nutrients are made available to periphyton in bays, particularly at the lake-proximate sampling locations used in this study.

Conclusion

Although this chapter examined multiple hypotheses regarding periphyton response, primary productivity predictor variables, and GIS watershed analysis, they all stem from the guiding hypothesis that periphyton response differs between bays with watersheds that have varying anthropogenic activity. It was surprising that no differences in periphyton accrual or final biomass were detected to a high degree of confidence in relation to watershed land use and suggests that for Coeur d'Alene Lake the use of periphyton substrates using this method is not an adequate tool to examine the effects of land use on nutrient accrual in the bays, unlike in Pend Oreille Lake (IDEQ 2014). An alternate study design that has a higher number of samples and more focus on key differences in in-bay processes may be able to discern differences between bays. Conversely, it could also suggest that the relationship between watershed land use and nutrient/macrophyte accrual in bays is complicated by other external or indirect in-bay factors as explained above. This is further supported by the fact that bays did not have different water column nutrient concentrations at the locations where sampling occurred. Watershed characteristics, particularly regarding indicators of human activity (e.g., population density), were evaluated to corroborate that bays did differed in anthropogenic activity as predicted. If this was not the case and watersheds had similar human activity characteristics, we would not expect periphyton response in bays to differ because the

watersheds themselves did not have different nutrient loading potential. However, watersheds varied based on all four factors analyzed, with percent forest clearing as the most related factor to periphyton maximum biomass.

I conclude that productivity parameters are not useful indicators of periphyton trends in Coeur d'Alene Lake, and that watersheds are characteristically different. The similar periphyton response in the bays indicated that the artificial substrate method as deployed in this study for monitoring periphyton is not suitable for Coeur d'Alene Lake because it was susceptible to a poor signal to noise ratio when measuring periphyton biomass over time. As such, I recommend that all of these potential confounding influences on this method's detection of periphyton response to nutrients need to be examined in detail to further evaluate this approach. Future application of this method to the system and others like it would need to better account for the influence of other in-bay factors like recreational boating, macrophytes, and sediment retention from stream inflows.

Literature Cited

Ané, C. 2017. Model selection. Univ. Wisconsin-Madison. Stat. 572 Stat. methods Biosci. II 1–53.

Ansari, A. A., S. S. Gill, and F. A. Khan. 2013. Eutrophication: Threat to aquatic ecosystems, p. 143–170. *In* A.A. Ansari, G.R. Lanza, S.S. Gill, and W. Rast [eds.], Eutrophication: Causes, Consequences, and Controls in Aquatic Ecosystems. Springer.

Barbour, M. T., J. Gerritsen, B. D. Snyder, and J. B. Stribling. 1999. Rapid bioassessment protocols for use in streams and wadeable rivers: periphyton, benthic macroinvertebrates and fish, Second Edition. US Environ. Prot. Agency Off. Water Washingt. DC 339. doi:EPA 841-B-99-002

Box, G. E. P., and D. R. Cox. 1964. An analysis of transformations (with discussion). J. R. Stat. Soc. B **26**: 211–252.

Canfield D.E. Jr. and Bachman R.W. 1981. Prediction of total phosphorus concentrations, chlorophyll *a*, and Secchi depths in natural and artificial lakes. Can J Fish Aquat. Sci. **38**:414–423.

Cattaneo, A. 1987. Periphyton in lakes of different trophy. Can. J. Fish. Aquat. Sci. **44**: 296–303.

Chislock, M. F., E. Doster, R. a. Zitomer, and A. E. Wilson. 2013. Eutrophication: Threat to aquatic ecosysstems, p. 143-170 *in* Eutrophication : Causes, consequences, and controls in aquatic ecosystems, A.A. Ansari, G.R. Lanza, S.S. Gill, and W. Rast [eds.]. Springer.

DeNicola, D. M., and M. Kelly. 2014. Role of periphyton in ecological assessment of lakes. Freshw. Sci. **33**: 619–638. doi:10.1086/676117

Dodds, W. K., V. H. Smith, and K. Lohman. 2002. Nitrogen and phosphorus relationships to benthic algal biomass in temperate streams. Can. J Fish. Aquat. Sci. **59**: 865-874. doi:10.1139/f02-063

Eaton, A. D., L. S. Clesceri, E. W. Rice, and M. A. Franson. 2005. Standard methods for the examination of water and wastewater. SM4500-P. American Public Health Association, 21st ed. American Public Health Association, American Water Works Association, Water Environment Federation.

Falter, C. M. 2004. Lake Pend Oreille littoral periphyton community: An updated trophic status assessment. Final report submitted to the Tri-State Water Quality Council.

Fox, J., and S. Weisberg. 2011. An R companion to applied regression. 2nd ed. Thousand Oaks, Sage xxii+ 495pp.

Goldman, C. R. 1988. Primary productivity, nutrients, and transparency during the early onset of eutrophication in ultra-oligotrophic Lake Tahoe, Califomia-Nevada. Limnol. Oceanogr. **33**: 1321–1333. doi:10.4319/lo.1988.33.6.1321

Hadwen, W. L., and S. E. Bunn. 2005. Food web responses to low-level nutrient and ^{15}N-tracer additions in the littoral zone of an oligotrophic dune lake. Limnol. Oceanogr. **50**: 1096–1105. doi:10.4319/lo.2005.50.4.1096

Hale, A., and F. W. Whilhelm. 2018. Waves of phosphorus: resuspension and release by recreational boating. Department of Fish and Wildlife Sciences. Senior thesis, University of Idaho, Moscow, ID, USA.

Havens, K. E., T. L. East, S.-J. Hwang, A. J. Rodusky, B. Sharfstein, and A. D. Steinman. 1999. Algal responses to experimental nutrient addition in the littoral community of a subtropical lake. Freshw. Biol. **42**: 329–344.

Hecky, R. E., and R. Hesslein. 1995. Contributions of benthic algae to lake food webs as revealed by stable isotope analysis JNAm. Benthol. Soc. **14**: 631–653.

IDEQ. 2014. Pend Oreille Lake productivity characterization. Idaho Dep. Environ. Qual. Rep.

IDEQ. 2018. Beneficial Uses. Idaho Department of Environmental Quality (DEQ). [Online] http://www.deq.idaho.gov/water-quality/surface-water/beneficial-uses/ (Accessed March 20, 2019).

Jacoby, J. M., D. D. Bouchard, and C. R. Patmont. 1991. Response of periphyton to nutrient enrichment in Lake Chelan, WA. Lake Reserv. Manag. **7**: 33–43. doi:10.1080/07438149109354252

Kann, J., and C. M. Falter. 1989. Periphyton as indicators of enrichment in Lake Pend Oreille, Idaho. Lake Reserv. Manag. **5**: 39–48. doi:10.1080/07438148909354397

Lambert, D., A. Cattaneo, and R. Carignan. 2008. Periphyton as an early indicator of perturbation in recreational lakes. Can. J. Fish. Aquat. Sci. **65**: 258–265. doi:10.1139/f07-168

Lavoie, I., S. Campeau, M. Grenier, and P. J. Dillon. 2006. A diatom-based index for the biological assessment of eastern Canadian rivers: An application of correspondence analysis (CA). Can. J. Fish. Aquat. Sci. **63**: 1793–1811. doi:10.1139/f06-084

Liboriussen, L., and E. Jeppesen. 2003. Temporal dynamics in epipelic, pelagic and epiphytic algal production in a clear and a turbid shallow lake. Freshw. Biol. **48**: 418–431. doi:10.1046/j.1365-2427.2003.01018.x

Loeb, S. L., J. E. Reuter, and C. R. Goldman. 1983. Littoral zone production of oligotrophic lakes, p. 161–167. *In* Periphyton of freshwater ecosystems. Springer Netherlands.

Mattila, J., and R. Raisanen. 1998. Periphyton growth as an indicator of eutrophication; an experimental approach. Hydrobiologia **377**: 15–23. doi:10.1023/A:1003265208397

McCormick, P. V, P. S. Rawlik, K. Lurding, E. P. Smith, and F. H. Sklar. 1996. Periphyton-water quality relationships along a nutrient gradient in the northern everglades. J. North Am. Benthol. Soc. **15**: 433–449.

MRLC. 2011. Multi-resolution land characteristics consortium (MRLC) National Land Cover Database 2011 (CONUS).

Omar, W. M. W. 2010. Perspectives on the use of algae as biological indicators for monitoring and protecting aquatic environments, with special reference to malaysian freshwater ecosystems. Trop. Life Sci. Res. **21**: 51–67.

Perrin, C., S. Bennett, and S. Linke. 2007. Bioassessment of streams in north-central British Columbia using the reference condition approach. Minist. Environ. **2a**: 135.

Phillips, N. D. 2018. YaRrr! The Pirate's Guide to R, BookDown.

Planas, D., M. Desrosiers, S.-R. Groulx, S. Paquet, and R. Carignan. 2000. Pelagic and benthic algal responses in eastern Canadian Boreal Shield lakes following harvesting and wildfires. Can. J Fish. Aquat. Sci. **57**: 136-145. doi:10.1139/f00-130

Potvin, C. 2001. ANOVA: Experimental layout and analysis, p. 63–76. *In* S.M. Scheiner and J. Gurevitch [eds.], Design and analysis of ecological experiments. Oxford University Press.

Rosenberger, E. E., S. E. Hampton, S. C. Fradkin, and B. P. Kennedy. 2008. Effects of shoreline development on the nearshore environment in large deep oligotrophic lakes. Freshw. Biol. **53**: 1673–1691. doi:10.1111/j.1365-2427.2008.01990.x

Sand-Jensen, K., and J. Borum. 1991. Interactions among phytoplankton, periphyton, and macrophytes in temperate freshwaters and estuaries. Aquat. Bot. **41**: 137–175. doi:10.1016/0304-3770(91)90042-4

Sartory, D. P., and J. U. Grobbelaar. 1984. Extraction of chlorophyll *a* from freshwater phytoplankton for spectrophotometric analysis. Hydrobiologia **114**: 177–187. doi:10.1007/BF00031869

Schindler, D. W., and J. R. Vallentyne. 2008. The Algal bowl: Overfertilization of the world's freshwaters and estuaries. University of Alberta Press.

Scofield, B., T. Harju, and D. Brandt. 2011. Lower Columbia River physical habitat and ecological productivity monitoring (Year 1-3): Study Period: 2008 - 2010. Clbmon#44 2008–2010.

U.S. Census Bureau. 2010. TIGER/Line® with selected demographic and economic data. Popul. Hous. Unit Counts -- Blocks Idaho.

USGS. 1999a. National elevation dataset for idaho (1 arc second | 30-meter). U.S. Geol. Surv. EROS Data Cent.

USGS. 1999b. National elevation dataset for Idaho (1/3 arc second | 10-meter). U.S. Geol. Surv. EROS Data Cent.

USGS. 2016. The StreamStats program for Idaho. U.S. Geol. Surv.

Vadeboncoeur, Y., S. P. Devlin, P. B. McIntyre, and M. J. Vander Zanden. 2014. Is there light after depth? Distribution of periphyton chlorophyll and productivity in lake littoral zones. Freshw. Sci. **33**:524–536 doi:10.1086/676315

Vadeboncoeur, Y., D. M. Lodge, and S. R. Carpenter. 2001. Whole-lake fertilization effects on distribution of primary production between benthic and pelagic habitats. Ecology **82**: 1065-1077. doi:10.2307/2679903

Vadeboncoeur, Y., G. Peterson, M. J. Vander Zanden, and J. Kalff. 2008. Benthic algal production across lake size gradients: Interactions among morphometry, nutrients, and light. Ecology **89**: 2542–2552. doi:10.1890/07-1058.1

Vadeboncoeur, Y., and M. E. Power. 2017. Attached algae: The cryptic base of inverted trophic pyramids in freshwaters. Ann. Rev. Ecol. Evol. Syst. **48**:255-279 doi:10.1146/annurev-ecolsys-121415

Venables, W. N., and B. D. Ripley. 2002. Modern applied atatistics with S. 4th ed. Springer.

Wetzel, R. G. 1983. Limnology, 2nd ed. Saunders College Publishing.

Woods, P. F., and M. A. Beckwith. 1997. Nutrient and trace-element enrichment of Coeur d'Alene Lake, Idaho. U.S. Geol. Surv. water-supply Pap. **2485** 1–93.

Zar, J. H. 1984. Biostatistical analysis. 2nd ed. Prentic-Hall, Inc.

Table 2.1: Estimated near-shore development and watershed loading in six northern bays of Coeur d'Alene Lake and their hypothesized effect on the lake (C. Cooper, Idaho Department of Environmental Protection, Coeur d'Alene Regional Office pers. comm.) bays.

Bay	Lake effect	Near-shore development	Watershed loading
Beauty	Mid	Low	Mid
Bennett	High	Mid	Mid
Blue	Mid	Mid	Mid
Kidd	Low	High	Mid
Neachen	Low	High	Mid
Wolf	High	Low	Mid

Table 2.2: Summary table of mean biomass ($mg \cdot m^{-2}$) represented by chlorophyll *a* for samples collected in 2017 for six northern bays of Coeur d'Alene Lake, Idaho.

	Date	6/29	7/6	7/13	7/19	7/27	8/2	8/9	8/16	8/24	8/31	9/13
Bay	Day	1	8	16	21	29	35	42	49	57	64	77
Beauty		0.44	1.85	6.59	10.81	9.91	11.42	13.88	23.49	23.07	22.99	23.65
Bennett		0.24	0.84	3.13	3.76	5.38	7.42	12.29	10.75	15.68	13.13	21.00
Blue Creek		0.65	3.25	5.97	5.08	10.34	14.18	20.74	19.98	17.62	16.75	18.93
Kidd Island		0.18	0.94	4.19	10.06	10.38	13.84	15.69	14.59	16.61	14.59	17.58
Neachen		0.51	2.04	8.10	12.57	11.54	14.04	15.53	19.08	21.10	22.78	24.42
Wolf Lodge		0.74	2.88	6.23	8.92	11.59	12.12	18.39	23.27	28.99	25.32	34.83

Table 2.3: Summary table of mean biomass ($mg \cdot m^{-2}$) represented by chlorophyll *a* for samples collected in 2018 for six northern bays of Coeur d'Alene Lake, Idaho.

	Date	6/14	6/28	7/12	7/26	8/10	8/23	9/6
Bay	Day	1	15	29	43	58	71	85
K_d		1.13	2.56	11.58	19.65	43.05	44.01	62.96
K_s		0.57	1.86	8.88	13.84	26.78	35.98	34.83
N_d		3.67	15.19	27.90	21.67	40.17	37.51	42.64
N_s		1.56	5.64	13.67	13.95	41.19	41.47	50.04

Table 2.4: Autotrophic index (AI) for six northern bays of Coeur d'Alene Lake, Idaho in Week 7 (August 9, 2017) based on ash-free dry mass (AFDM) and chlorophyll *a* biomass (chl *a*). Means and standard errors (SE) are presented.

Bay	AFDM		Mean chlorophyll *a* biomass		AI	
	$mg \cdot m^{-2}$	SE	$mg \cdot m^{-2}$	SE	mean	SE
Beauty	19,540	1,821	13.88	4.27	1,716	575.0
Bennett	14,860	5,526	12.29	2.59	1,356	578.2
Blue Creek	21,590	2,074	20.74	2.27	1,063	147.8
Kidd Island	26,960	8,960	15.69	4.68	2,384	1,140.0
Neachen	28,910	6,700	15.53	1.64	1,956	577.1
Wolf Lodge	23,160	3,048	18.39	2.26	1,261	69.78

Table 2.5: Autotrophic index (AI) for six northern bays of Coeur d'Alene Lake, Idaho in Week 7 (September 21, 2017) based on ash-free dry mass (AFDM) and chlorophyll *a* biomass (chl *a*). Means and standard errors (SE) are presented.

	AFDM		Chl *a* biomass		AI	
Bay	$mg \cdot m^{-2}$	SE	$mg \cdot m^{-2}$	SE	mean	SE
Beauty	27,400	1,778	23.65	2.32	1,175	102
Bennett	19,670	6,040	21.00	4.88	1,031	420
Blue Creek	26,730	2,173	18.93	2.14	1,441	181
Kidd Island	33,070	5,134	17.58	1.93	1,990	497
Neachen	34,430	8,556	24.42	4.88	1,439	231
Wolf Lodge	32,900	7,184	34.83	4.62	924	79

Table 2.6: Summary statistics for the 2017 productivity parameters dataset. Variables include orthophosphorus (OP), cumulative OP (OPC), total phosphorus (TP), cumulative TP (TPC), cumulative daylight hours (HrC), water column chlorophyll *a* (WC Chla), and substrate chlorophyll *a* (S Chla). Minimum and maximum nutrient and S Chla values represent single samples, not bay averages. The 25th and 75th quantiles are indicated as Q25 and Q75. Nutrient concentrations marked with an asterisk indicate values flagged as below the reporting limit (RL). The RL of 2.47 $\mu g \cdot L^{-1}$ was substituted in their place.

Variable	OP	OPC	TP	TPC	HrC	W Chla	S Chla
Units	$\mu g \cdot L^{-1}$	$\mu g \cdot L^{-1}$	$\mu g \cdot L^{-1}$	$\mu g \cdot L^{-1}$	Hr.	$\mu g \cdot L^{-1}$	$mg \cdot m^{-2}$
N	90	90	90	90	99	78	99
Mean	5.44	40.07	7.06	50.05	14.83	0.64	12.32
SD	2.88	21.22	3.68	28.23	0.95	0.16	8.49
SE	0.30	2.24	0.39	2.98	0.10	0.02	0.85
Min	2.47*	2.47*	2.47*	2.47*	13.00	0.34	0.16
Q25	3.52	26.78	4.71	30.00	14.00	0.50	5.30
Q75	7.40	51.33	8.82	70.00	15.7	0.73	18.69
Max	14.00	98.00	15.88	122.35	16.00	1.17	37.05

Table 2.7: Summary statistics for the 2018 productivity parameters dataset. Variables include orthophosphorus (OP), cumulative OP (OPC), total phosphorus (TP), cumulative TP (TPC), cumulative daylight hours (HrC), water column chlorophyll *a* (WC Chla), and substrate chlorophyll *a* (S Chla). S Chla.d and S Chla.s represent deep and shallow substrates. The 25th and 75th quantiles are indicated as Q25 and Q75. Nutrient concentrations marked with an asterisk indicate values flagged as below the reporting limit (RL). The RL of 2.47 $\mu g \cdot L^{-1}$ was substituted in their place.

Variable	OP	OPC	TP	TPC	HrC	S Chla.d	S Chla.s
Units	$\mu g \cdot L^{-1}$	$\mu g \cdot L^{-1}$	$\mu g \cdot L^{-1}$	$\mu g \cdot L^{-1}$	Hr.	$\mu g \cdot L^{-1}$	$mg \cdot m^{-2}$
N	41	41	41	41	41	41	41
Mean	4.53	57.74	5.82	73.32	15.24	24.68	20.72
SD	1.42	15.21	2.19	22.41	1.12	18.04	19.42
SE	0.22	2.38	0.34	3.50	0.65	2.82	3.03
Min	2.47*	30.33	3.15	44.07	13.00	0.97	0.51
Q25	3.56	48.22	4.07	55.37	14.20	11.11	3.45
Q75	5.48	70.00	7.22	86.67	16.0	36.88	37.92
Max	9.00	87.11	11.76	123.53	17.0	69.73	71.84

Table 2.8: Summary statistics for the linear regressions of potential productivity variables over time for 2017. All estimates are in $\mu g \cdot L^{-1}$ except daylight hours. All intercept p-values were <0.001. Variables include orthophosphorus (OP), cumulative OP (OPC), total phosphorus (TP), cumulative TP (TPC), cumulative daylight hours (HrC), and water column chlorophyll a (WC Chla).

Parameter	OP	OPC	TP	TPC	HrC	WC Chla
Intercept	8.42	56.24	8.58	62.25	16.30	0.60
Slope	-0.08	-0.42	-0.05	-0.38	-0.04	0.001
(p-value)	<0.001	<0.001	0.01	0.01	<0.001	0.11
Multiple R^2	0.39	0.21	0.07	0.07	0.98	0.03
Adjusted R^2	0.39	0.20	0.06	0.06	0.98	0.02

Table 2.9: 2018 summary statistics for the linear regressions of potential productivity variables over time for 2018. All estimates are in $\mu g \cdot L^{-1}$ except daylight hours. All intercept p-values were <0.001. Variables include orthophosphorus (OP), cumulative OP (OPC), total phosphorus (TP), cumulative TP (TPC), and cumulative daylight hours (HrC).

Parameter	OP	OPC	TP	TPC	HrC
Intercept	5.83	62.86	7.64	16.92	16.96
Slope	-0.03	-0.12	-0.04	-0.19	-0.04
(p-value)	<0.001	0.16	<0.001	0.14	<0.001
Multiple R^2	0.37	0.05	0.30	0.06	0.97
Adjusted R^2	0.35	0.03	0.29	0.03	0.97

Table 2.10: 2017 summary statistics for the linear regressions of substrate chlorophyll *a* as a function of each potential productivity variable. All estimates are in $\mu g \cdot L^{-1}$ except daylight hours. All intercept p-values were <0.001. Variables include orthophosphorus (OP), cumulative OP (OPC), total phosphorus (TP), cumulative TP (TPC), cumulative daylight hours (HrC), and water column chlorophyll a (WC Chla).

Parameter	OP	OPC	TP	TPC	HrC	WC Chla
Intercept	22.14	21.28	14.80	15.19	118.2	8.05
Slope	-1.67	-0.21	-0.48	-0.08	-7.14	6.65
(p-value)	<0.001	<0.001	0.04	0.01	<0.001	0.32
Multiple R^2	0.32	0.26	0.05	0.07	0.63	0.01
Adjusted R^2	0.31	0.25	0.03	0.06	0.63	<0.001

Table 2.11: 2018 summary statistics for the linear regressions of substrate chlorophyll *a* as a function of each potential productivity variable. All estimates are in $\mu g \cdot L^{-1}$ except daylight hours. All intercept p-values were <0.001. Variables include orthophosphorus (OP), cumulative OP (OPC), total phosphorus (TP), cumulative TP (TPC), and cumulative daylight hours (HrC).

Parameter	OP	OPC	TP	TPC	HrC
Intercept	58.62	43.02	40.81	25.08	255.2
Slope	-7.49	-0.32	-2.77	-0.01	-15.0
(p-value)	<0.001	0.09	0.03	0.97	<0.001
Multiple R^2	0.35	0.07	0.11	<0.001	0.58
Adjusted R^2	0.33	0.05	0.09	<0.001	0.57

Table 2.12: 2017 Summaries for the three-variable models of substrate chlorophyll *a* as a function of time with Day of Study and Bay as β_1 and β_2. The column gives the model fit of the third model parameter. All estimates are in $\mu g \cdot L^{-1}$ except daylight hours. All slope p-values were <0.001. Variables include orthophosphorus (OP), cumulative OP (OPC), total phosphorus (TP), cumulative TP (TPC), cumulative daylight hours (HrC), and water column chlorophyll *a* (WC Chla).

Parameter	Base	OP	OPC	TP	TPC	HrC	WC Chla
Multiple R^2	0.72	0.72	0.73	0.73	0.73	0.73	0.77
Adjusted R^2	0.70	0.70	0.71	0.71	0.71	0.71	0.75
AIC	593.93	542.99	539.26	533.54	532.75	591.88	468.99

Table 2.13: 2018 Summaries for the three-variable models of substrate chlorophyll *a* over time with Day of Study and Bay as β_1 and β_2. The column gives the model fit of the third model parameter. All estimates are in $\mu g \cdot L^{-1}$ except daylight hours. All intercept p-values were <0.001. Variables include orthophosphorus (OP), cumulative OP (OPC), total phosphorus (TP), cumulative TP (TPC), and cumulative daylight hours (HrC).

Parameter	Base	OP	OPC	TP	TPC	HrC
Multiple R^2	0.67	0.69	0.68	0.69	0.70	0.60
Adjusted R^2	0.66	0.66	0.66	0.66	0.68	0.57
AIC	314.60	314.36	315.24	314.44	312.13	349.29
ANOVA (p-value)	-	0.16	0.27	0.17	0.05	0.83

Table 2.14: Watershed variables per type of anthropogenic activity as reported by GIS analysis.

Bay	Population density (Population·km^{-2})	Dwelling density (Housing units·km^{-2})	Forest clearing (%)	Other land use (%)
Beauty	0.36	0.47	4.07	0.72
Bennett	24.16	10.78	35.54	16.55
Blue	4.44	2.14	28.32	1.36
Kidd	9.40	5.71	37.27	4.26
Neachen	3.63	4.31	19.67	3.66
Wolf	0.82	0.44	11.09	1.51

Table 2.15: Rank order for bays according to magnitude of anthropogenic activity variable. Rank values are on a scale of 1 to 6, with 1 indicating that the bay scored lowest for that variable and 6 being the highest. For example, Beauty Bay has the lowest population density (1) and Bennett Bay has the highest population density (6). Sum equals the total number of rank points for each bay, and percent is the ratio of points earned to total points available (84).

	Beauty	Bennett	Blue	Kidd	Neachen	Wolf
Population density	1	6	4	5	3	2
Dwelling density	2	6	3	5	4	1
% Forest clearing	1	5	4	6	3	2
% Other	1	6	2	5	4	3
Sum	5	23	13	21	14	8
Percent	6%	27%	15%	25%	17%	10%

Table 2.16: Summary statistics for the single linear regression models of maximum chlorophyll *a* biomass by each anthropogenic activity indicator.

	Population density	Dwelling density	Forest clearing	Other land use
Intercept	25.52	26.33	30.48	24.69
(p-value)	0.002	0.002	0.002	0.002
Slope	-0.30	-0.76	-0.31	-0.27
(p-value)	0.39	0.34	0.14	0.61
Multiple R^2	0.19	0.23	0.46	0.07
Adjusted R^2	-0.02	0.03	0.32	-0.16

Table 2.17: Model parameters and summary statistics for top-competing models of maximum chlorophyll *a* biomass predicted by anthropogenic activity characteristics. Variable abbreviations are β_p for population density, β_h for housing unit density, β_c for percent other land use, and β_o for percent forest clearing. ANOVA values are p-values for the two-way ANOVA comparing that model to the single-factor percent forest clearing model (Factor level 1).

Factor level	Variables	Multiple R^2	Adjusted R^2	AIC	ANOVA
1	β_c	0.4071	0.3700	120.41	-
2	$\beta_p + \beta_o$	0.4512	0.3781	121.01	0.29
3	$\beta_p + \beta_h + \beta_o$	0.5278	0.4266	120.31	0.20
4	$\beta_p + \beta_h + \beta_o + \beta_c$	0.5698	0.4375	120.63	0.23

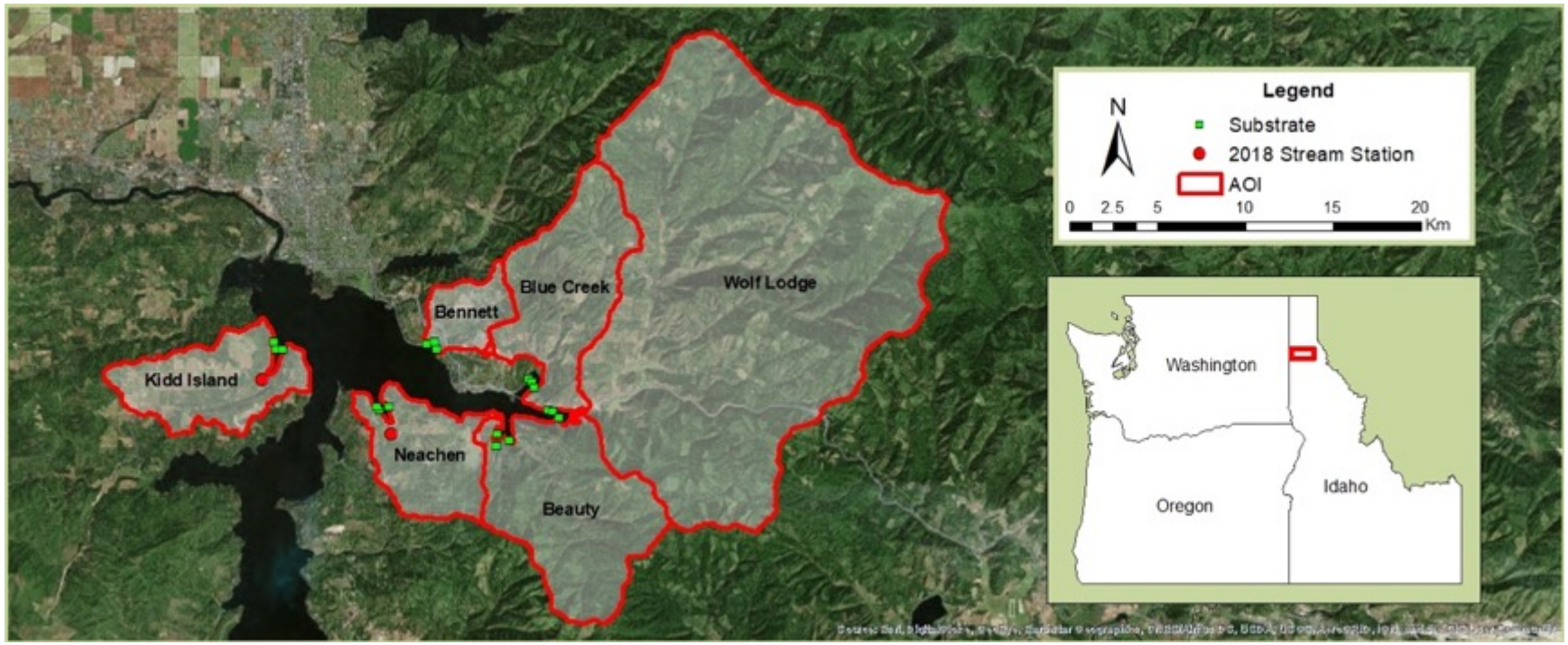

Figure 2.1: Site map of the six north-end bays and corresponding subwatersheds studied in 2017 and 2018 for the Coeur d'Alene Lake Periphyton Study. Subcatchments are delineated by the area of interest (AOI) markings and green squares indicate the locations of the three substrates deployed at 4 m in each bay during both years. In 2018, three additional 1.8 m substrates were installed in close proximity to the three 4 m substrates. Two stream sites were used in 2018 for stream nutrient load calculations and are marked by red circles in Kidd Island and Neachen bays.

Figure 2.2: Site map of Beauty Bay, Coeur d'Alene Lake, ID. Yellow flag icons mark the locations of substrates placed at 4 m in 2017 and 2018. One substrate at 1.8 m was placed in close proximity to each yellow flag in 2018, totaling six substrates per bay. The region of suitable placement locations for the 4 m substrates is indicated by the 10 and 15 ft. bathymetry contour lines.

Figure 2.3: Site map of Bennett Bay, Coeur d'Alene Lake, ID. Yellow flag icons mark the locations of substrates placed at 4 m in 2017 and 2018. One substrate at 1.8 m was placed in close proximity to each yellow flag in 2018, totaling six substrates per bay. The region of suitable placement locations for the 4 m substrates is indicated by the 10 and 15 ft. bathymetry contour lines.

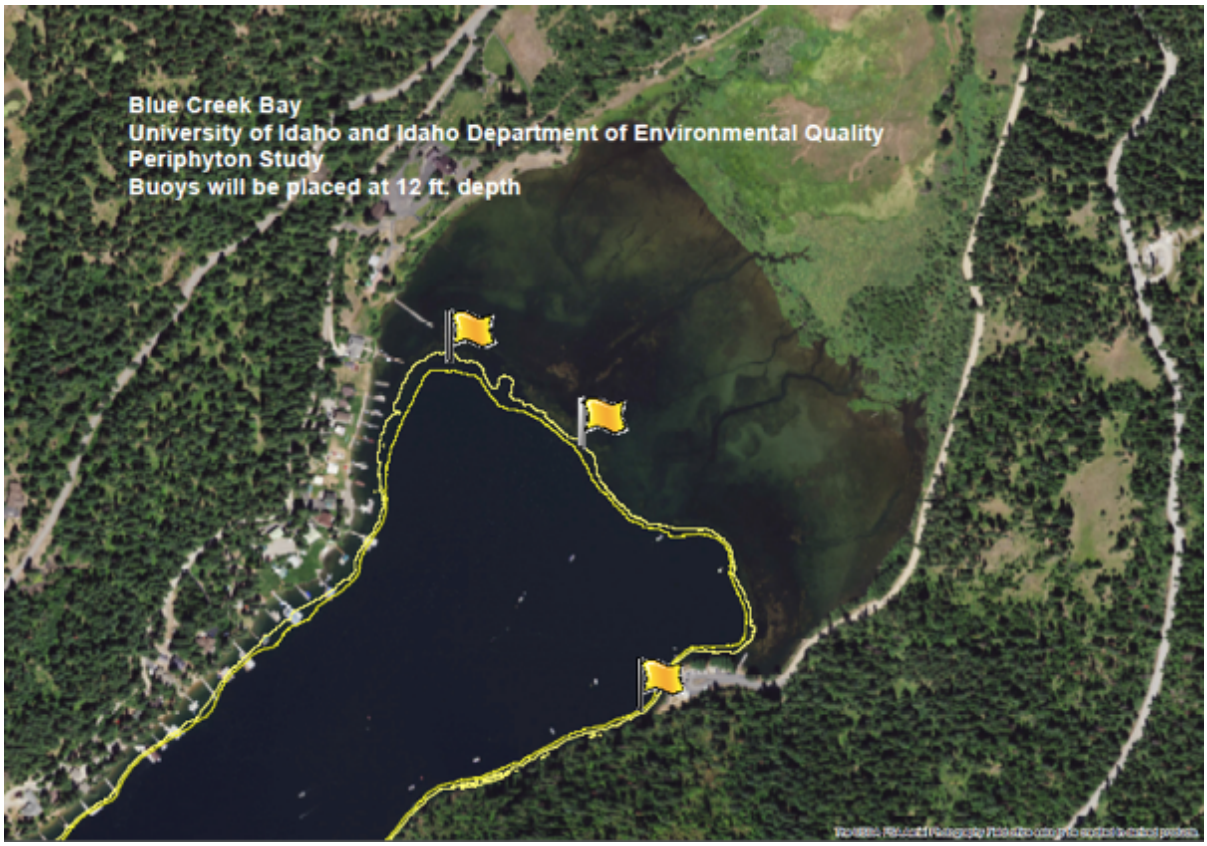

Figure 2.4: Site map of Blue Creek Bay, Coeur d'Alene Lake, ID. Yellow flag icons mark the locations of substrates placed at 4 m in 2017 and 2018. One substrate at 1.8 m was placed in close proximity to each yellow flag in 2018, totaling six substrates per bay. The region of suitable placement locations for the 4 m substrates is indicated by the 10 and 15 ft. bathymetry contour lines.

Figure 2.5: Site map of Kidd Island Bay, Coeur d'Alene Lake, ID. Yellow flag icons mark the locations of substrates placed at 4 m in 2017 and 2018. One substrate at 1.8 m was placed in close proximity to each yellow flag in 2018, totaling six substrates per bay. The region of suitable placement locations for the 4 m substrates is indicated by the 10 and 15 ft. bathymetry contour lines.

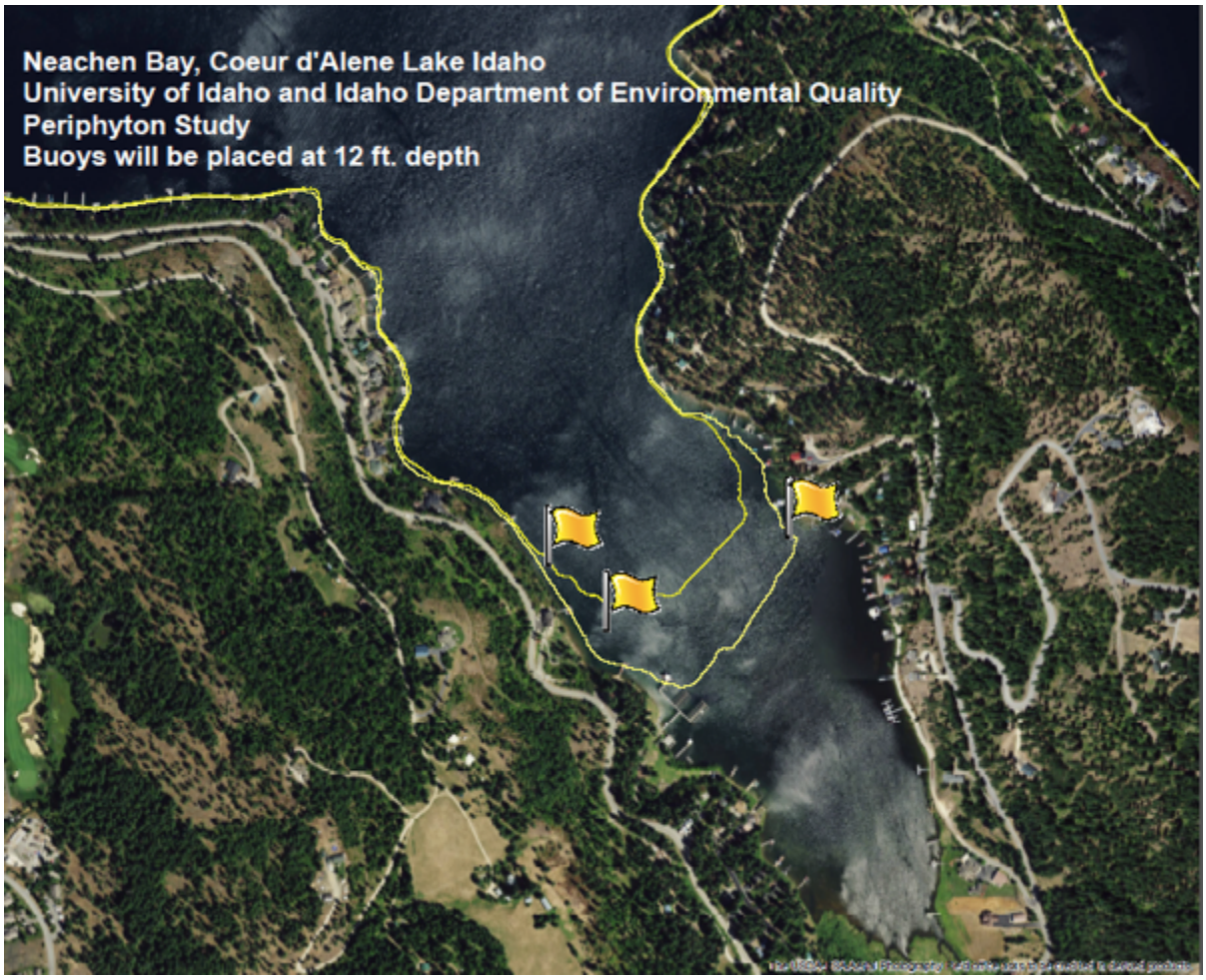

Figure 2.6: Site map of Neachen Bay, Coeur d'Alene Lake, ID. Yellow flag icons mark the locations of substrates placed at 4 m in 2017 and 2018. One substrate at 1.8 m was placed in close proximity to each yellow flag in 2018, totaling six substrates per bay. The region of suitable placement locations for the 4 m substrates is indicated by the 10 and 15 ft. bathymetry contour lines.

Figure 2.7: Site map of Wolf Lodge Bay, Coeur d'Alene Lake, ID. Yellow flag icons mark the locations of substrates placed at 4 m in 2017 and 2018. One substrate at 1.8 m was placed in close proximity to each yellow flag in 2018, totaling six substrates per bay. The region of suitable placement locations for the 4 m substrates is indicated by the 10 and 15 ft. bathymetry contour lines.

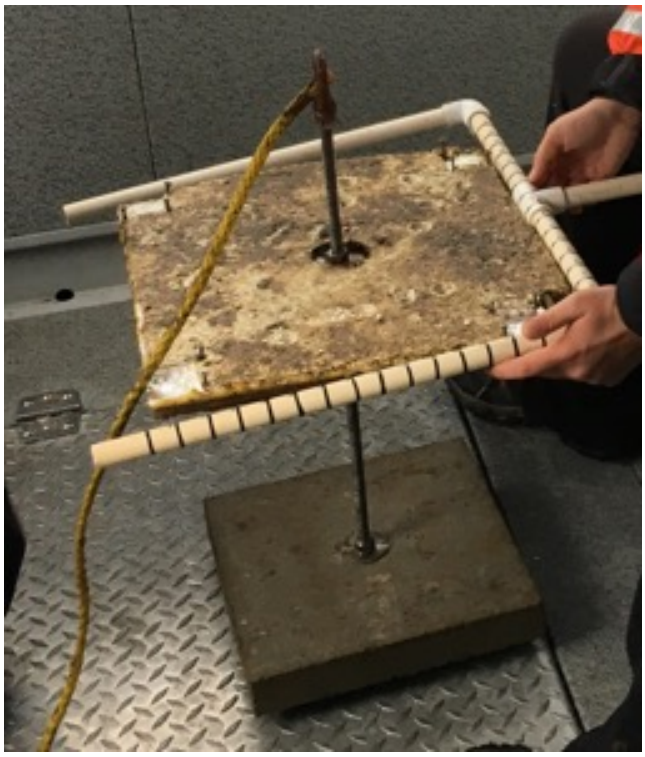

Figure 2.8: Artificial substrate apparatus photo taken on the last day of the 2017 study period (Day 77; September 13, 2017).

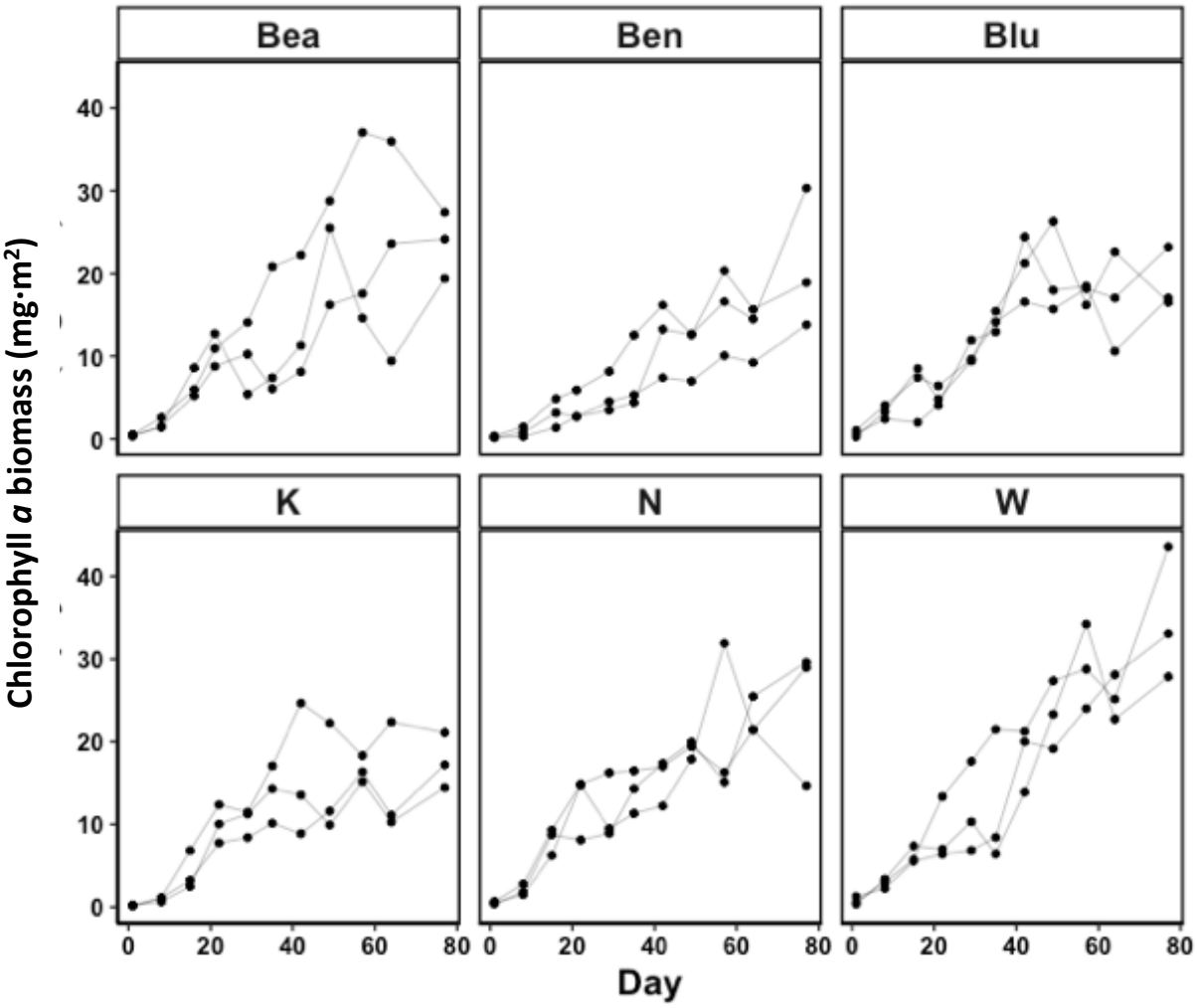

Figure 2.9: Periphyton biomass accrual over the 2017 growing season. Day 1 was on June 29, 2017, two weeks after substrate installation in the lake. Final samples were collected on September 13, 2017 (Day 77). Each frame of the figure displays biomass as a function of time for each substrate within a bay. Biomass (represented by chlorophyll *a* concentration) increased linearly from approx. 0 mg m^{-2} and reached its maximum biomass between 20 and 50 mg m^{-2} with increasing variation between substrates over time.

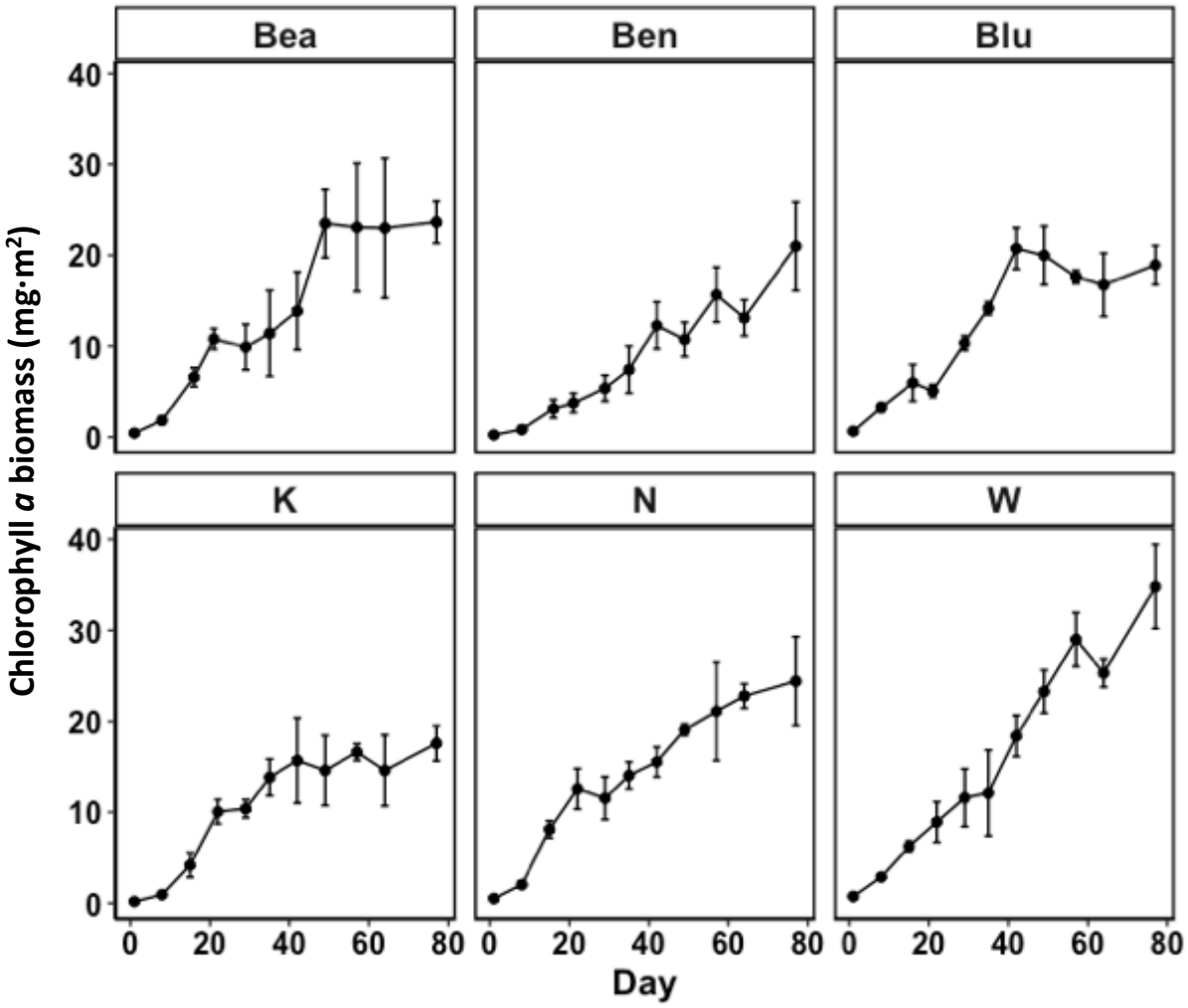

Figure 2.10: Mean periphyton biomass accrual over the 2017 growing season. Means include three substrates sampled within the bay at each sampling event. See Figure 2.9 (caption) for more details.

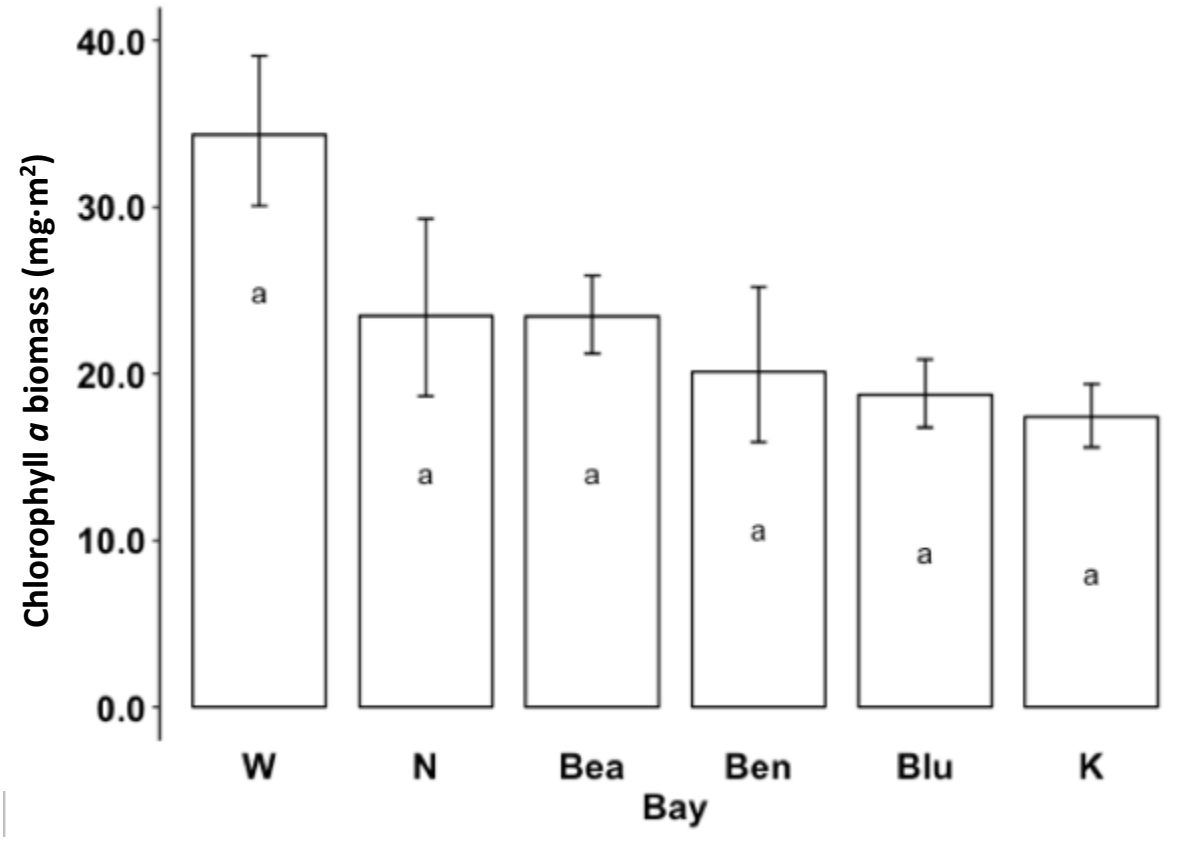

Figure 2.11: Maximum biomass ANOVA for bays sampled in 2017. All bays reached their highest mean biomass in Week 11 (Sept. 13, 2017; Day 77). Because back-transformed data after statistical analysis are shown here, error bars are uneven. Similar means are indicated by similar letters inside the bars.

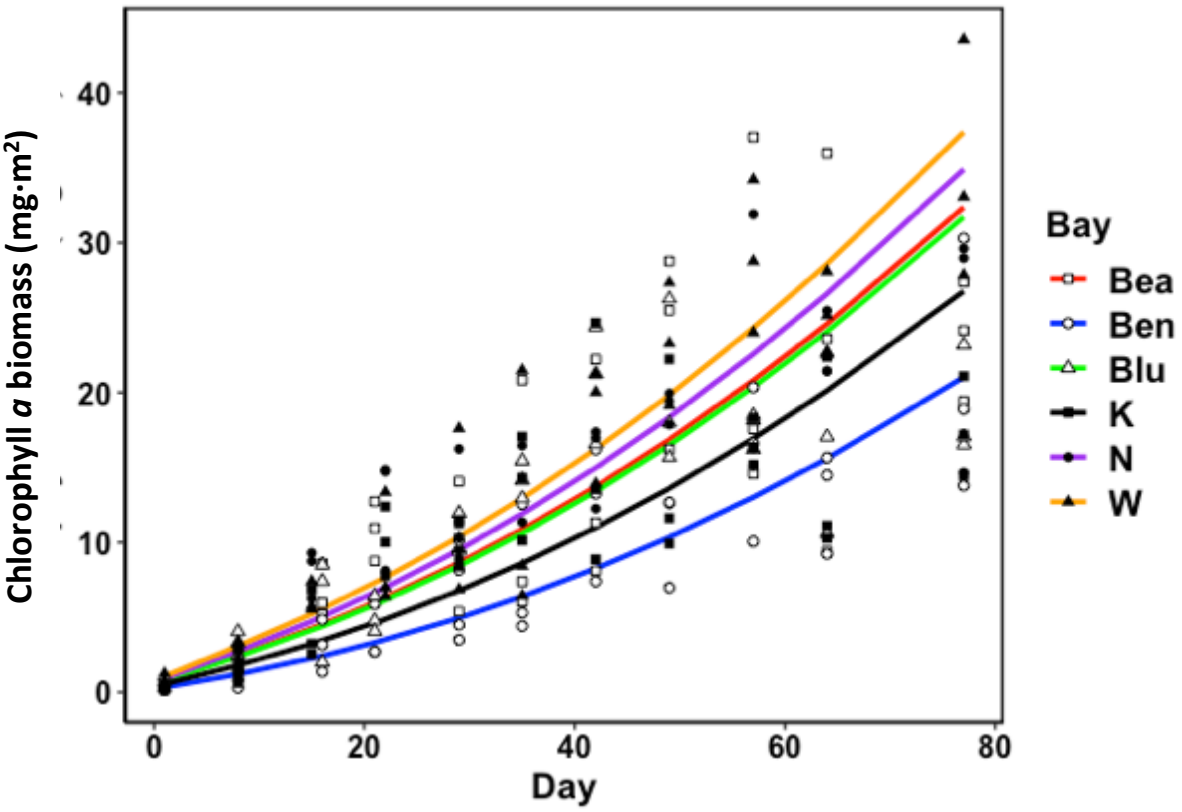

Figure 2.12: 2017 slope analysis using ANCOVA. Chlorophyll *a* as a function of day of experiment (Day 1 was June 14, 2018). Lines specified by the transformed data are plotted on normal axes for ease of interpretation.

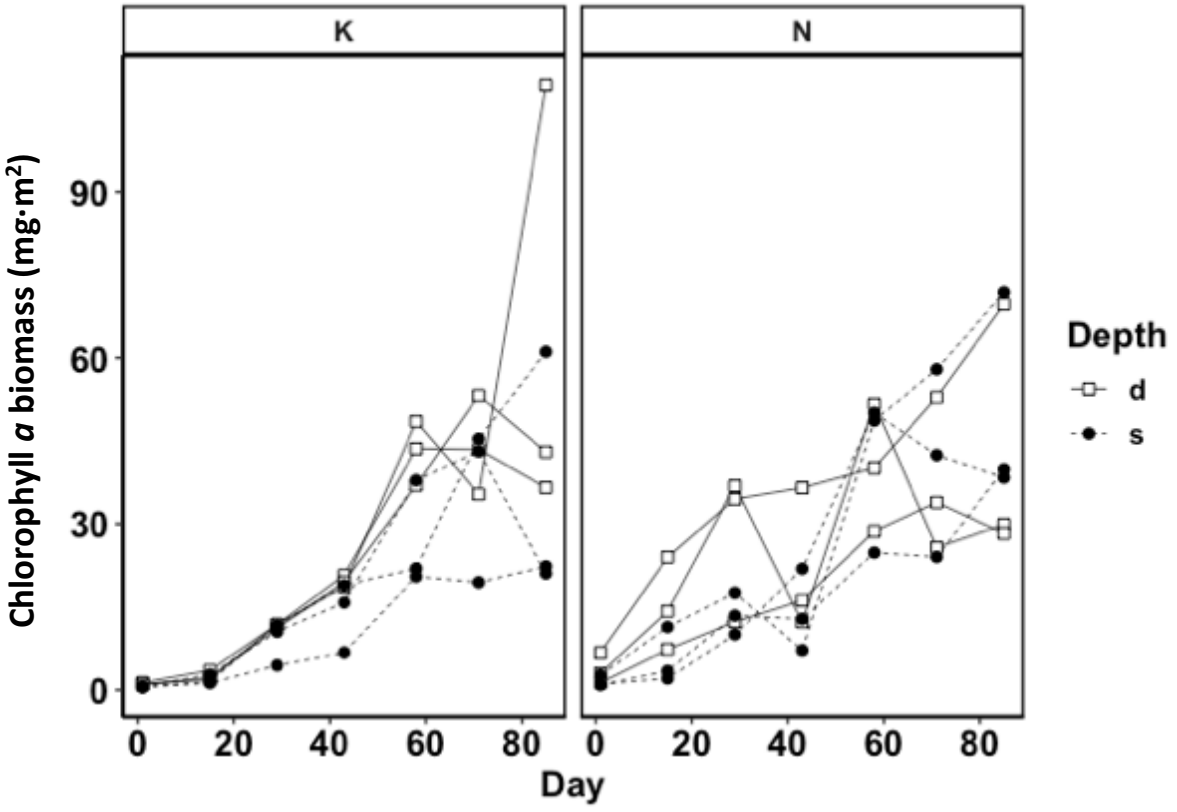

Figure 2.13: 2018 periphyton biomass accrual during 2018 in Kidd (K) and Neachen (N) bays in Coeur d'Alene Lake, Idaho. Day 1 occurred on June 16, 2018, two weeks after substrate installation in the lake. Final samples were collected on September 9, 2018 (Day 85). Each fame contains periphyton biomass (represented by chlorophyll *a* concentration) as a function of time at depths of 1.8 m (s; shallow) or 4 m (d; deep).

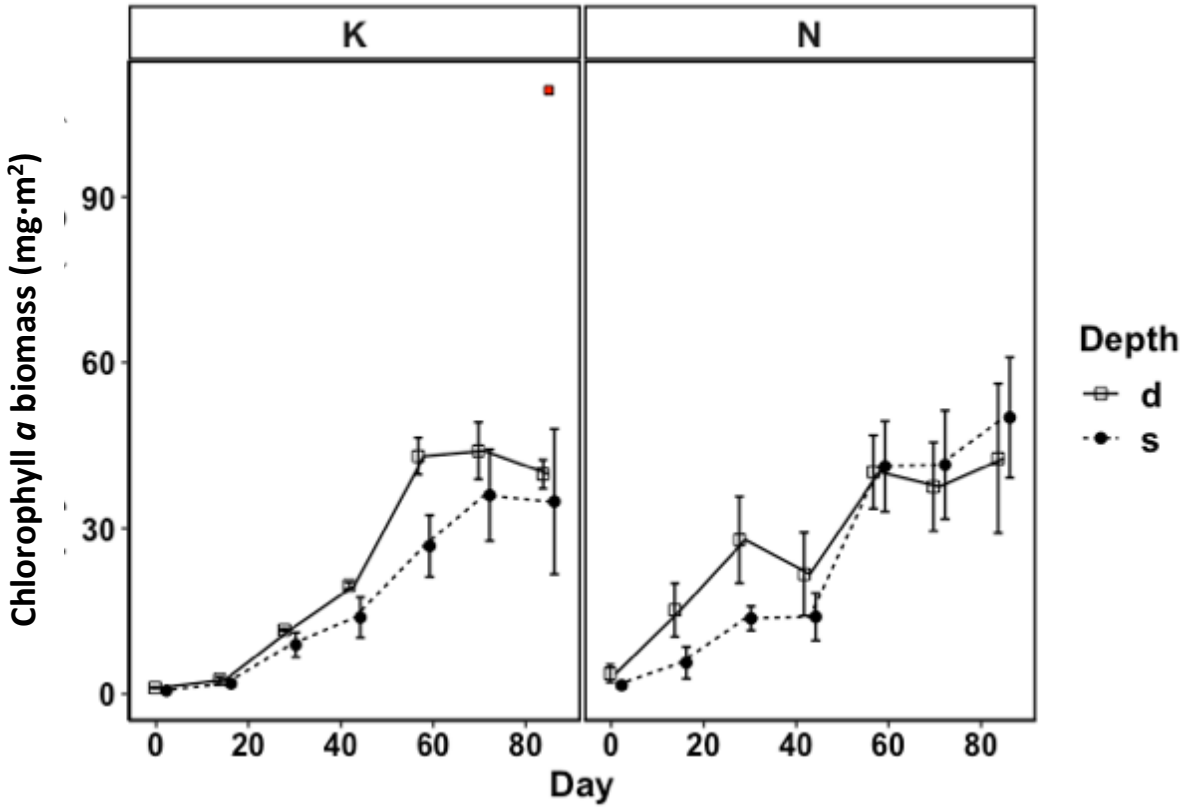

Figure 2.14: 2018 periphyton mean biomass accrual during 2018 in Kidd (K) and Neachen (N) bays in Coeur d'Alene Lake, Idaho. Day 1 occurred on June 16, 2018, two weeks after substrate installation in the lake. Final samples were collected on September 9, 2018 (Day 85). Each fame contains periphyton biomass (represented by chlorophyll *a* concentration) as a function of time at depths of 1.8 m (s; shallow) or 4 m (d; deep). One outlier (K_{d3} on Day 85) was removed (marked in red). Point positions are adjusted ±5 days to remove overlap for visual clarity but all analyses were run on the non-adjusted data points.

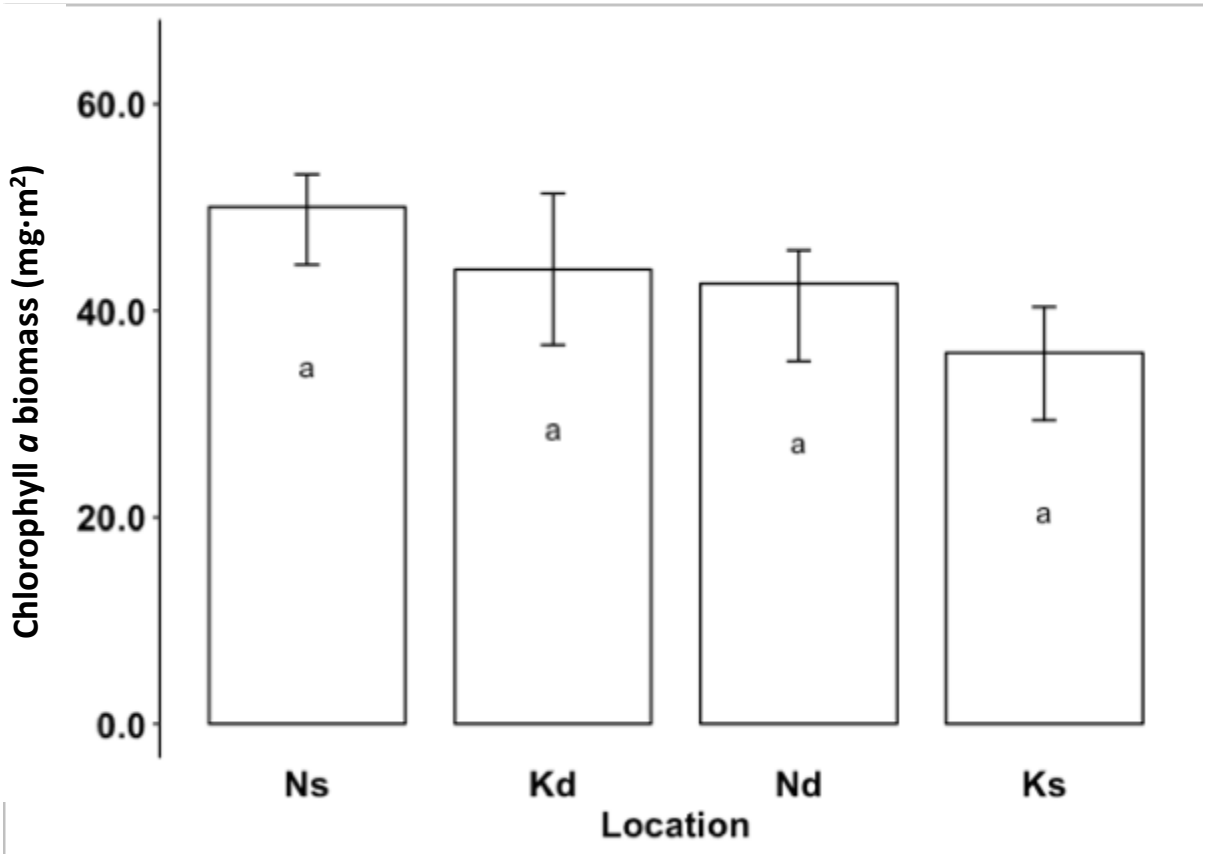

Figure 2.15: Comparison of maximum periphyton biomass from substrates on Day 71 for Kidd Island (K) and Day 85 for Neachen (N) bays in Coeur d'Alene Lake in 2018. Lower case s and d refer to shallow (1.8 m) and deep (4) m depth locations of substrates in each bay, respectively. Bars with similar letters indicate similar means (ANOVA) and error bars represent ±standard error. Note analyses were completed on transformed data to meet assumptions of analysis but I present back-transformed data for ease of interpretation which is the reason for the unequal error bars.

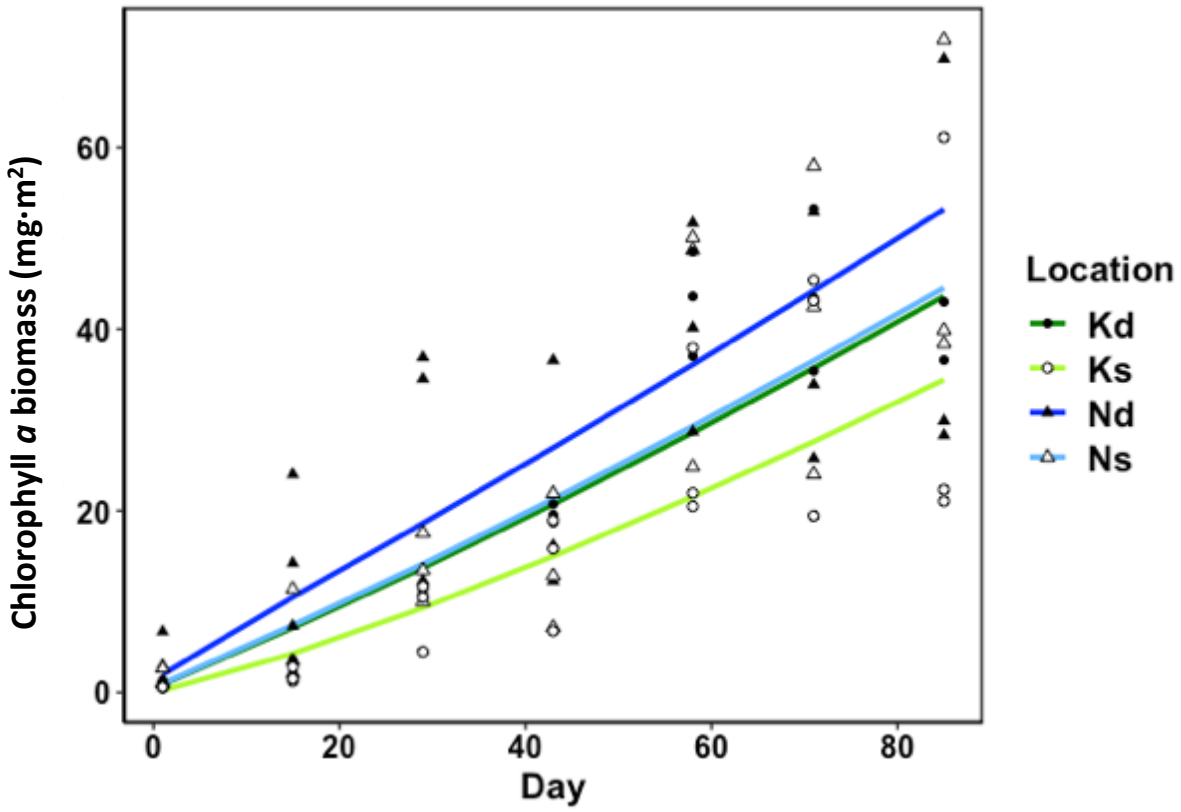

Figure 2.16: Chlorophyll *a* as a function of day of experiment (Day 1 was June 14, 2018). Lines specified by the transformed data are plotted on normal axes for ease of interpretation.

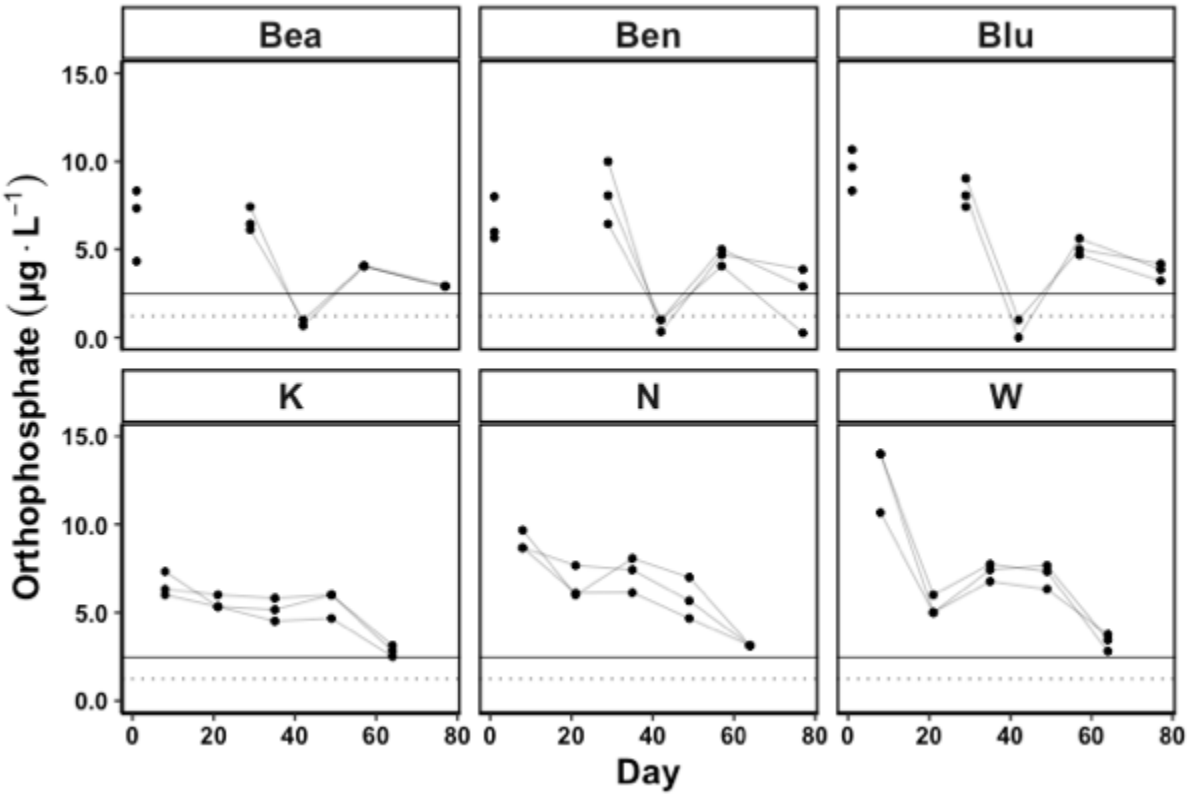

Figure 2.17: Orthophosphorus concentrations of water samples from the six bays sampled in 2017 as a function of day of experiment. Abbreviations for bays are as follows: Beauty (Bea), Bennett (Ben), Blue Creek (Blu), Kidd Island (K), Neachen (N), and Wolf Lodge (W) bays. Line represents water samples taken at one of three substrate locations in each bay. The solid horizontal line is the method reporting limit of 2.47 $\mu g \cdot L^{-1}$ and the dotted line is the method detection limit of 1.23 $\mu g \cdot L^{-1}$. Samples below the reporting limit are shown here but were not included in statistical analyses.

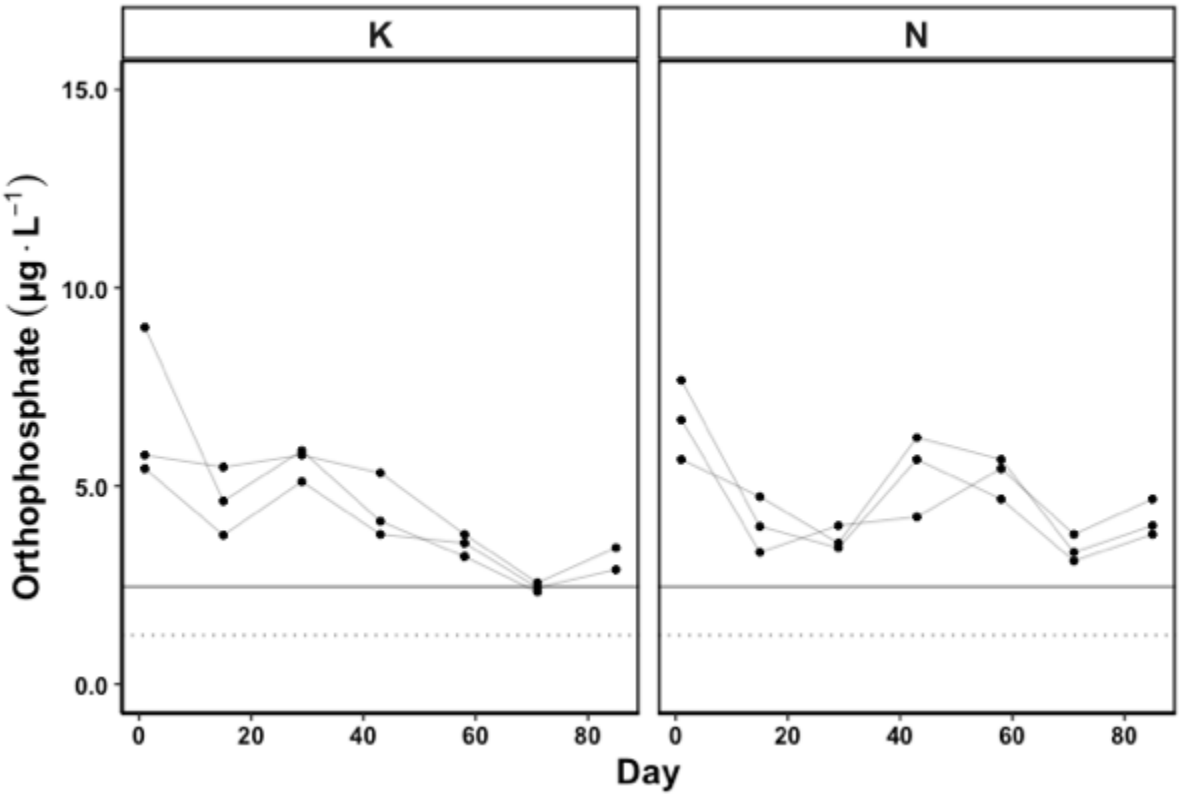

Figure 2.18: Orthophosphorus concentrations of water samples from the six bays sampled in 2018 as a function of day of experiment. Abbreviations for bays are as follows: Kidd Island (K), Neachen (N) bays. Line represents water samples taken at one of three substrate locations in each bay. The solid horizontal line is the method reporting limit of 2.47 $\mu g \cdot L^{-1}$ and the dotted line is the method detection limit of 1.23 $\mu g \cdot L^{-1}$. Samples below the reporting limit are shown here but were not included in statistical analyses.

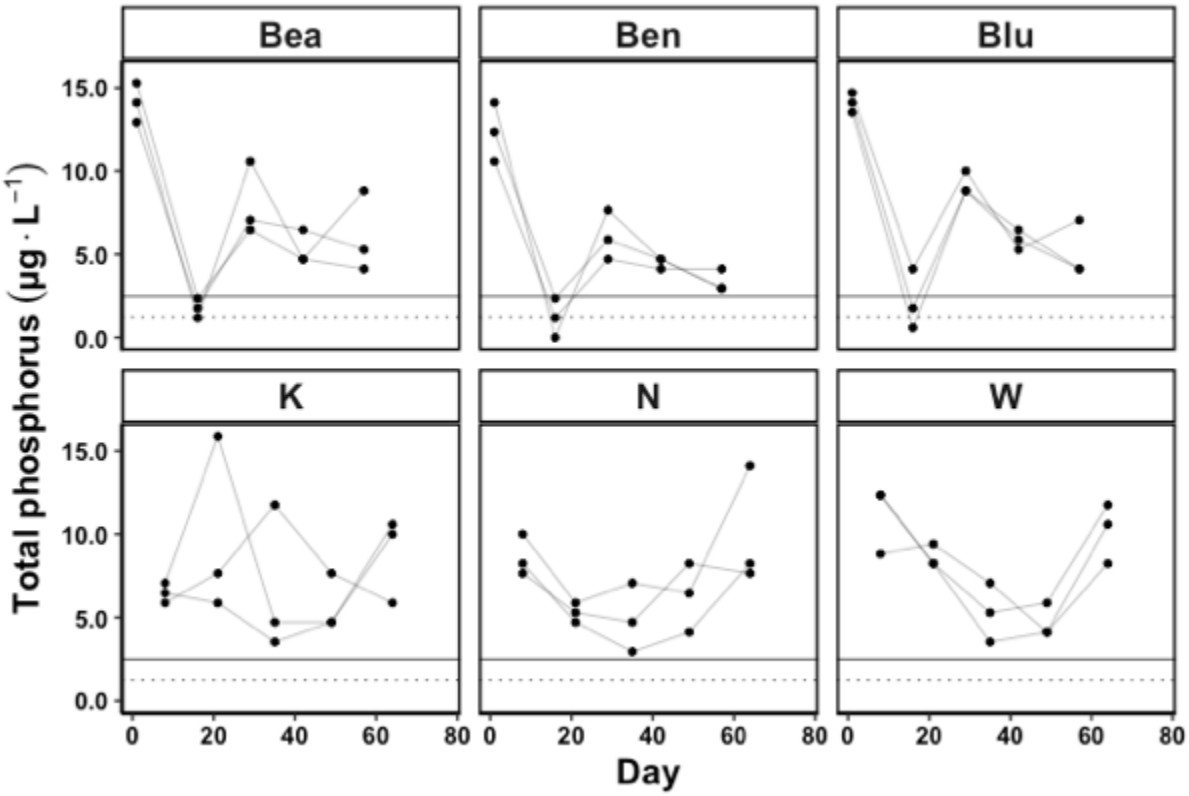

Figure 2.19: Total phosphorus concentrations of water samples from the six bays sampled in 2017 as a function of day of experiment. Abbreviations for bays are as follows: Beauty (Bea), Bennett (Ben), Blue Creek (Blu), Kidd Island (K), Neachen (N), and Wolf Lodge (W) bays. Line represents water samples taken at one of three substrate locations in each bay. The solid horizontal line is the method reporting limit of 2.47 $\mu g \cdot L^{-1}$ and the dotted line is the method detection limit of 1.23 $\mu g \cdot L^{-1}$. Samples below the reporting limit are shown here but were not included in statistical analyses.

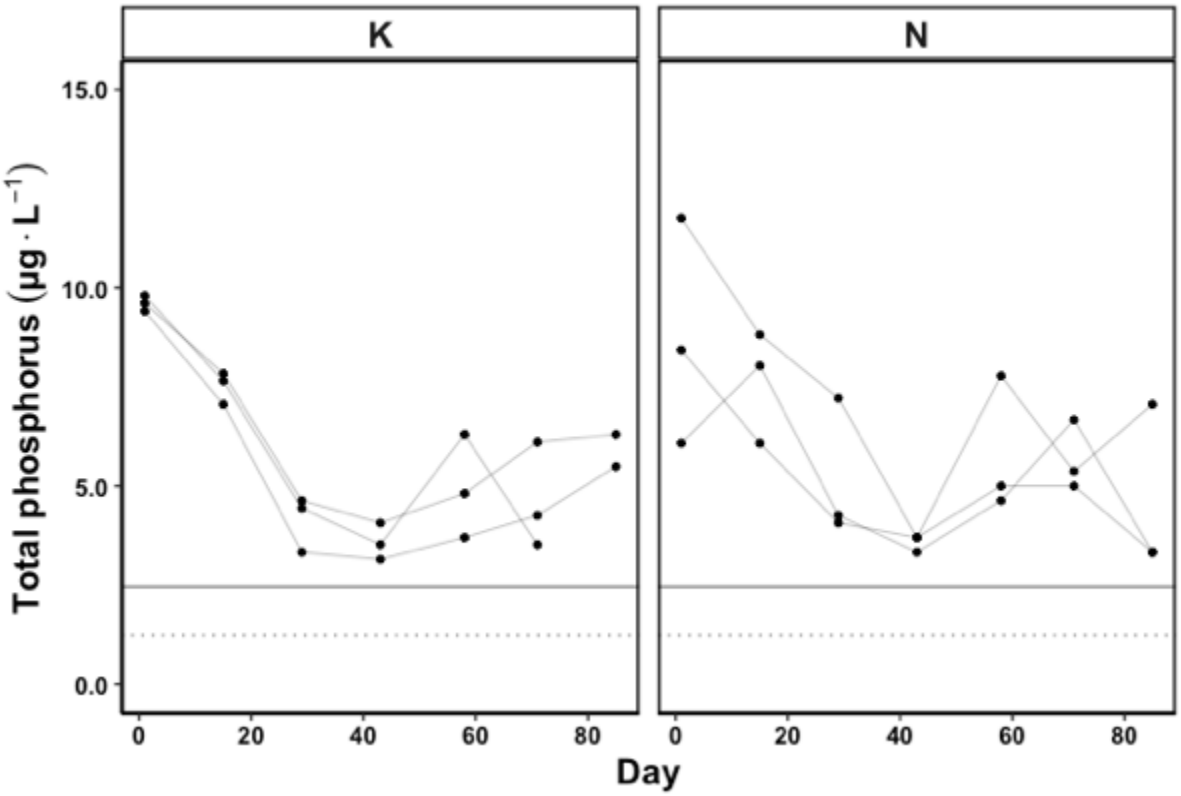

Figure 2.20: Total phosphorus concentrations of water samples from the six bays sampled in 2018 as a function of day of experiment. Abbreviations for bays are as follows: Kidd Island (K), Neachen (N) bays. Line represents water samples taken at one of three substrate locations in each bay. The solid horizontal line is the method reporting limit of 2.47 $\mu g \cdot L^{-1}$ and the dotted line is the method detection limit of 1.23 $\mu g \cdot L^{-1}$. Samples below the reporting limit are shown here but were not included in statistical analyses.

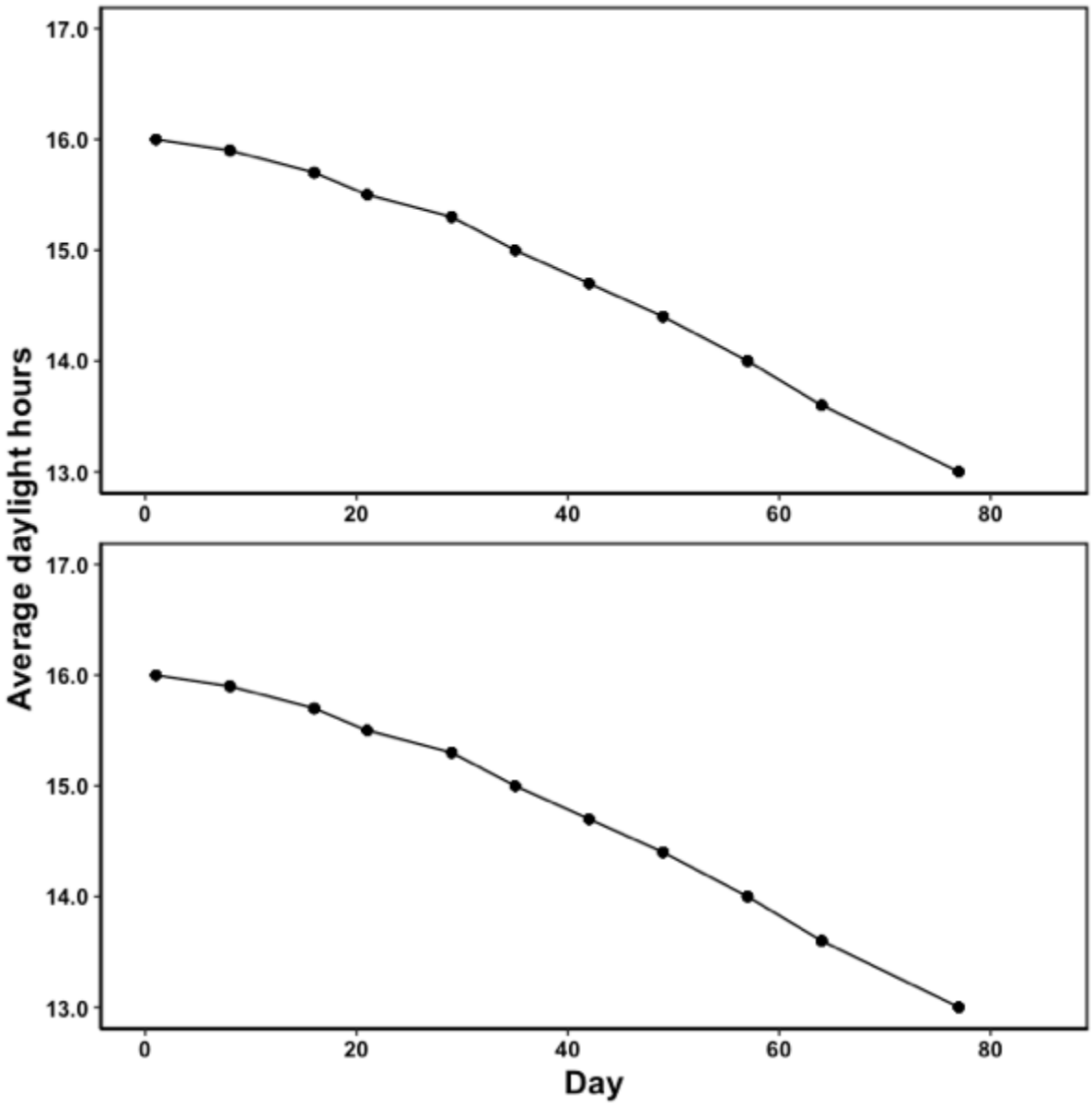

Figure 2.21: Plot of number of average daily lighted hours between sampling periods for 2017 (top) and 2018 (bottom). Each point marks a sampling event, and the y-value for cumulative hours equals the sum of daylight hours available since the last sampling event.

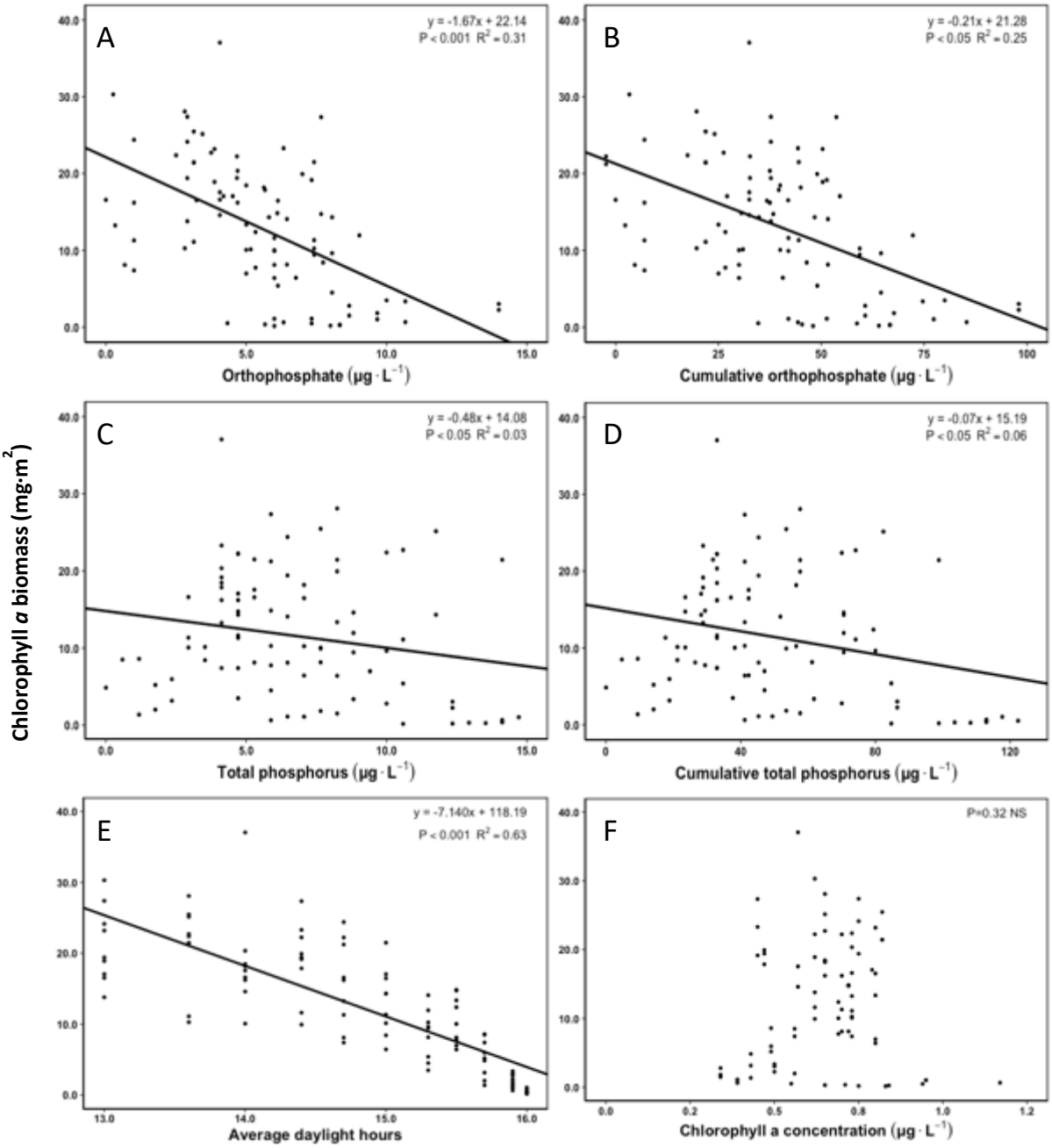

Figure 2.22: 2017 Chlorophyll *a* biomass as a function of watershed productivity indicators: (A) orthophosphorus, (B) cumulative orthophosphorus, (C) total phosphorus, (D) cumulative total phosphorus, € average daylight hours, and (F) water column chlorophyll *a* concentration. Only significant trendlines are displayed. Note regression equations and coefficients are given in frames for which the relationships were significant.

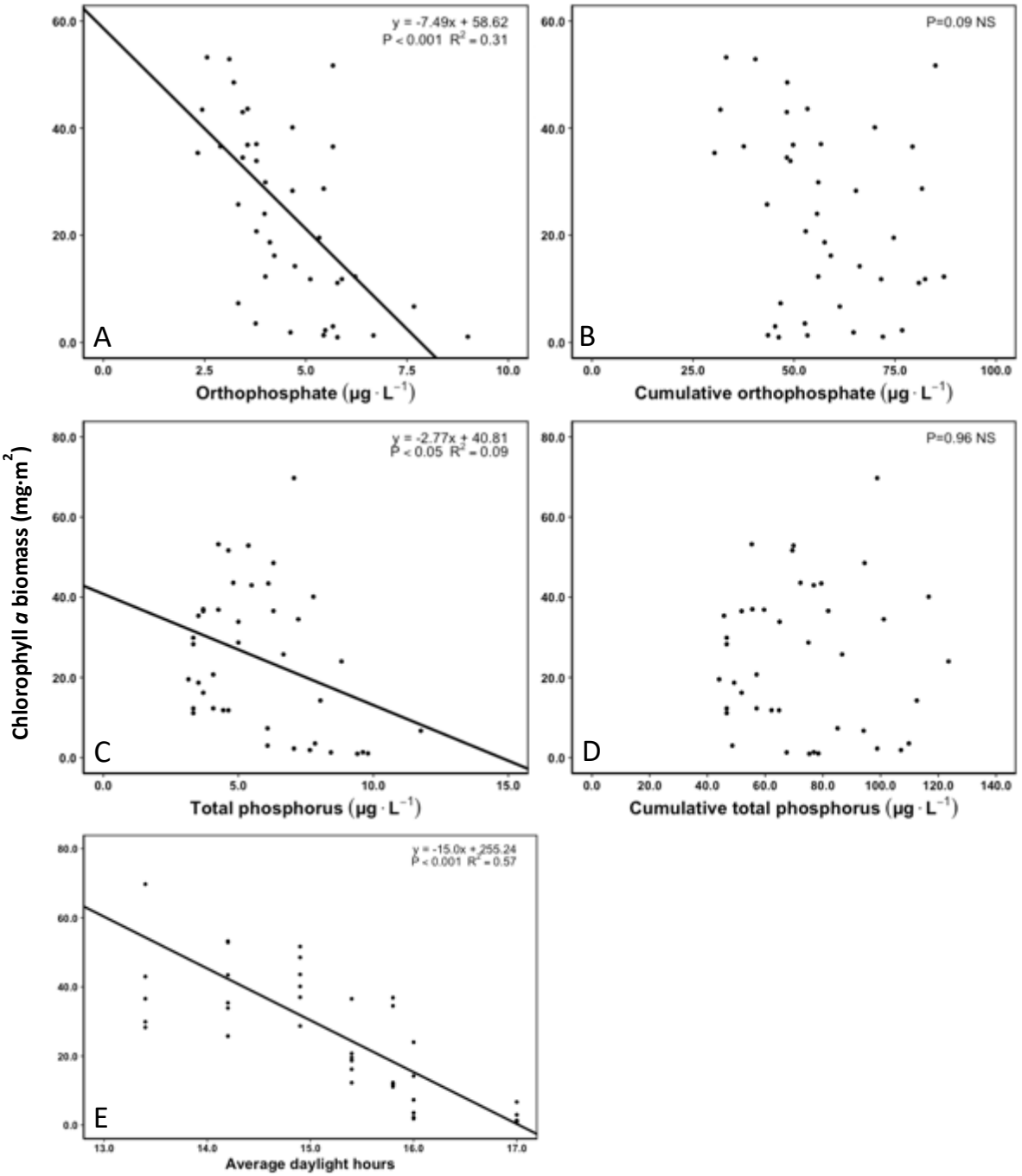

Figure 2.23: 2018 Chlorophyll *a* biomass as a function of watershed productivity indicators: (A) orthophosphorus, (B) cumulative orthophosphorus, (C) total phosphorus, (D) cumulative total phosphorus, € average daylight hours, and (F) water column chlorophyll *a* concentration. Only significant trendlines are displayed. Note each regression formula given in facets with significant relationships.

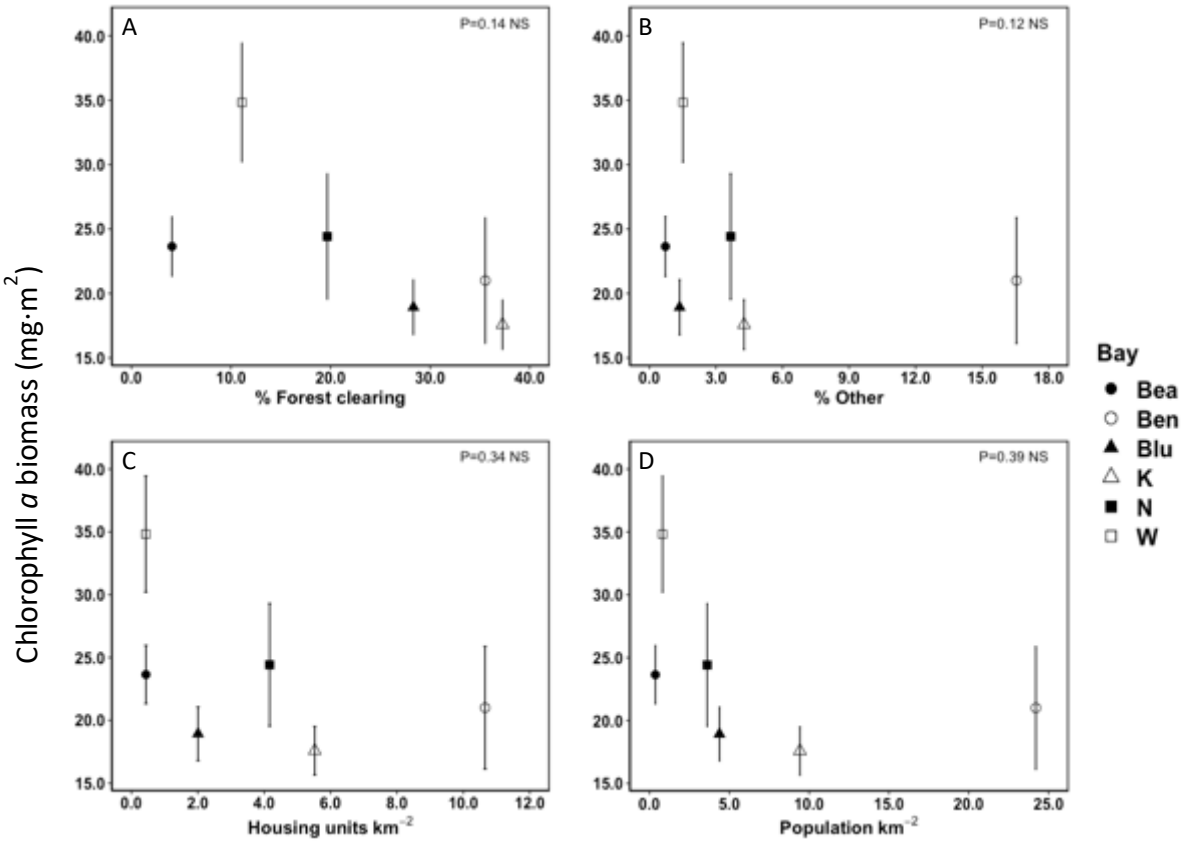

Figure 2.24: Chlorophyll *a* biomass as a function of watershed anthropogenic activity indicators: (A) Percent forest clearing, (B) % other, (C) Housing unit density, and (D) population density. Each point represents the bay-average maximum biomass in 2017 (n = 3).

Chapter 3: Estimates of the seasonal influx of total residue and phosphorus to Kidd Island and Neachen bays of Coeur d'Alene Lake via the main intermittent stream to each bay

Abstract

Nutrient input from the watershed to bays occurs primarily via streams and rivers in a natural landscape, along with other sources such as atmospheric wet and dry deposition and point and non-point sources. These sources are magnified by the expanding human population that is increasingly modifying the natural world which increases the rate of nutrient delivery to aquatic ecosystems. Here my goal was to estimate the particulate matter and associated nutrient load delivered to two north-end bays in Coeur d'Alene Lake which had similar-sized watersheds and topology but differed in population density and land use. Automated samplers were used to collect daily grab samples for the analysis of total residue and total phosphorus. Stream discharge was measured biweekly from cross-sections of wetted width and velocity measurements for the period of April 28 to July 13, 2018, ending when stream depth became too low for reliable measurement and constituent load was minimal. Average discharge, total phosphorus (TP) and total residue (TR) loads were higher in Kidd Creek than in Neachen Creek. Once normalized for watershed area (km^2), Kidd Creek had 86% higher discharge, and >400% higher TP and >150% higher TR per day per km^2 than Neachen Creek. These results suggest that some factor(s) other than watershed size, such as differences in land use, interact to cause differential nutrient loading between bays. This study produced data for spring freshet nutrient and sediment deposition, which more than likely represents the majority of the annual load to the bays. These data can be used by lake managers to examine the contribution of watersheds with different land use characteristics, and for the calibration and enhancement of existing and future nutrient loading modeling efforts.

Introduction

The hydrology of the Western United States is intimately linked to snowpack (Neal et al. 2002; Mote 2003; Hamlet et al. 2005; Luce et al. 2013), unlike other portions of the US where the hydrograph is dominated by rain. Snow melt contributes the most water to the overall water budget in the Western U.S. (Yang et al. 2003; Stewart et al. 2004). In these systems, snowpack serves as a reservoir of water that becomes available to the landscape during the melt period. Water in excess of soil-saturation becomes surface runoff, a quantity measurable by stream gages as discharge. Runoff timing in the Pacific Northwest is changing (Stewart et al. 2004; Barnett et al. 2005; Rood et al. 2008; Clark 2010) as melting begins earlier (Stewart et al. 2004) and less precipitation falls as snow (Clark 2010). The duration of the melt period in a watershed varies but is regionally defined as April to July by Stewart et al (2004). Stewart (2005) also notes that runoff timing at lower elevations (compared to alpine) are experiencing shifts in earlier runoff of between one to four weeks, which could edge the start of the runoff period into March in some areas.

Erosion is the predominant source of sediment and its associated nutrients to standing water bodies (Ward and Trimble 2003; Kendy and Bredehoeft 2006), and is highest during the runoff period. Following the runoff period, Western streams are dominated by groundwater inputs (Mote 2003; Ward and Trimble 2003; Kendy and Bredehoeft 2006). It follows then that spring runoff deposition of nutrients is a critical period for stream research, particularly when seeking to quantify the influence of watershed characteristics, rather than groundwater, on nutrient deposition to lakes and bays. Nutrient loads from streams in watersheds can differ based on the composition of land use (Beaulac and Reckhow 1983; Rajkovich 2014). Therefore, in situations in which annual sediment load calculations are not possible, seasonal investigations should be timed with peak runoff to capture the signature of watershed influence on erosion rather than groundwater inputs.

It is true that the vast majority of sediment-associated nutrients enter Coeur d'Alene Lake through its two major tributary rivers, the Coeur d'Alene and the St. Joe rivers (Wood and Beckwith 2008), but these deposits rarely mix into the bays because lake residence time is short, indicating that sediment-laden water flushes quickly through Coeur d'Alene Lake. Retention of sediments in the lake is evidenced by south-to-north nutrient concentration

gradients, with concentrations decreasing as sediment plumes settle while traveling northward toward the outlet at the Spokane River (Wood and Beckwith 2008). According to Wood and Beckwith (2008), faster flushing rates cause lakes to be more dependent on watershed influences because of the continual input of nutrients and lack of time to establish internal loading. Conversely, lakes with long retention times are less influenced by watershed characteristics and more by internal processes.

Wood and Beckwith (2008) explain that the effect of plumes from large riverine inputs is high because the magnitude of temperature, density, and concentration of constituents is high between the lake and river. Conversely, they state that small inflows, such as the sub-catchment streams measured in this study, less significantly influence overall lake conditions because they mix more-readily upon deposition. This rapid mixing occurs in bays because faster equilibration of temperatures occurs. Although Wood and Beckwith (2008) discuss plume influence in terms of the importance of riverine inputs, these considerations also justify this study's focus on littoral zones in bays. While riverine and main-lake processes are crucial to understand current and future pelagic conditions, the characteristically different sediment dynamics of bays indicated in their analysis imply that littoral productivity is strongly influenced by in-bay processes.

In general, to relate summer periphyton growth to land use activity in the watershed, nutrient inputs from streams need to be understood. Specifically, the relationship between nutrient flux into the bay from the watershed and its retention in the bay must be known. Without this, it is not possible to conclude if primary productivity in the bay is derived from the watershed or internal sources. The guiding hypothesis for the Coeur d'Alene Periphyton Study is that the recruitment of periphyton on substrates during the summer varies in bays with differential watershed characteristics regarding human activity. To explore the relationship between watershed characteristics and stream nutrient loading, the tributary streams of two bays were instrumented for sampling in 2018. This chapter includes three parts: First, the installation and maintenance of stream samplers to collect samples for nutrient analysis, and second, the calculation of nutrient loads. Finally, I compared nutrient loads and periphyton growth to the extent possible, between bays to determine if spring nutrient load influenced summer periphyton growth.

Methods

Sample collection and analysis

One ISCO 2900 automated water sampler (Teledyne ISCO, Lincoln, NE) was installed and maintained in each of the single tributary streams of Kidd Island and Neachen bays. These streams were chosen for several reasons, but mainly to represent end-member bays along the continuum of most to least disturbed watersheds of the six bays sampled in 2017 (Chapter 2). The Kidd Island watershed is highly modified because of anthropogenic activities including agriculture and residential developments along the shoreline. As well, there is currently little information available for Kidd Island Bay in the IDEQ Nutrient Inventory. Neachen Bay was selected to contrast Kidd Island Bay because it has a mainly forested watershed with the least human disturbance of the six bays examined in 2017 (Chapter 2). The bays had similar surface areas and shapes (Figures 2.2 and 2.7).

ISCO samplers were installed on April 7, 2018 in Kidd Creek and April 28, 2018 in Neachen Creek, before peak spring runoff. Samplers were placed as close to the creek-bay confluence as possible at sites that were easily accessible and not at risk of flooding from high lake elevations or stream discharge. Sampling concluded on July 13, 2018 at both sites when flow past the sampler intake ceased. A 500 ml stream water sample was collected daily at 15:00 and samples were retrieved every 14 days. Samples were transported on ice to the UI Limnology Laboratory where they were refrigerated at 4°C until analysis.

From the 500 ml sample, triplicate 20 ml aliquots were used for the analysis of total phosphorus (TP) according to SM4500-P.E with potassium persulfate digestion and no preservative (Eaton et al. 2005). The average of the three concentrations was considered the daily TP concentration of the stream. Total residue (TR) was measured according to SM2540-B with the remaining 440 ml of sample (Eaton et al. 2005), evaporating at 105°C to dryness in pre-tared ceramic crucibles.

Collection of discharge data and establishment of a stage-discharge curve to calculate nutrient load

To obtain daily discharge values, I constructed a stage-discharge relationship for each stream by manually measuring discharge and depth every two weeks when I retrieved the samples from the ISCO samplers (Appendix A). This relationship was used to estimate discharge from a continuously recording HOBO U20-001-01 depth logger (Onset Computer

Corporation, Bourne, MA) set to record water depth every 15 minutes. The stream depth logger data were corrected for changes in atmospheric pressure by a similar level logger located on land near each ISCO sampler. From March 31 to June 15, 2018, the HOBO logger file for stream water level at Kidd Creek was corrupted and no data were retrievable. Daily water level was estimated using linear interpolation for these missing dates. In addition, the atmospheric pressure sensor was not active from April 27 to March 3, and from June 15 to June 29, 2018. Barometric pressure (BP) data from the Coeur d'Alene Regional Airport (NCEI 2018) was used in place of site-collected BP data according to methods developed by LaCroix (2015).

To calculate discharge, I calculated cross-sectional area and measured velocity using an Ott MF Pro (Ott, Loveland, CO, USA) and top-setting rod set to 60% depth in each section according to USGS methods (Appendix A; Rantz 1988; Gordon et al. 2004). Daily discharge was calculated from stream-specific stage-discharge relationships (Appendix A; Rantz 1988; Gordon et al. 2004; Squires et al. 2017).

Statistical analysis

To calculate daily and seasonal TP and TR loads for both streams using daily depth and biweekly discharge measurements and concentrations, I first converted bi-weekly stage and discharge measurements (Appendix A) to daily discharge values using the HOBO water level data. Second, bi-weekly stage and discharge data were regressed to determine a stage/discharge (rating) curve for each stream (Appendix A). Third, the estimated daily discharge, and daily constituent concentrations (Appendix B and C) were used in the nonparametric smearing approach to calculate daily TP and TR loads for each stream (Appendix D; Duan 1983; Cohn 1995; Helsel and Hirsch 2002). Finally, the overall seasonal load from each stream was calculated as the sum of daily constituent loads over the study period. Because Neachen Creek (April 28, 2018 to July 13, 2018) was instrumented for fewer days than Kidd Creek (April 7, 2018 to July 13, 2018), daily loads for both streams were summed only for the days during which the collection of data from each stream overlapped to have directly comparable data.

I used least squares regression to examine TP ($\mu g \cdot s^{-1}$) as a function of TR ($\mu g \cdot s^{-1}$) to see if TP was related to TR. A positive relationship would indicate that increased nutrient loading occurs with sediment addition to the stream. TR was also regressed against stream

discharge to determine if increases in TR occurred with high stream velocity. Secondly, TP and TR seasonal loads ($kg \cdot period^{-1}$) were normalized by watershed area (km^2), to control for the influence of shear watershed size on nutrient transport, so that loads could be compared based on watershed characteristics (Miatke 2015).

Results

Hydrograph and daily loads

Hydrographs for each stream indicated higher daily average discharge in Kidd Creek compared to Neachen Creek (Figure 3.1, Table 3.1). The daily average discharge was 0.67 ± 0.0014 (mean ± SE) $m^3 \cdot s^{-1}$ at Kidd Creek and 0.40 ± 0.004 $m^3 \cdot s^{-1}$ at Neachen Creek. The daily average discharge of Kidd Creek ranged from 0.54 to 1.04 $m^3 \cdot s^{-1}$, which occurred on March 31 and March 12, 2018, respectively. The daily average discharge at Neachen Creek was lower and ranged from 0.31 to 0.56 $m^3 \cdot s^{-1}$ on March 31 and March 7, 2018, respectively.

Daily average TP and TR loads reached their maximums and minimums on the same days as discharge. TP load from Kidd Creek (Figure 3.2) ranged from 2.66 to 8.00 $kg \cdot day^{-1}$ and Neachen's TP load ranged from 0.51 to 0.95 $kg \cdot day^{-1}$. TR in Kidd Creek ranged from 5.47 to 12.77 $tonnes \cdot day^{-1}$ and Neachen's TR ranged from 2.51 to 3.21 $tonnes \cdot day^{-1}$. See Table 3.1 for all summary statistics for discharge, TP, and TR. Quantile analysis on each dataset (Figure 3.4, Table 3.1) revealed larger upper than lower quantiles and far more upper outliers than lower outliers in Kidd Creek. In Neachen Creek, upper and lower quantiles were even and there were fewer outliers on either end (Figure 3.4, Table 3.1).

Relationship between total phosphorus and total residue

A significant positive regression slope for the relationship between TP and TR indicated that TP was related to TR in both streams (Table 3.2, Figures 3.5 and 3.6). The regression slope for Kidd Creek was 1.21 ($N=96$, $P<0.001$) and 0.79 ($N=75$, $P=0.008$) for Neachen Creek (Table 3.2). After TP and TR seasonal loads were normalized for watershed area (Table 3.3), loads were compared. The normalized load to Kidd Island Bay was 15.6 $kg \cdot km^{-2}$ while to Neachen Bay it was 3.6 $kg \cdot km^{-2}$. The normalized TR load to Kidd Island Bay was 30.4 $tonnes \cdot km^2$ and to Neachen bay it was 14.7 $tonnes \cdot km^2$.

Discussion

The hydrographs showed that at its maximum peak on March 12, 2018, Kidd Creek discharged 86% more water volume per second than Neachen (Figure 3.1). Overall, discharge was always higher in Kidd than Neachen, with a typical difference of approximately 0.2 $m^3 \cdot s^{-1}$ or 60% at baseflow. Upper quantile discharge (Figure 3.4) also had more variation and outliers, representing a flashier hydrology in Kidd, rather than the steady discharge in Neachen. This difference in volume and hydrograph shape reflects the fact that watershed size is not the sole determinant of drainage volume and timing from a watershed.

Because of the manner in which loads were calculated they were reflective of the hydrograph in each stream. Comparatively, mean TP and TR were 436% and 156% higher in Kidd Creek than in Neachen Creek. Although the Kidd Island Bay watershed is only 24% larger than Neachen's (Table 3.4), the mean TP and TR loads were >400% and >150% higher per day per area at peak flow to Kidd Island than Neachen bays. This means that variation in TP and TR load between streams was disproportional to the difference in watershed size. This disparity in loads could be related to the differences in land use and anthropogenic activities in the respective watersheds.

Two non-exclusive processes may be at play in these watersheds that caused this disparity in load versus area. First, the simple difference in discharge could influence creek constituent load. As discharge increased, so did TP and TR (Figure A.7 and A.8) because greater movement of water across the landscape increases its erosive power and ability to transport sediment. As such, because Kidd Creek drains more water per area, the extra force may be moving more sediment into the stream compared to Neachen. Drainage volume and timing characteristics rely on elevation and aspect, along with soil properties like elevation, and vegetative interception could play a role in causing the disproportionate area-normalized discharge rates.

A second explanation, analyzed in Chapter 2, is that some variable(s) controlling nutrient and sediment load to streams differ between the two watersheds. In this case, Kidd Island's higher area-normalized daily loads would be considered the result of watershed characteristics such as land use, topology, and human impacts that alter erosion coefficients across the landscape. Analysis of the anthropogenic activity indicators, population density, housing density, percent forest clearing, and percent other land use indicated that Kidd and

Neachen differed in the amount of watershed disturbance characteristic of humans. Kidd Island was higher by 61% in population density, 25% in housing density, 47% in forest clearing, and 14% in other land use (Table 3.4). In light of this chapter's quantified difference in stream loads, plus the Chapter 2 finding of unequal disturbance characteristics, it follows that the difference in load could be caused by the alterations to the natural landscape and hydrology that in turn increase sediment transport in Kidd over Neachen. Realistically, both of these explanations are possible and can operate together. Further research into 2018 snowpack, precipitation, and soil characteristics is necessary to examine if more specific conclusions regarding the differences in discharge, TP, and TR between these two watersheds can be reached.

Because this study resulted in two seasonal nutrient loads, statistical analysis regarding nutrient load and periphyton response was not possible. One proposed option for the interpretation of stream nutrient loads in the context of periphyton is to convert nutrient loads to potential phytoplankton concentrations in their respective bays using known chlorophyll *a*: TP ratios (Dillon and Rigler 1974; Jones et al. 2015). In this way, the researcher is asking, "Do these streams deposit different enough TP loads to produce measurable differences in phytoplankton in these bays?" Potential phytoplankton would then be analyzed in light of trophic level indicators, questioning how much TP would need to be added to bays by streams to cause trophic-level changes. This ultimately puts measured TP loads in the context of primary productivity, but it is computationally and theoretically complex, causing its exploration to fall outside the scope of this study. Simply to calculate the initial potential phytoplankton concentrations requires bathymetric volume calculations to determine how nutrient loads (kg) would translate into concentrations ($\mu g \cdot L^{-1}$). Additionally, the method assumptions are tenuous, such as the assumption that nutrients from streams are directly converted to phytoplankton only rather than other forms of biomass or abiotic sinks, which extremely oversimplifies the system. Although this method of quantifying the relationship between stream loads and primary productivity was proposed, it was not pursued further.

Conclusion

Stream work in Kidd and Neachen creeks during 2018 provided me valuable experience in instrumenting and monitoring streams for the analysis of constituent load and watershed hydrology. Key findings for this chapter included the interesting differences in stream discharge patterns as visualized in the hydrographs, and the conclusion that seasonal nutrient and sediment loads to bays per day were >50% higher in Kidd Creek when normalized for watershed area. Analysis in this chapter pointed to a need for in-depth analyses of the abiotic environmental processes that govern watershed hydrology at these sites. With more information, researchers could better determine the cause of these load disparities, particularly examining the influence of shear water volume contributing to greater erosion vs. the hypothesis that land use influences erosion of sediment to streams. Concerning periphyton, this chapter has advanced, but not completed, the complex pursuit of conceptually and quantitatively tying watershed activity to summer primary productivity. Streams are critical nutrient and sediment transport mechanisms in any watershed and quantifying seasonal loads from Kidd and Neachen creeks allowed for introductory reconnaissance for information about sediment dynamics in these bays. Finally, data for discharge, TP, and TR, including daily instantaneous sample concentrations, estimated daily average constituent loads, and total seasonal load were shared with DEQ personnel for their use. Current DEQ projects will benefit from additional data in these bays, which currently face data constraints in existing Nutrient Inventory calculations and nutrient loading models.

Literature Cited

Barnett, T. P., J. C. Adam, and D. P. Lettenmaier. 2005. Potential impacts of a warming climate on water availability in snow-dominated regions. Nature **438**: 303–309. doi:10.1038/nature04141

Beaulac, M. N., and K. H. Reckhow. 1983. Water resources bulletin: An examination of land use-Nutrient export relationships. Am. Water Resour. Assoc. **18**: 1013–1024.

Clark, G. M. 2010. Changes in patterns of streamflow from unregulated watersheds in Idaho, western wyoming, and Northern Nevada. J. Am. Water Resour. Assoc. **46**: 486–497. doi:10.1111/j.1752-1688.2009.00416.x

Cohn, T. A. 1995. Recent advances in statistical methods for the estimation of sediment and nutrient transport in rivers, U.S. National Report to the International Union Geodesy and Geophysics 1991–1994, Reviews of Geophysics, Supplement., **33**: 1117–1123.

Dillon, P. J., and F. H. Rigler. 1974. The phosphorus-chlorophyll relationship in lakes. Limnol. Oceanogr. **19**: 767–773. doi:10.4319/lo.1974.19.5.0767

Duan, N. 1983. Smearing estimate: A Nonparametric retransformation method. Source J. Am. Stat. Assoc. **78**: 605-610.

Eaton, A. D., L. S. Clesceri, E. W. Rice, and M. A. Franson. 2005. Standard methods for the examination of water and wastewater. SM4500-P. American Public Health Association, 21st ed. American Public Health Association, American Water Works Association, Water Environment Federation.

Gordon, N. D., T. A. McMahon, B. L. Finlayson, C. J. Gippel, and R. J. Nathan. 2004. Stream hydrology: An introduction for ecologists. Ecol. Eng. **2**: 166–169. doi:10.1016/0925-8574(93)90041-D

Hamlet, A. F., P. W. Mote, M. P. Clark, and D. P. Lettenmaier. 2005. Effects of temperature and precipitation variability on snowpack trends in the western United States. Climate **18**: 4545–4561.

Helsel, D. R., and R. M. Hirsch. 2002. Statistical methods in water resources, *In* Techniques of Water-Resources Investigations of the United States Geological Survey: Book 4, Hydrologic Analysis and Interpretation.

Jones, J. R., R. W. Bachmann, J. R. Jones, and W. Roger. 2015. Prediction of phosphorus levels in lakes. Water Pollut. Control Fed. **48**: 2176–2182.

Kendy, E., and J. D. Bredehoeft. 2006. Transient effects of groundwater pumping and surface-water-irrigation returns on streamflow. Water Resour. Res. **42**. doi:10.1029/2005WR004792

Luce, C. H., J. T. Abatzoglou, and Z. A. Holden. 2013. The missing mountain water: Slower westerlies decrease orographic enhancement in the Pacific Northwest USA. Science **342**: 1360–1364. doi:10.1126/science.1242335

Miatke, B. G. 2015. Quanitfying nutrient and sediment loads during spring runoff in the Missiquoi River Basin. Honors College senior thesis, University of Vermont, Burlington, VT, USA.

Mote, P. W. 2003. Trends in snow water equivalent in the Pacific Northwest and their climatic causes. Geophys. Res. Lett. **30**. doi:10.1029/2003GL017258

NCEI. 2018. Climate data online for the Coeur d'Alene Regional Airport (WBAN:24136) for the period April 1 - July 31, 2018. Natl. Cent. Environ. Information. Natl. Ocean. Atmos. Assoc. (NOAA).

Neal, E. G., M. Todd Walter, and C. Coffeen. 2002. Linking the pacific decadal oscillation to seasonal stream discharge patterns in Southeast Alaska. J. Hydrol. **263**: 188–197.

Rajkovich, H. 2014. Research in the Willow Creek watershed: Estimates of sediment and phosphorus loads from sub-catchments; gauging public response to a constructed wetland; and a quantitative assessment of a conceptual constructed wetland. MS thesis, University of Idaho, Moscow, ID, USA.

Rantz, S. E. et al. 1988. Measurement and computation of streamflow: Volume 1. Measurement of stage and discharge. U.S. Geological Survey. Water-supply paper 2175.

Rood, S. B., J. Pan, K. M. Gill, C. G. Franks, G. M. Samuelson, and A. Shepherd. 2008. Declining summer flows of Rocky Mountain rivers: Changing seasonal hydrology and probable impacts on floodplain forests. J. Hydrol. **349**: 397–410. doi:10.1016/j.jhydrol.2007.11.012

Squires, A. L., J. Boll, and E. S. Brooks. 2017. On the role of spatial, temporal, and climatic forces on stream sediment loading from rural and urban ecosystems. JAWRA J. Am. Water Resour. Assoc. **53**: 1195–1211. doi:10.1111/1752-1688.12566

Stewart, I. T., D. R. Cayan, and M. D. Dettinger. 2004. Changes in snowmelt runoff timing. Clim. Change **62**: 217–232. doi:10.1023/B:CLIM.0000013702.22656.e8

Ward, A., and S. Trimble. 2003. Environmental hydrology, 2nd ed. CRC Press.

Wood, M. S., and M. A. Beckwith. 2008. Coeur d'Alene Lake, Idaho: Insights gained from limnological studies of 1991–92 and 2004–06. USGS Sci. Investig. Rep. 2008-5168 52.

Yang, D., D. Robinson, Z. Yuanyuan, T. Estilow, and B. Ye. 2003. Streamflow response to seasonal snow cover extent changes in large Siberian watersheds. J. Geophys. Res. **108**: 4578. doi:10.1029/2002JD003149

Table 3.1: Summary statistics for discharge (Q, $m^3 \cdot sec^{-1}$), total phosphorus (TP, $kg \cdot day^{-1}$), total residue (TR, $tonnes \cdot day^{-1}$) for stream data collected from April 28, 2018 to July 13,2018, which is the overlapping sample period for Kidd (K) and Neachen (N) creeks. Table includes the number of samples (N), mean, standard deviation (SD), standard error (SE), minimum (Min), 25th (Q25) and 75th (75) quantiles, and maximum (Max).

Stream	Statistic	N	Mean	SD	SE	Min	Q25	Q75	Max
K	Q	76	0.66	0.11	0.0014	0.54	0.60	0.67	1.04
	TP	76	3.70	1.22	0.0161	2.66	3.08	3.85	8.00
	TR	76	7.25	1.61	0.0215	5.77	6.40	7.51	12.73
N	Q	76	0.40	0.05	0.0004	0.31	0.37	0.43	0.56
	TP	76	0.69	0.10	0.0017	0.51	0.62	0.74	0.95
	TR	76	2.83	0.16	0.0016	2.51	2.72	2.91	3.21

Table 3.2: Comparative relationships between total phosphorus (TP; $kg \cdot day^{-1}$) and total residue (TR; $tonnes \cdot day^{-1}$) at both sites for the 2018 study period. General linear regression equation is in the form y=mx+b, where m is the slope and b is the intercept. CI is the 95% confidence interval, N equals the number of observations, and R^2 is the coefficient of determination. N is lower for Neachen because it was sampled for a shorter period of the 2018 field season.

Stream	Slope	95% CI	Intercept	95% CI	R^2	N	P
Kidd	1.21	(1.02, 1.40)	-3.13	(-5.30, -0.96)	0.62	96	<0.001
Neachen	0.79	(0.48, 1.09)	1.13	(-1.97, 4.23)	0.27	75	0.008

Table 3.3: Normalized total phosphorus (TP) and total residue (TR) loads in Kidd and Neachen creeks in 2018.

		Load	Watershed area	Normalized load
Constituent	Stream	kg	km^2	$kg \cdot km^{-2}$
TP	Kidd	287	18.349	15.6
	Neachen	53	14.832	3.6
	Δ	81%	19%	77%
TR	Kidd	557	18.349	30.4
	Neachen	218	14.832	14.7
	Δ	61%	19%	52%

Table 3.4: Watershed characteristics analyzed in Chapter 2 and used in this chapter to compare the watersheds drained by Kidd and Neachen creeks.

Bay	Area	Population density	Dwelling density	Forest clearing	Other land use
	km^2	Population·km^{-2}	Housing units·km^{-2}	%	%
Kidd	18.35	9.4	5.71	37.27	4.26
Neachen	14.83	3.63	4.31	19.67	3.66
Difference	24%	61%	25%	47%	14%

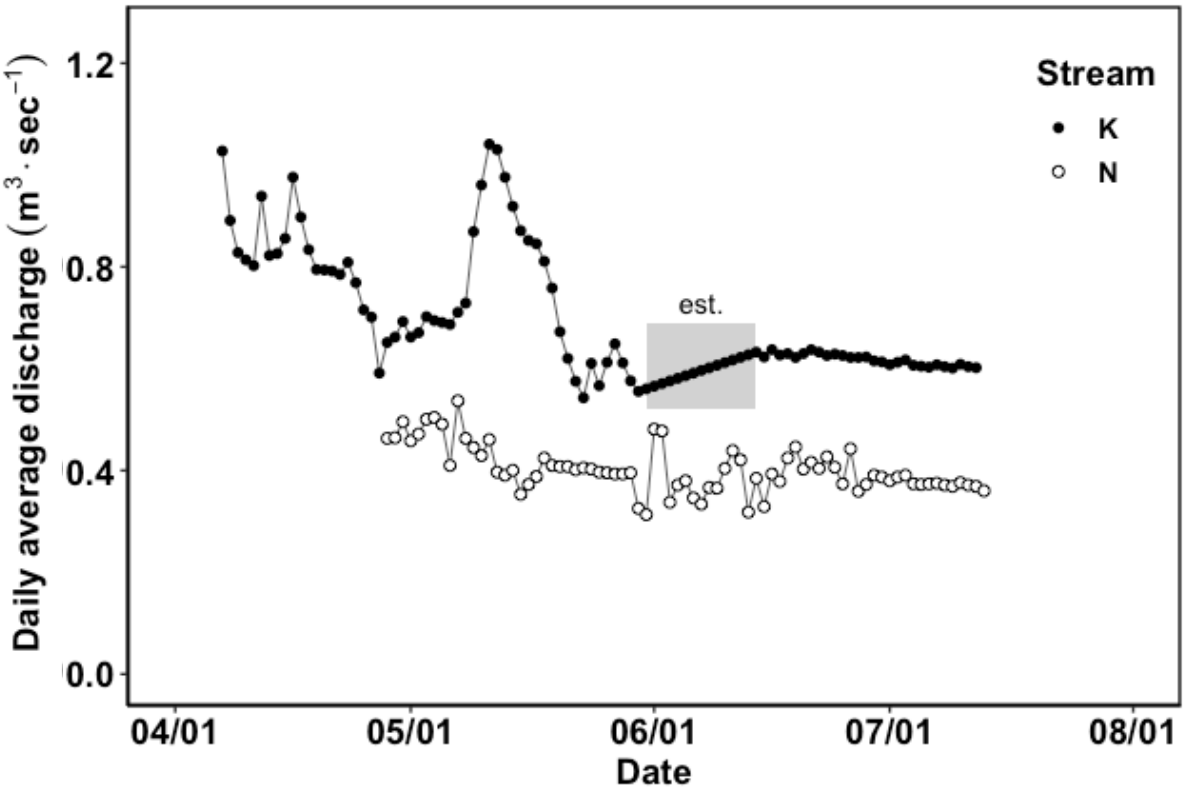

Figure 3.1: Hydrograph of daily average discharge ($m^3 \cdot sec^{-1}$) at both sites over the course of the study period which occurred from April 7, 2018 to July 13, 2018 for Kidd Creek (K) and April 28, 2018 to July 13, 2018 for Neachen Creek (N). Shaded gray box highlights estimated discharge values for May 31, 2018 to June 14, 2018 at Kidd Creek. See Methods for an explanation of estimation techniques.

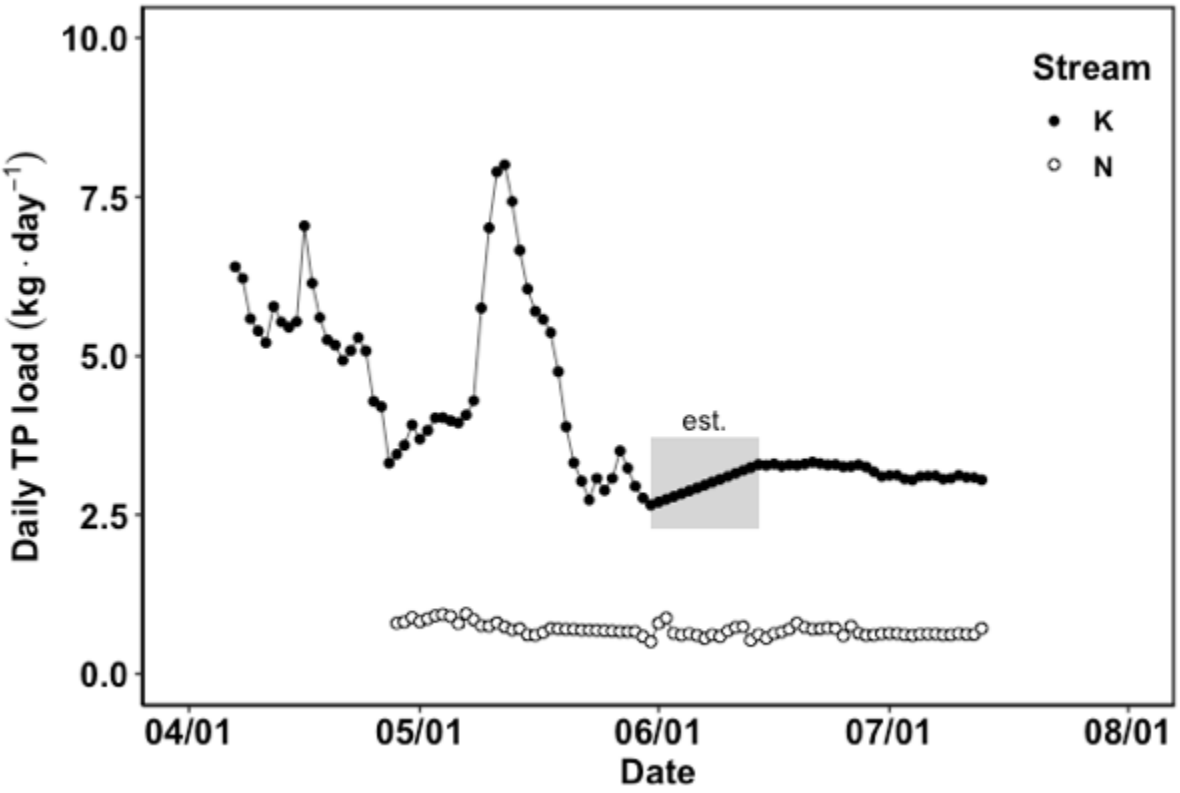

Figure 3.2: Daily total phosphorus (TP) load in (kg· day^{-1}) at both sites over the course of the study period which occurred from April 7, 2018 to July 13, 2018 for Kidd Creek (K) and April 28, 2018 to July 13, 2018 for Neachen Creek (N). Shaded gray box highlights estimated discharge values for May 31, 2018 to June 14, 2018 at Kidd Creek. See Methods for an explanation of estimation techniques.

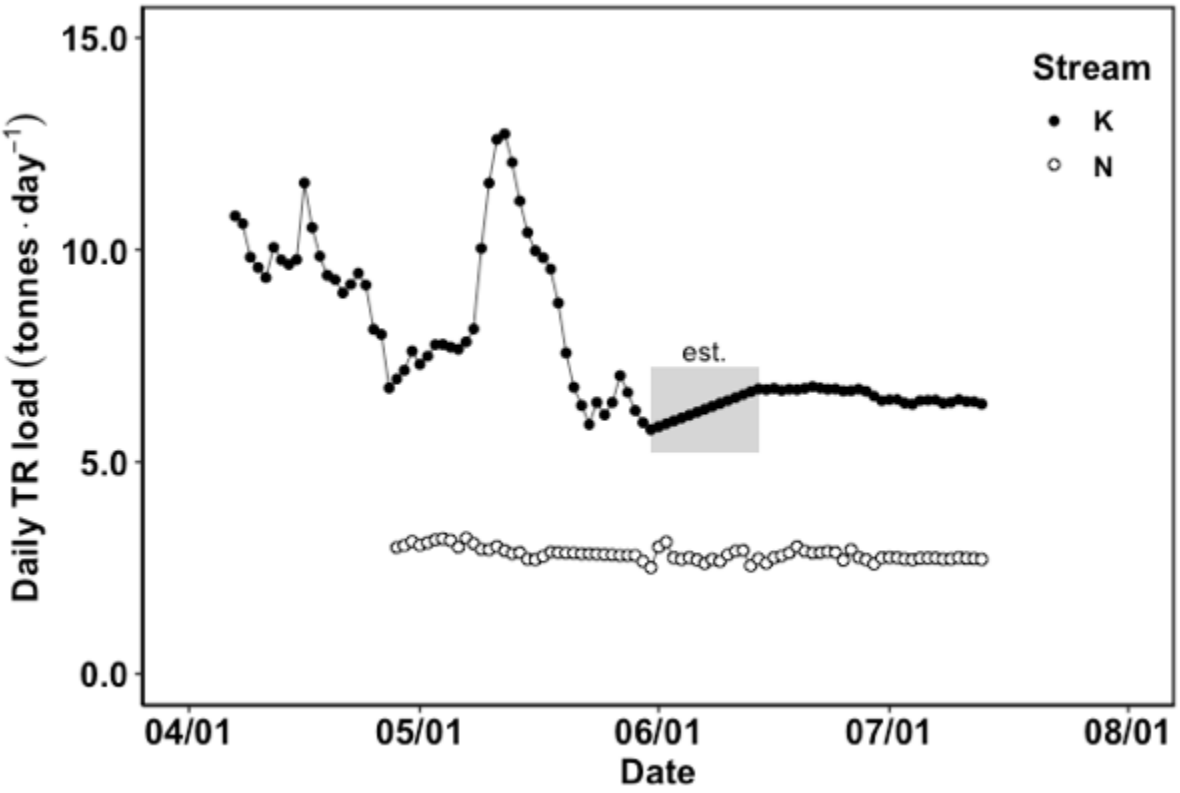

Figure 3.3: Daily total residue (TR) load in (tonnes· day^{-1}) at both sites as a function of time for the period April 7, 2018 to July 13, 2018 for Kidd Creek (K) and April 28, 2018 to July 13, 2018 for Neachen Creek (N). Shaded gray box highlights estimated discharge values for May 31, 2018 to June 14, 2018 at Kidd Creek. See Methods for an explanation of estimation technique.

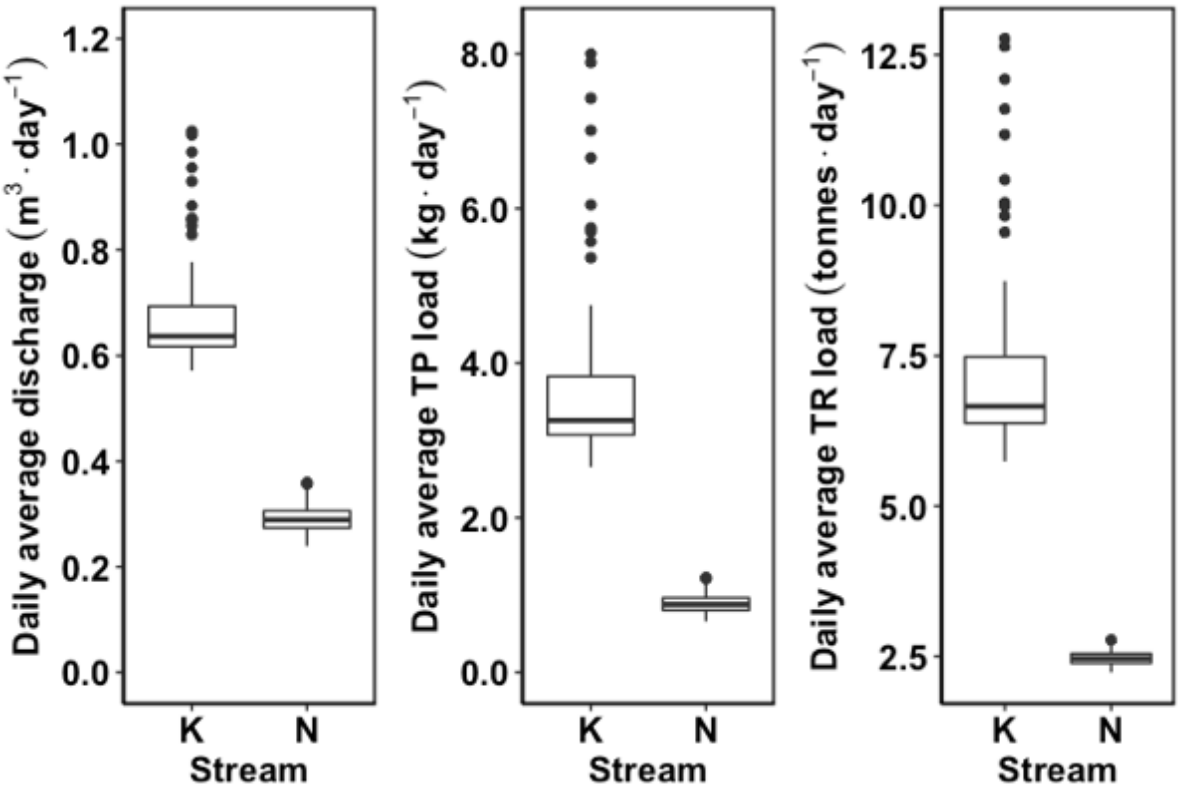

Figure 3.4: Boxplot summaries of key variables in stream analysis for Kidd (K) and Neachen (N) creeks. The center line of each boxplot is the median. Outside lines represent the 25th and 75th percentiles. Whiskers end at the greatest value, excluding outliers. Outliers are defined as values >1.5x the upper or lower quartile, respectively.

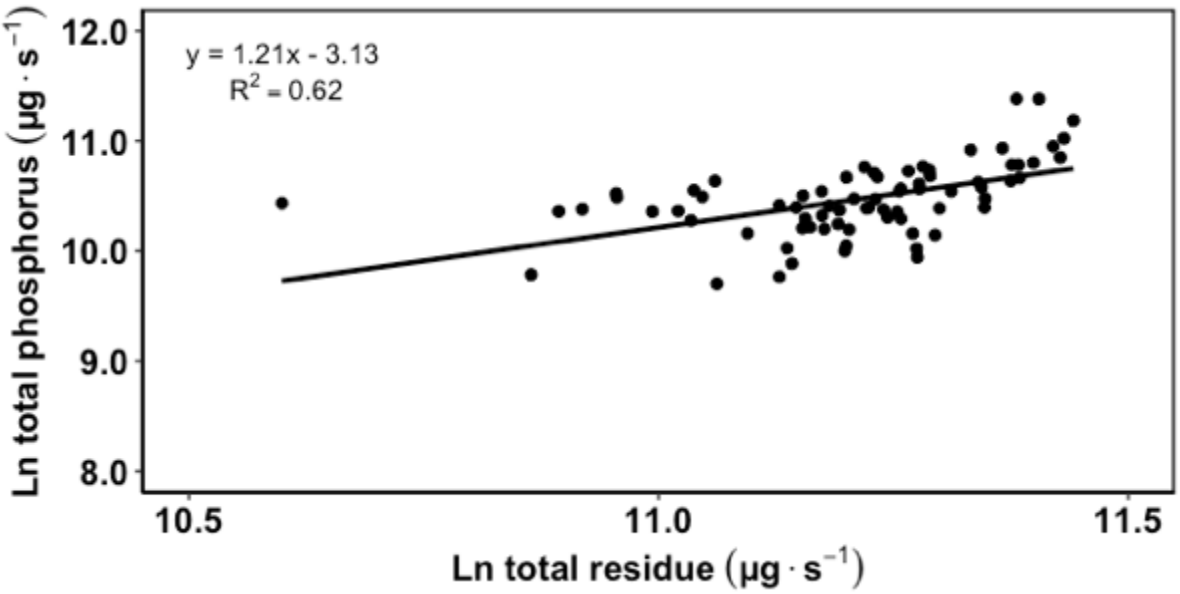

Figure 3.5: Natural log of total phosphorus (TP) as a function of Ln total residue (TR) for Kidd Creek in 2018.

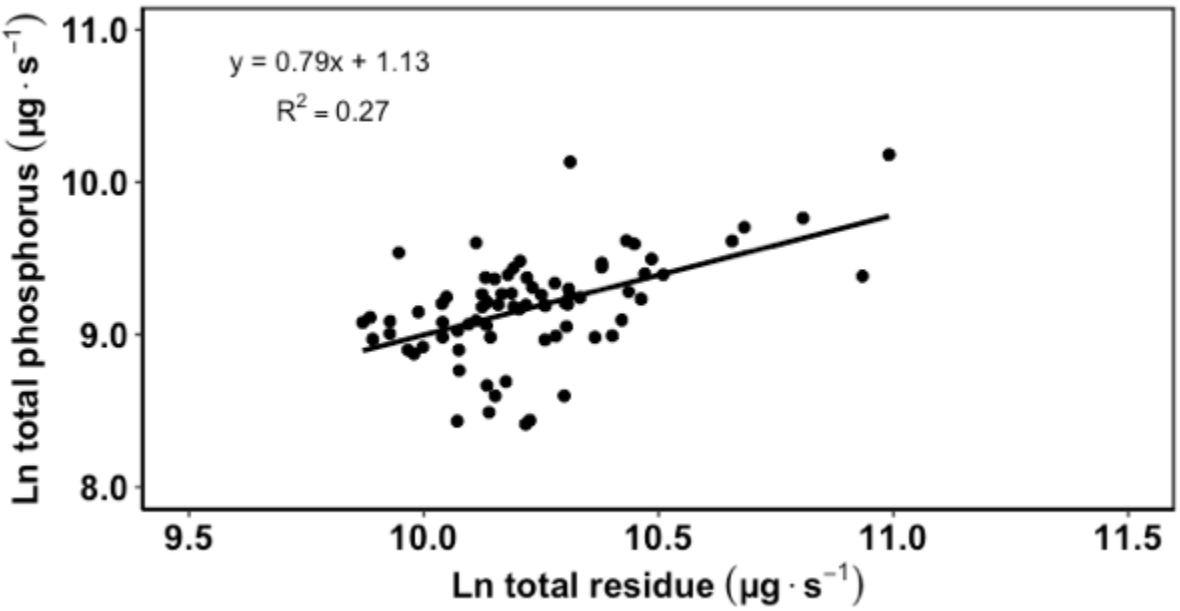

Figure 3.6: Natural log of total phosphorus (TP) as a function of Ln total residue (TR) for Neachen Creek in 2018.

Chapter 4: The analysis of total phosphorus

"Lessons Learned: A 'who done it?' investigation in search of mistakes in laboratory methods, the solution, and resulting data." *LakeLine* vol. 38, 2019, pp. 38-40[1].

Abstract

This chapter summarizes tests undertaken to identify and correct issues that arose with respect to the analysis of total phosphorus (TP) during my research. The issues included: results of ortho-phosphate, a fractional form of total phosphorus in a sample, that were greater than TP in most samples; inconsistencies between split samples analyzed by third party labs contracted by the Idaho Department of Environmental Quality (IDEQ) and my analyses; and TP concentrations that were below TP concentrations in water samples previously collected by the IDEQ from the same location. I also review TP analysis methods and quality assurance/quality control steps for future students conducting TP analyses using the spectrophotometric ascorbic acid method in the UI Limnology lab. Overall, the problem was calculating the concentration of P from acidified samples using a standard curve made with unacidified standards. A series of re-analyses and back calculations allowed correction of this issue: TP concentrations were then higher than OP concentrations; split samples with the 3rd party laboratory were similar, and samples matched historic concentrations. Recommendations for future students include increasing quality controls used for low-level detection methods, storing water samples without acid preservation, and careful calculation of method reporting limits.

[1] This chapter is an edited version of Notte, R. 2018. *Lessons Learned: A "who done it?" investigation in search of mistakes in laboratory methods, the solution, and resulting data.* LakeLine **38**: 38-40 See Appendix F for the print version of the article.

LakeLine Article

Lessons Learned: A "who done it?" investigation in search of mistakes in laboratory methods, the solution, and resulting data

Crime scene

"It's physically and theoretically impossible," I cautiously explained to my thesis committee member, "but the weekly results are like this consistently. What am I doing wrong?"

I knew that something had gone sideways in my laboratory analysis, but I never guessed that only one month into my graduate studies I had identified a chemistry conundrum that would follow me through the first year of my program. So, like a criminal investigator supported by the chief of police and a high-ranking forensic scientist (read: my Master's thesis advisor and chemistry-lead committee member), I set out to find and correct the error before the end of the field season.

Opening the investigation

As with every serious investigation, just as in scientific pursuits, it is critical to establish the storyline and lay out the facts. Beginning in June 2017, the Coeur d'Alene Lake Management periphyton project was established to develop and implement a periphyton monitoring method to observe potential changes in trophic status within littoral zones in the lake (Figure 4.1). Along with periphyton biomass samples from artificial substrates, weekly sampling for various water quality parameters included pH, temperature, conductivity, chlorophyll-*a*, total nitrogen, and the ever-fateful total and ortho-phosphorus samples (TP and OP, respectively).

Collected at a depth of 4 meters from near the artificial substrates, TP and OP samples were dispensed from the same Kemmerer sampler into their respective, acid-washed and native-rinsed 125 ml bottles. In the case of OP samples, water was filtered through a pre-rinsed 0.45 µm nitrocellulose filter within 15 minutes of collection prior to bottling according to common methods (SM 4500-P; APHA 2005). TP samples were preserved with sulfuric acid until digestion and OP was unpreserved but processed within 48 hours.

Laboratory methods were equally locked into place and well-worn. Generations of previous graduate students in the University of Idaho Limnology Lab had followed these lab methods for the colorimetric determination of TP and OP, although none before me had encountered my error.

Despite using routine methods, week after week the near-bottom water samples from Coeur d'Alene Lake were returning OP concentrations two to five times higher than TP samples from the same location. This, of course, was impossible. OP is a fraction of TP, and should never be higher than TP. Immediately, a list was made of possible explanations including contamination, faulty filters, minimum detection limits on the machines, etc. With a list made, the scientific process of elimination began. Contamination tests were executed on every piece of equipment and reagent present in the field or lab. Laboratory machinery was interrogated for reliability, minimum detection and reporting limits calculated, and percent recovery determined. Filters, those used by the group as well as other comparable brands, were tested on samples collected specifically for the investigation. All together, these tests yielded no reliable leads (Appendix A).

Trail growing cold

With little headway gained in that line of questioning, minute variables of the colorimetry method were tested (Appendix B). Although others before me had used non-digested standards for spectrophotometer calibration, I determined that slight changes in TP were indeed occurring with digested standards compared to non-digested standards, a method that more closely matched the sample handling methods. However, this distinction only occurred at higher concentrations than those seen in my low-level lake samples, making it a suspect without probable cause, incapable of altering my results significantly.

So, new experiments were devised to compare to historical TP and OP data available from Coeur d'Alene Lake (Appendix C). I moved along to question an expert witness, the technician from the local lab that had analyzed phosphorus samples from previous lake management projects at our site. The interview was promising but yielded few results. Detail after detail checked out and all my steps seemed to be in order, despite the technician's perfect record and my dismal one.

By fall, the case was growing as cold as the lake, signaling the end of my field season and my window to bring justice to the dataset. A year had passed and everyone in my greater

academic circle had been consulted, if not begged, for information. It seemed time to close the case file, to move on without the data and draw conclusions about water-column nutrients some other way.

New evidence

Spring came, with fresh pursuits and new cases on my academic docket. They brought with them new expert witnesses, one ultimately providing the detail that would resurrect my cold case and solve it for good. The issue of sample digestion and handling was raised while training on an automated TP method in a new lab. Groups of grad students with varying phosphorous colorimetry methods were forced to amass a lab-wide, officially accepted method and through the discussions, an idea was born. “The calibration standards! Have the standards been treated *exactly* like the lake samples?”

Like a witness casually interviewed at the scene by first responders, calibration standard handling procedures had always appeared harmless and had been taken for granted. Preservation of samples, a step unique to TP but unemployed in OP samples, had been evaluated early on. Preserved samples in split tests had shown reduced TP concentrations when preserved, but not to a level of significance necessary for a trial judge’s (or thesis advisor’s) sentencing (Appendix C). However, by my own fault, both preserved and non-preserved samples had been analyzed according to un-preserved standards in that test, the fatal mistake. Simple lab tests of the theory produced the smoking gun (Appendix D).

Case Closed

All along, TP concentrations had been suppressed when I calculated concentrations from a standard curve made with un-preserved standards—the acidity between the samples and calibrants was wildly different and falsified the relationship between concentration and measured absorbance. The suppression had caused TP values to fall below the OP values, those samples which had not been affected by the preservation mix-up because they had never been preserved.

Effectively, a year’s worth of stress had come down to the slope of a calibration line (Figure 4.2). Unpreserved standards had a steeper slope in the regression between calibrant concentration and machine-read absorbance values, meaning that for the same sample, the unpreserved standard curve resulted in a lower TP concentration than from a curve based on preserved standards.

At long last, I had my answer.

With so much time invested in this mistake, I had to ask myself, “How did this happen?” Simply, no other students following the Limnology Lab methods had ever preserved their TP samples, yet I had insisted on the practice based on recommendations from others. Despite the confusion, there was ultimately clarity, my lessons learned: in a mystery novel, never overlook the seemingly-harmless bystander. And in science, your data is only as accurate as your calibration.

Moving Forward

After the trial, it was time to reconcile my new-found knowledge to my victimized dataset. Fortunately, lab experiments showed a linear calibration relationship using preserved standards, allowing for the back-calculation of the first season’s TP values (Appendix D). Better yet, corrected TP was greater than OP in all cases except when indistinguishable by the equipment reporting limit (4.90 $\mu g \cdot L^{-1}$). In conclusion, I’d like to draw the jury’s attention to the final evidentiary exhibit, Figure 4.3, where data from a selected site displays the results of the TP back-calculation. Although unpreserved TP values hang victimized below OP for most of the summer, corrected preserved concentrations rise above, resolved.

Literature Cited

Eaton, A. D., L. S. Clesceri, E. W. Rice, and M. A. Franson. 2005. Standard methods for the examination of water and wastewater. SM4500-P. American Public Health Association, 21st ed. American Public Health Association, American Water Works Association, Water Environment Federation.

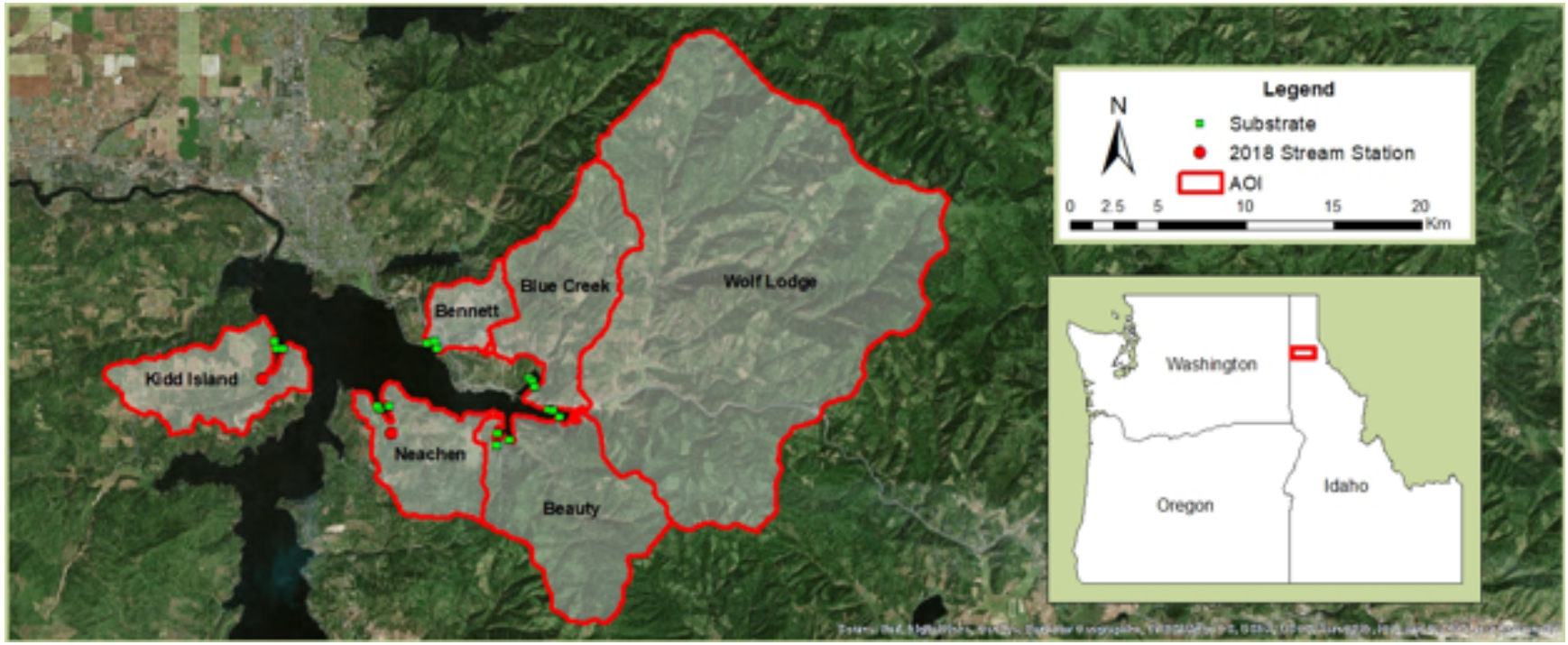

Figure 4.1: Site map of northern Coeur d'Alene Lake. Water quality and periphyton samples taken at substrate points. Area of interest (AOI) polygons represent bay watersheds generated from a 30 m DEM.

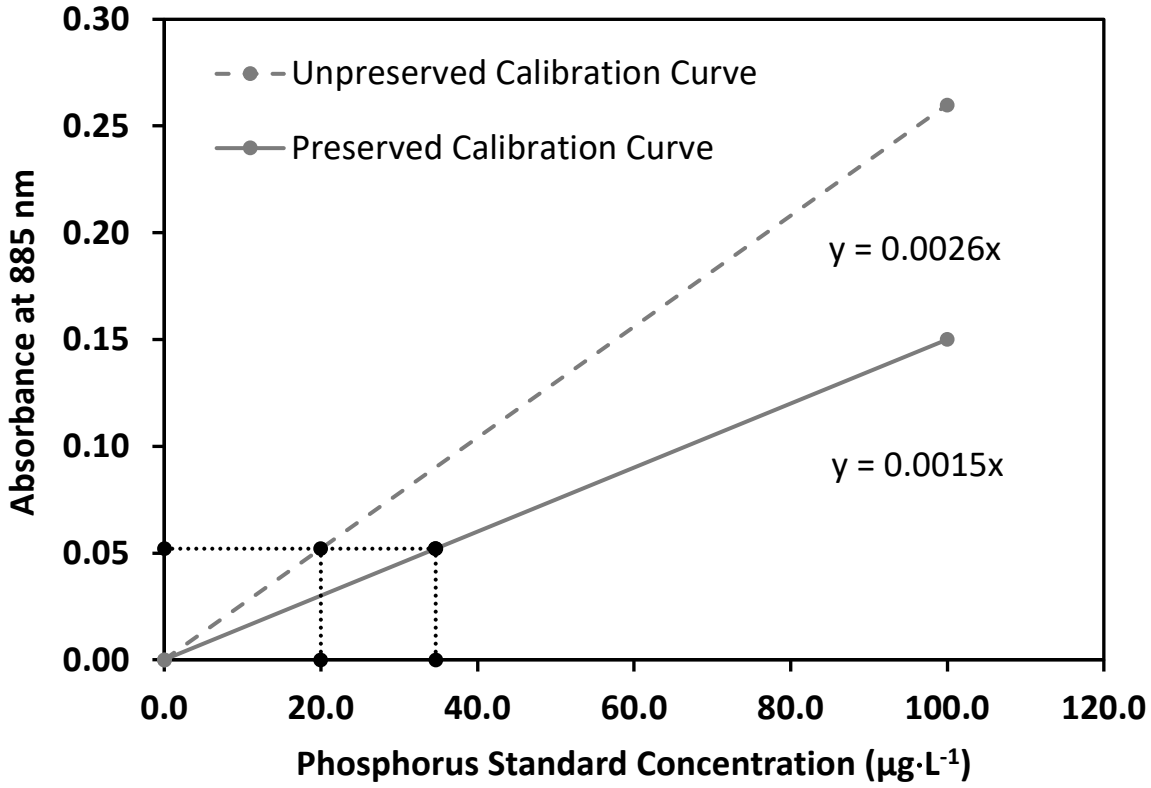

Figure 4.2: Absorbance as a function of phosphorus standard for preserved and unpreserved standards showing how preservation of standards with acid caused a suppression of absorbance.

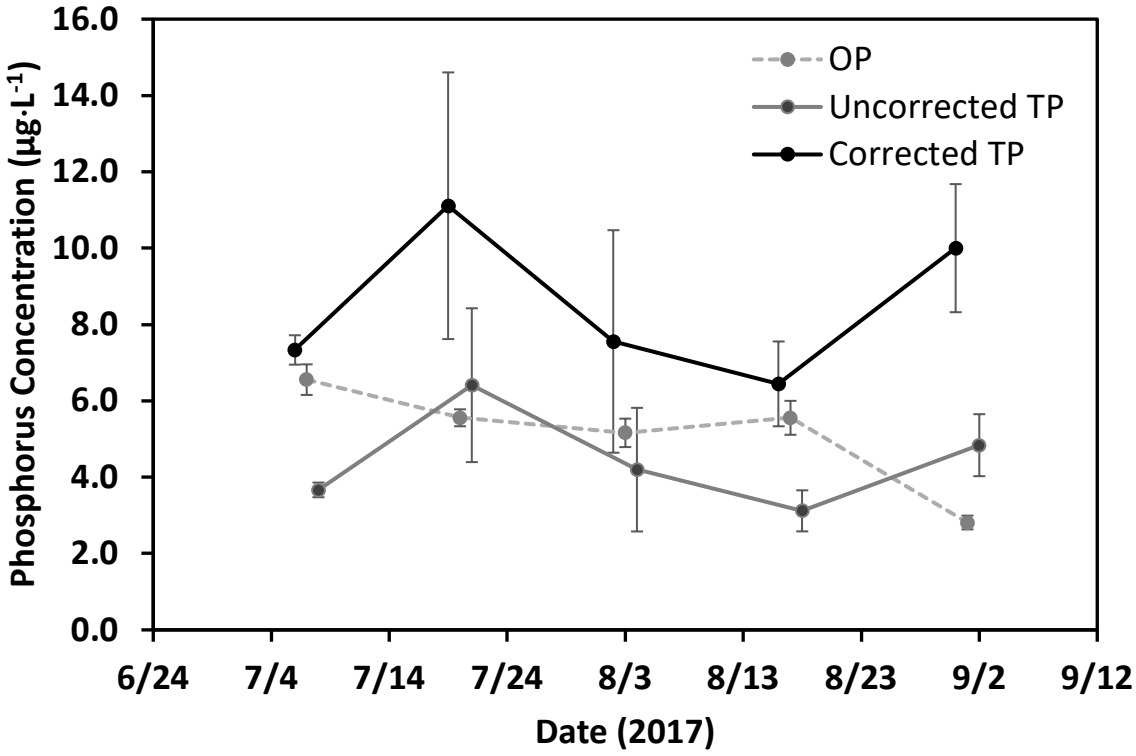

Figure 4.3: Mean ± SE (n = 3) orthophosphorus (OP) and total phosphorus (TP) concentrations for samples from Kidd Island Bay during the 2017 field season. Uncorrected refers to the original dataset calculated without preserving the calibration standards. Corrected TP refers to the back-calculated TP values using preserved calibration standards. Data points are offset in one-day increments to visualize error bars. All analyses were conducted with non-offset data. Error bars represent one standard error.

Chapter 5: Conclusion

Project summary

Coeur d'Alene Lake is a vital regional freshwater resource, benefitting the local economy, quality of life for residents, and providing habitat and ecological services to the area. Like many lakes globally, the threat of eutrophication is a concern in Coeur d'Alene Lake (Ansari et al. 2013). Studies in 1991-1992 and 2004-2006 showed that trophic level indicators such as total phosphorus concentrations and water column chlorophyll *a* had increased over time (Woods and Beckwith 1997; Wood and Beckwith 2008). Littoral zones in the bays of Coeur d'Alene Lake are likely the locations of the earliest signs of eutrophication, particularly cultural eutrophication that is tied to human activities such as shoreline development and land use changes in the watershed (Lambert et al. 2008; Rosenberger et al. 2008). In the littoral zone, nutrients deposited by streams encounter biotic and abiotic processes that influence their fate. Biologically, sediment-associated nutrients can be taken up (Loeb et al. 1983; Goldman 1988; Jacoby et al. 1991; Hadwen and Bunn 2005) and incorporated into biomass rather than being transported to the pelagic zone. Because the littoral zone functions as the first line of defense against nutrient loading to the whole lake, early changes to littoral zone dynamics in nutrients and primary producers can indicate coming changes to the main lake over time (Jacoby et al. 1991; Havens et al. 1999; Hadwen and Bunn 2005; Lambert et al. 2008; Rosenberger et al. 2008).

Periphyton, a group of primary producers in the littoral zone, theoretically function as indicators of nutrient levels because their location is stationary. Thus, they rapidly take up nutrients, and they are methodologically easy to sample, providing a straightforward indicator system. Previous studies of lakes in northern Idaho have monitored periphyton biomass to investigate if nutrient loads from watersheds negatively influenced littoral productivity (Kann and Falter 1989; Falter 2004; PBS&J 2006; PBS&J, Land & Water Consulting 2009; IDEQ 2014). The purpose of my thesis was to test the methods used in Pend Oreille Lake to see if periphyton monitoring could be used successfully in Coeur d'Alene Lake and to specifically ask if the response of periphyton was related to different land use activities in watersheds of northern bays of the lake.

Chapter review

For Chapter 2, I deployed artificial substrates in six bays of Coeur d'Alene Lake to analyze the recruitment and response characteristics of periphyton over time. The results from this experiment, chiefly the variation in slope and maximum biomass accrued on the substrates, were used to rigorously evaluate the suitability and limitations of this monitoring method in Coeur d'Alene Lake. While periphyton grew on the substrates, the rate of accrual, and final biomass did not differ between bays to a high degree of confidence, even when statistically controlling for the increase in variation in substrate biomass over time. This was surprising given the differing land uses in the watersheds, which was the impetus for their inclusion in the study. While disappointing, it indicates that this method, as used, may not be suitable to monitor the influence of nutrient transport from watersheds with different land uses to bays of Coeur d'Alene Lake. Modifications that reduce the signal-to-noise ratio could make the method suitable for use. It is also possible that a myriad of other confounding in-bay factors generated sufficient variation to obscure the link to land use and requires further investigation.

It is also interesting that none of the multi-factor models (including light availability and water chemistry) improved estimates of periphyton growth than the time-only model. This suggests that the influence of water chemistry on periphyton accrual is temporally complex. Future research should examine these relationships in more detail to identify drivers of periphyton growth. One must also remember that the discrete periphyton samples taken from the substrates represent biomass that has integrated water chemistry over time. Thus, more complex analyses that incorporate a lag time function (which were beyond the scope of this thesis) may be needed to discover underlying relationships. Two in-bay process stand out that could potentially influence such an approach as well. These are the retention time of the inflows and recreational activities. The first is important because it would determine the fate of nutrient influx to a bay and its availability to contribute to periphyton biomass via a lag effect. For example, inflow that simply passes through a bay would contribute little to local productivity compared to an inflow that deposits materials in a bay. Therefore, it is conceivable that watersheds with different land uses and different nutrient exports could result in similar biomass accrual on substrates. The latter is important as well, because it is well known that recreational activities such as boating, especially wake-boating

and jet-propelled watercraft, can resuspend sediment and associated nutrients (Hale 2018), especially during summer when inflows are low. Such activity could elevate the nutrient signal in bays and potentially mask watershed influences. These factors should be examined in detail in future studies to identify how they influence the accrual (rate and biomass) of periphyton.

In Chapter 3, watershed contribution to nutrient loading was quantified using automated samplers at Kidd and Neachen creeks during the summer of 2018. I calculated daily total phosphorus (TP) and total residue (TR) concentrations and used continuous water level data to estimate daily discharge and constituent loads for each stream. Stream discharge and loads normalized for watershed area were higher in Kidd Creek for the study period (April 28, 2018 to July 13, 2018) than in Neachen Creek. This disproportional discharge and constituent load could be reflective of the different land uses in the two watersheds; the Kidd Island Bay subwatershed was identified as having high anthropogenic activity, while the Neachen subwatershed was identified as relatively pristine with a high forest cover. Based on my analyses, I am unable to exclude potential differences in hydrology (e.g., gradient) and geology (e.g., soil type and depth) as factors besides land use that could have contributed to the higher flow and constituent load in Kidd Creek. Future research should examine such factors. In addition, my study was limited to a portion of the year rather than a full annual hydrograph, I feel that it is imperative to obtain empirical data for an entire year to accurately estimate loads to each of the bays. This should be a long-term goal of the lake monitoring program, as changes in bays and nearshore areas will occur before any change in overall trophic status is measured at offshore pelagic sites.

Individual constituent loads do not provide sufficiently robust information to predict how periphyton will respond in bays, especially considering the complexity of the bay environments. This chapter impressed the conclusion that numerous intermediate steps govern how, when, and where periphyton growth occurs in bays; and more importantly it reinforced the conclusion that the artificial substrate periphyton monitoring method is insufficient to approximate real-world primary productivity in a substantially quantifiable manner. Three substrates randomly placed in bays exhibited levels of variation sufficiently high to mask any detectable differences that may have occurred between bays overall. The Chapter 3 initial findings of differential nutrient load, although not substantial, further hint

that periphyton substrates do not represent the variation in watershed characteristics a hypothesized. Because GIS analysis in Chapter 2 and these preliminary load calculations show that sediment loads from watersheds differ, yet periphyton response did not differ between bays, it follows that critical drivers of periphyton growth were not captured in this study.

Future work

Data gaps exist with regard to the intermediate processes that influence periphyton growth, both temporally and spatially. The lag time between spring freshet and the summer growing season leaves the fate of the influx of nutrients unknown. Immediate settling of nutrients at the mouth of the stream and interception by beds of macrophytes present the initial challenges to understand nutrient dynamics in a bay. Next, fluid dynamics such as the routing of sediments as interflow, underflow, or overflow (Gustavson 1975; Wetzel 2001) governed by physics (temperature and density), as well as the temporal dynamics of bioavailability also influence the availability of nutrients to periphyton during the summer (Ellison and Brett 2006).

Approximating bay residence time using traditional equations (Pilson 1985) would provide a rough estimate of water exchange with the main lake. Bay bathymetry, a designated "end of bay" demarcation, and spatial analysis software would be needed to calculate the bay volumes required for these calculations. While residence time is an important consideration in modeling sediment retention from streams, further research into the physical limnological processes that occur within a bay during the runoff season need to be evaluated before a retention study is undertaken as the next step to understand the fate of sediments from Kidd and Neachen creeks. Water exchange with the main lake could be a major driver of sediment dynamics in a bay, but the constituents of the water leaving the bay must be known as well, not simply the water volume. Methods for determining a nutrient budget for bays, adapted from lakes with measurable stream outflows, are needed to plan a retention study to quantify nutrient flux post-runoff.

Undergraduate researcher Abigail Hale conducted interesting research in Kidd Island Bay during 2018 that informs the potential of in-bay sediment and nutrient dynamics that could influence the accrual of periphyton on artificial substrates (Hale and Whilhelm 2018). They examined the resuspension of sediment and phosphorus into the water column as a

function of boat wakes along the shoreline. Results indicated that recreational boat wakes in a bay increased total phosphorus in the nearshore environment. Periphyton substrates in the Coeur d'Alene Lake Periphyton study were placed in the shallow littoral zone near the shoreline where boat wake resuspension of nutrients could have been a factor contributing to periphyton growth. Considering the high recreational activity pressure on several of the bays in the Coeur d'Alene Lake Periphyton Study (pers. Obs.), it is possible that mixing of the shallow waters could have masked any watershed land use effects.

I also noticed that the sampling of the substrates could have introduced some variability in the data. For example, because we used an uncommonly long period of deployment, the substrates accrued high biomass, which may have been subject to soughing when I raised them to obtain samples. Sloughing of attached algae, although observed in other studies (Wood and Beckwith 2008) is relatively poorly understood and deserves further investigation. I did deploy quality control duplicate substrates in close proximity to three normal substrates in two bays with the intent to analyze potential differences between substrate biomass at the end of the season of regularly sampled and undisturbed substrates. These datasets could be useful for comparison but were beyond the scope of this work. They are available for future use. Its full analysis should be a priority before additional in-lake substrates are deployed to inform any modifications to the sampling/deployment designs. This dataset also includes transect sampling across the substrates on the last sampling date to examine potential spatial differences on the substrates themselves. This also needs to be examined to learn if the substrate size used is appropriate for Coeur d'Alene Lake; selection of the substrate size was informed by a similar study by IDEQ in Lake Pend Oreille.

Overall conclusion

This thesis details the evaluation of a novel periphyton monitoring method, particularly unique in the length of substrate deployment, substrate apparatus design and periphyton chlorophyll *a* analysis methodology. Research in this thesis also provided a single-study comparison of four key land use indicators of nutrient loading and their relationship with periphyton biomass in bays of lakes. The Idaho Department of Environmental Quality, a major partner in the funding and completion of this research, benefits from the detailed methodological evaluation that can be used to decide if and when artificial substrate periphyton monitoring should be included in regular lake monitoring

efforts. The IDEQ also benefits from the data collected regarding stream discharge and constituent loading in Kidd and Neachen creeks, which previously had few long-term hydrologic data points available for the Nutrient Inventory analysis. Furthermore, methods for the calculation of nutrient loads to bays from streams can be compared to existing methods used by the IDEQ to enhance their understanding of stream nutrient loads.

Despite the fact that the guiding hypothesis—that periphyton response in bays would vary between bays with watersheds of different anthropogenic activity—was not supported by the results in Chapter 2, supporting research completed in this study indicates that noteworthy explanatory and intermediate physical processes may be at play in masking the watershed effect on periphyton growth in bays. Several contradictory conclusions in this study warrant further analysis before the guiding hypothesis should be rejected. GIS analysis in Chapter 2 suggests that anthropogenic activity does differ between bays and may be the reason for the differential nutrient loads observed in Chapter 3. Altogether, this research project concludes that periphyton monitoring is a good indicator of early eutrophication, its application in bays of Coeur d'Alene Lake is complex and not straightforward, warranting further investigation.

Literature Cited

Ansari, A. A., S. S. Gill, and F. A. Khan. 2013. Eutrophication: Threat to aquatic ecosystems, p. 143–170. *In* A.A. Ansari, G.R. Lanza, S.S. Gill, and W. Rast [eds.], Eutrophication: Causes, consequences, and controls in aquatic ecosystems. Springer.

Consulting, P. L. & W. 2006. Water quality status and trends monitoring system for the Clark Fork-Pend Oreille watershed summary monitoring report 2006.

Ellison, M. E., and M. T. Brett. 2006. Particulate phosphorus bioavailability as a function of stream flow and land cover. **40**: 1258-1268. doi:10.1016/j.watres.2006.01.016

Falter, C. M. 2004. Lake Pend Oreille littoral periphyton community: An updated trophic status assessment. Final report submitted to the Tri-State Water Quality Council.

Goldman, C. R. 1988. Primary productivity, nutrients, and transparency during the early onset of eutrophication in ultra-oligotrophic Lake Tahoe, Califomia-Nevada. Limnol. Oceanogr. **33**: 1321–1333. doi:10.4319/lo.1988.33.6.1321

Gustavson, T. C. 1975. Sedimentation and physical limnology in proglacial Malaspina Lake, Southeastern Alaska, p. 249-263 *In* Glaciofluvial and glaciolacustrine sedimentation. *Edited by* A.V. Jopling and B.C. McDonald; Society of Economic Paleontologists and Mineralogists. Special publication. No.23. United States. ISSN: 0097-3270

Hadwen, W. L., and S. E. Bunn. 2005. Food web responses to low-level nutrient and ^{15}N-tracer additions in the littoral zone of an oligotrophic dune lake. Limnol. Oceanogr. **50**: 1096–1105. doi:10.4319/lo.2005.50.4.1096

Hale, A., and F. W. Wilhelm. 2018. Waves of phosphorus: resuspension and release by recreational boating. Department of Fish and Wildlife Sciences. Senior thesis, University of Idaho, Moscow, ID, USA.

Havens, K. E., T. L. East, S.-J. Hwang, A. J. Rodusky, B. Sharfstein, and A. D. Steinman. 1999. Algal responses to experimental nutrient addition in the littoral community of a subtropical lake. Freshw. Biol. **42**: 329–344.

IDEQ. 2014. Pend Oreille Lake productivity characterization. Idaho Dep. Environ. Qual. Rep.

Jacoby, J. M., D. D. Bouchard, and C. R. Patmont. 1991. Response of periphyton to nutrient enrichment in Lake Chelan, WA. Lake Reserv. Manag. **7**: 33–43.

doi:10.1080/07438149109354252

Kann, J., and C. M. Falter. 1989. Periphyton as indicators of enrichment in Lake Pend Oreille, Idaho. Lake Reserv. Manag. **5**: 39–48. doi:10.1080/07438148909354397

Lambert, D., A. Cattaneo, and R. Carignan. 2008. Periphyton as an early indicator of perturbation in recreational lakes. Can. J. Fish. Aquat. Sci. **65**: 258–265. doi:10.1139/f07-168

Loeb, S. L., J. E. Reuter, and C. R. Goldman. 1983. Littoral zone production of oligotrophic lakes, p. 161–167. *In* Periphyton of Freshwater Ecosystems. Springer Netherlands.

PBS&J Land & Water Consulting. 2009. Water quality status and trends in the Clark Ford-Pend Oreille watershed time trends analysis for the 1984-2007 period.

Pilson, M. E. Q. 1985. On the residence time of water in Narragansett Bay. Estuaries **8**: 2. doi:10.2307/1352116

Rosenberger, E. E., S. E. Hampton, S. C. Fradkin, and B. P. Kennedy. 2008. Effects of shoreline development on the nearshore environment in large deep oligotrophic lakes. Freshw. Biol. **53**: 1673–1691. doi:10.1111/j.1365-2427.2008.01990.x

Wetzel, R. G. 2001. Limnology, 3rd ed. Academic Press.

Wood, M. S., and M. A. Beckwith. 2008. Coeur d'Alene Lake, Idaho: Insights gained from limnological studies of 1991–92 and 2004–06. USGS Sci. Investig. Rep. 2008-5168 52.

Woods, P. F., and M. A. Beckwith. 1997. Nutrient and trace-element enrichment of Coeur d'Alene Lake, Idaho. U.S. Geol. Surv. water-supply Pap. 2485 1–93.

Appendix A - Bi-weekly water quality samples from bays of Coeur d'Alene Lake in 2017 and 2018

Table A.1: 2017 total phosphorus ($\mu g \cdot L^{-1}$) concentrations for Beauty, Bennett, and Blue Creek bays.

Date	Beauty					Bennett					Blue Creek				
	x_i	x_{ii}	x_{iii}	$\bar{x}$	± SE	x_i	x_{ii}	x_{iii}	$\bar{x}$	± SE	x_i	x_{ii}	x_{iii}	$\bar{x}$	± SE
29-Jun	15.29	14.12	12.94	14.12	0.68	10.59	14.12	12.35	12.35	1.02	13.53	14.71	14.12	14.12	0.34
13-Jul	2.35	1.18	1.76	1.76	0.34	1.18	0.00	2.35	1.18	0.68	0.59	4.12	1.76	2.16	1.04
27-Jul	6.47	10.59	7.06	8.04	1.29	4.71	7.65	5.88	6.08	0.85	8.82	10.00	8.82	9.22	0.39
9-Aug	4.71	4.71	6.47	5.29	0.59	4.12	4.71	4.71	4.51	0.20	5.88	5.29	6.47	5.88	0.34
24-Aug	4.12	8.82	5.29	6.08	1.41	4.12	2.94	2.94	3.33	0.39	4.12	7.06	4.12	5.10	0.98

Table A.2: 2017 total phosphorus ($\mu g \cdot L^{-1}$) concentrations for Kidd Island, Neachen, and Wolf Lodge bays.

	Kidd Island					Neachen					Wolf Lodge				
Date	x_i	x_{ii}	x_{iii}	$\bar{x}$	± SE	x_i	x_{ii}	x_{iii}	$\bar{x}$	± SE	x_i	x_{ii}	x_{iii}	$\bar{x}$	± SE
6-Jul	7.06	5.88	6.47	6.47	0.34	10.00	8.24	7.65	8.63	0.71	8.82	12.35	12.35	11.18	1.18
19-Jul	15.88	7.65	5.88	9.80	3.08	5.88	4.71	5.29	5.29	0.34	9.41	8.24	8.24	8.63	0.39
2-Aug	4.71	11.76	3.53	6.67	2.57	7.06	2.94	4.71	4.90	1.19	7.06	3.53	5.29	5.29	1.02
16-Aug	4.71	7.65	4.71	5.69	0.98	6.47	4.12	8.24	6.27	1.19	4.12	4.12	5.88	4.71	0.59
31-Aug	10.00	5.88	10.59	8.82	1.48	14.12	8.24	7.65	10.00	2.07	10.59	8.24	11.76	10.20	1.04

Table A.3: 2017 ortho-phosphorus ($\mu g \cdot L^{-1}$) concentrations for Beauty, Bennett, and Blue Creek bays.

	Beauty					Bennett					Blue Creek				
Date	x_i	x_{ii}	x_{iii}	$\bar{x}$	± SE	x_i	x_{ii}	x_{iii}	$\bar{x}$	± SE	x_i	x_{ii}	x_{iii}	$\bar{x}$	± SE
29-Jun	4.33	7.33	8.33	6.67	1.20	6.00	5.67	8.00	6.56	0.73	8.33	9.67	10.67	9.56	0.68
13-Jul	2.47	2.47	2.47	2.47	0.00	2.47	2.47	2.47	2.47	0.00	2.47	2.47	2.47	2.47	0.00
27-Jul	6.45	6.13	7.42	6.67	0.39	10.00	6.45	8.06	8.17	1.03	7.42	8.06	9.03	8.17	0.47
9-Aug	2.47	2.47	2.47	2.47	0.00	2.47	2.47	2.47	2.47	0.00	2.47	2.47	2.47	2.47	0.00
24-Aug	4.06	4.06	4.06	4.06	0.00	4.69	4.06	5.00	4.58	0.28	4.69	5.63	5.00	5.10	0.28

Table A.4: 2017 ortho-phosphorus ($\mu g \cdot L^{-1}$) concentrations for Kidd Island, Neachen, and Wolf Lodge bays.

	Kidd Island					Neachen					Wolf Lodge				
Date	x_i	x_{ii}	x_{iii}	$\bar{x}$	± SE	x_i	x_{ii}	x_{iii}	$\bar{x}$	± SE	x_i	x_{ii}	x_{iii}	$\bar{x}$	± SE
6-Jul	6.00	6.33	7.33	6.56	0.40	8.67	8.67	9.67	9.00	0.33	10.67	14.00	14.00	12.89	1.11
19-Jul	5.33	6.00	5.33	5.56	0.22	6.11	7.67	6.00	6.59	0.54	5.00	6.00	5.00	5.33	0.33
2-Aug	4.52	5.81	5.16	5.16	0.37	6.13	7.42	8.06	7.20	0.57	6.77	7.74	7.42	7.31	0.28
16-Aug	4.67	6.00	6.00	5.56	0.44	4.67	5.67	7.00	5.78	0.68	6.33	7.33	7.67	7.11	0.40
31-Aug	2.50	2.81	3.13	2.81	0.18	3.13	3.13	3.13	3.13	0.00	3.75	2.81	3.44	3.33	0.28

Table A.5: 2018 total phosphorus concentrations ($\mu g \cdot L^{-1}$) for Kidd Island and Neachen bays.

Date	Kidd Island					Neachen				
	x_i	x_{ii}	x_{iii}	$\bar{x}$	± SE	x_i	x_{ii}	x_{iii}	$\bar{x}$	± SE
14-Jun	9.61	9.80	9.41	9.61	0.11	11.76	6.08	8.43	8.76	1.65
28-Jun	11.76	6.08	8.43	8.76	1.65	8.82	8.04	6.08	7.65	0.82
12-Jul	4.63	4.44	3.33	4.14	0.40	7.22	4.26	4.07	5.19	1.02
26-Jul	4.07	3.52	3.15	3.58	0.27	3.70	3.33	3.70	3.58	0.12
10-Aug	4.81	6.30	3.70	4.94	0.75	7.78	4.63	5.00	5.80	0.99
23-Aug	6.11	3.52	4.26	4.63	0.77	5.37	6.67	5	5.68	0.51
6-Sep	6.3	4.07	5.49	5.29	0.65	7.06	3.33	3.33	4.58	1.24
21-Sep	4.12	3.53	4.12	3.92	0.20	4.12	5.1	3.92	4.38	0.36

Table 0.6: 2018 ortho-phosphorus concentrations ($\mu g \cdot L^{-1}$) for Kidd Island and Neachen bays.

Date	Kidd Island					Neachen				
	x_i	x_{ii}	x_{iii}	$\bar{x}$	± SE	x_i	x_{ii}	x_{iii}	$\bar{x}$	± SE
14-Jun	5.44	9.00	5.78	6.74	1.13	7.67	5.67	6.67	6.67	0.58
28-Jun	3.76	4.62	5.48	4.62	0.50	3.98	4.73	3.33	4.01	0.40
12-Jul	5.11	5.89	5.78	5.59	0.24	3.44	3.56	4.00	3.67	0.17
26-Jul	3.78	4.11	5.33	4.41	0.47	5.67	6.22	4.22	5.37	0.60
10-Aug	3.56	3.22	3.78	3.52	0.16	4.67	5.67	5.44	5.26	0.30
23-Aug	2.44	2.33	2.56	2.44	0.06	3.11	3.33	3.78	3.41	0.20
6-Sep	2.89	3.22	3.44	3.19	0.16	3.78	4	4.67	4.15	0.27
21-Sep	12.2	3.44	3.78	6.48	2.87	3.78	4.11	4.33	4.07	0.16

Appendix B - Stage-discharge relationships

The methods for this section were previously used by past MS students in the UI Limnology Laboratory (Rajkovich 2014; LaCroix 2015) to produce rating curves for each stream monitored in 2018. The rating curve estimates the relationship between creek water level (stage) and discharge. This relationship is used to interpolate continuous estimates of stream discharge from bi-weekly measured stage and discharge measurements. Stage was measured at both creeks from a metal yardstick wire-tied to a steel U-channel sign post driven into the creek bed near the automated sampler's intake hose. Discharge was measured using the traditional cross-sectional area velocity method (Rantz 1988; Rajkovich 2014; LaCroix 2015). The relationship between stage and discharge was best modeled with ordinary least squares regression according to the formula:

$$y = mx + b$$

The linear regression was completed in the statistical software R. Bi-weekly stage and discharge values measurements are shown in Table B.1. The fitted parameters for each stream's rating curve are in Table B.2. Rating curve regressions are given in Figures B.1 and B.2.

Literature Cited

LaCroix, T. 2015. A Nutrient mass balance of Fernan Lake, Idaho, and directions for future research. MS thesis, University of Idaho, Moscow, ID, USA.

Rajkovich, H. 2014. Research in the Willow Creek watershed: Estimates of sediment and phosphorus loads from sub-catchments; gauging public response to a constructed wetland; and a quantitative assessment of a conceptual constructed wetland. MS thesis, University of Idaho, Moscow, ID, USA.

Rantz, S. E. et al. 1988. Measurement and computation of streamflow: Volume 1. Measurement of stage and discharge. U.S. Geological Survey. Water-supply paper 2175.

Table B.1: Stage and discharge values measured bi-weekly at the Kidd Island and Neachen Bay stream sites in 2018. Both streams were not always serviced on the same day, so "-" days indicate that the stream was not measured on that date.

Date	Kidd		Neachen	
	Stage (m)	Discharge ($m^3 \cdot sec^{-1}$)	Stage (m)	Discharge ($m^3 \cdot sec^{-1}$)
4/7/18	0.508	0.198	-	-
4/19/18	0.533	0.217	-	-
4/28/18	-	-	0.267	0.161
5/3/18	0.406	0.026	-	-
5/18/18	0.305	0.026	0.206	0.043
5/30/18	0.356	0.005	0.159	0.012
6/15/18	0.343	0.003	0.178	0.008
6/29/18	0.330	0.002	0.146	0.004
7/13/18	0.321	0.028	0.137	0.002

Table B.2: Fitted parameters for rating curves used to calculate continuous discharge. The equation takes the form y=mx+b.

Stream	Slope	95% CI	Intercept	95% CI	R^2	N	P
Kidd	-0.31	(0.29, 0.37)	0.95	(-0.45, -0.16)	0.85	8	<0.001
Neachen	-0.18	(-0.29, -0.07)	1.21	(0.63, 1.79)	0.87	6	0.005

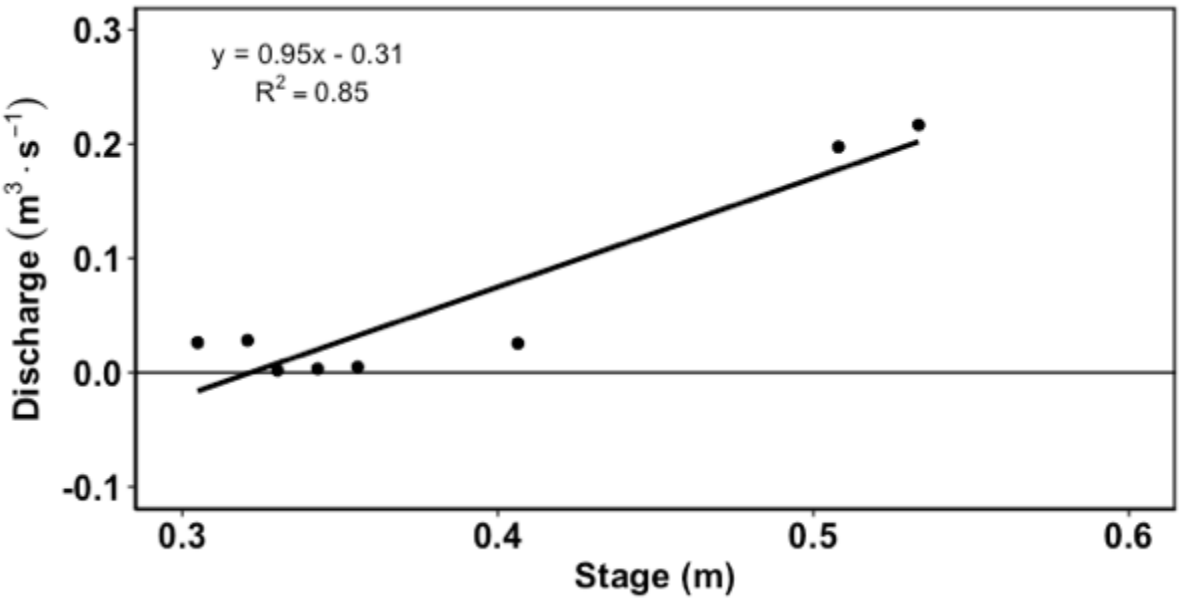

Figure B.1: Rating curve for Kidd Creek at Kidd Island Bay. Ordinary least squares regression of discharge as a function of time (y=mx+b) is shown as the solid line.

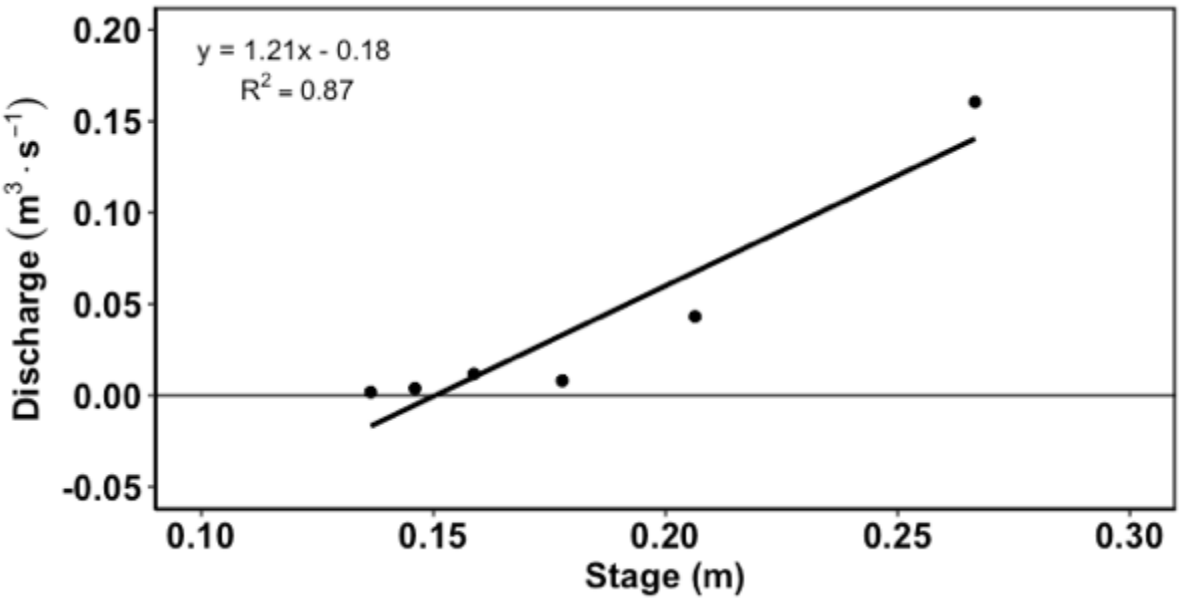

Figure B.2: Rating curve for Neachen Creek at Neachen Bay. Ordinary least squares regression of discharge as a function of time (y=mx+b) is shown as the solid line.

Appendix C - Daily stream TP data including instantaneous sample concentrations and estimated daily loads

Table C.5: Total phosphorus (TP) data from Kidd and Neachen creeks for 2018. TP in $\mu g \cdot L^{-1}$ is the instantaneous concentrations of each day's water sample. Estimated TP loads were calculated using the smearing method. Neachen was not sampled until April 28, 2018.

	Kidd			Neachen		
Date	TP $\mu g \cdot L^{-1}$	± SE	Est. TP load $kg \cdot day^{-1}$	TP $\mu g \cdot L^{-1}$	± SE	Est. TP load $kg \cdot day^{-1}$
7-Apr	75.51	2.33	6.37	-	-	-
8-Apr	120.64	18.58	6.19	-	-	-
9-Apr	80.38	1.39	5.57	-	-	-
10-Apr	70.13	1.58	5.39	-	-	-
11-Apr	68.72	0.92	5.21	-	-	-
12-Apr	189.36	1.12	5.76	-	-	-
13-Apr	87.18	5.16	5.53	-	-	-
14-Apr	74.23	2.50	5.44	-	-	-
15-Apr	84.49	1.12	5.53	-	-	-
16-Apr	206.54	8.77	6.99	-	-	-
17-Apr	106.41	5.21	6.12	-	-	-
18-Apr	82.88	1.35	5.59	-	-	-
19-Apr	151.03	8.30	5.25	-	-	-
20-Apr	61.79	1.43	5.17	-	-	-
21-Apr	60.77	0.22	4.94	-	-	-
22-Apr	58.59	2.27	5.09	-	-	-
23-Apr	63.72	2.19	5.29	-	-	-
24-Apr	72.69	1.35	5.08	-	-	-
25-Apr	66.92	2.14	4.31	-	-	-
26-Apr	67.18	0.71	4.22	-	-	-
27-Apr	69.19	4.00	3.35	-	-	-
28-Apr	71.67	1.22	3.49	77.26	2.02	0.80
29-Apr	64.36	2.24	3.63	30.40	4.51	0.82
30-Apr	64.23	1.46	3.94	29.87	1.07	0.89
1-May	65.26	0.71	3.72	27.20	3.45	0.83
2-May	67.31	0.44	3.86	37.87	1.99	0.87
3-May	124.10	2.18	4.05	38.13	0.48	0.92
4-May	50.77	1.02	4.05	41.87	0.96	0.94
5-May	50.64	0.71	4.01	43.20	0.83	0.91
6-May	46.28	4.04	3.98	40.13	1.57	0.79
7-May	51.92	1.02	4.10	40.40	1.97	0.95
8-May	51.67	2.68	4.32	39.73	1.04	0.86
9-May	48.08	2.12	5.74	47.73	2.02	0.76
10-May	50.13	1.34	6.96	45.47	0.81	0.75
11-May	52.69	1.55	7.82	36.00	1.01	0.81

Table C.1 Continued

	Kidd			Neachen		
Date	TP $\mu g \cdot L^{-1}$	± SE	Est. TP load $kg \cdot day^{-1}$	TP $\mu g \cdot L^{-1}$	± SE	Est. TP load $kg \cdot day^{-1}$
12-May	51.28	0.68	7.92	37.07	0.35	0.74
13-May	54.74	1.48	7.37	41.87	0.48	0.69
14-May	52.44	0.46	6.62	41.73	0.71	0.71
15-May	53.21	1.56	6.03	40.67	1.48	0.62
16-May	57.05	1.48	5.69	40.80	0.23	0.61
17-May	56.79	1.86	5.57	39.07	1.16	0.65
18-May	114.55	3.56	5.36	87.33	6.98	0.72
19-May	56.25	1.27	4.76	40.93	2.98	0.71
20-May	60.69	5.08	3.92	33.87	3.54	0.70
21-May	61.67	4.81	3.36	30.57	2.39	0.70
22-May	55.69	1.19	3.07	34.14	1.77	0.69
23-May	57.08	0.64	2.78	32.99	0.41	0.69
24-May	51.53	1.32	3.12	34.14	1.58	0.69
25-May	50.28	1.81	2.93	34.37	1.69	0.68
26-May	58.47	2.64	3.11	35.17	1.50	0.68
27-May	60.14	2.17	3.54	33.22	4.14	0.67
28-May	61.11	3.57	3.27	28.16	2.99	0.67
29-May	61.11	0.77	2.99	34.60	0.23	0.67
30-May	146.67	3.35	2.81	67.82	1.81	0.59
31-May	55.14	1.14	2.70	31.26	0.11	0.51
1-Jun	54.72	2.05	2.75	29.66	0.53	0.80
2-Jun	65.69	1.08	2.79	31.38	1.24	0.88
3-Jun	61.39	1.60	2.83	30.00	0.69	0.64
4-Jun	54.44	0.77	2.88	30.23	0.94	0.61
5-Jun	54.86	0.14	2.92	30.23	1.33	0.64
6-Jun	56.53	1.14	2.96	30.92	1.44	0.61
7-Jun	45.14	10.30	3.01	36.78	0.61	0.56
8-Jun	48.89	0.14	3.05	36.44	0.57	0.61
9-Jun	70.14	0.37	3.10	39.66	2.74	0.59
10-Jun	53.75	2.68	3.15	45.29	2.38	0.68
11-Jun	50.28	0.61	3.19	31.26	0.46	0.73
12-Jun	56.11	1.53	3.24	26.55	1.11	0.75
13-Jun	52.15	0.73	3.28	30.11	1.78	0.53
14-Jun	50.67	3.10	3.33	31.84	2.59	0.62
15-Jun	107.99	3.58	3.32	71.33	8.14	0.56
16-Jun	58.72	2.86	3.34	31.07	2.36	0.64
17-Jun	51.15	1.15	3.31	29.33	1.14	0.66

Table C.1 Continued

	Kidd			Neachen		
Date	TP $\mu g \cdot L^{-1}$	± SE	Est. TP load $kg \cdot day^{-1}$	TP $\mu g \cdot L^{-1}$	± SE	Est. TP load $kg \cdot day^{-1}$
18-Jun	40.51	3.82	3.33	28.27	1.62	0.71
19-Jun	36.67	1.68	3.32	40.00	0.40	0.80
20-Jun	35.26	1.05	3.34	35.87	1.04	0.73
21-Jun	45.75	6.60	3.37	38.27	1.27	0.70
22-Jun	71.87	10.94	3.34	36.67	0.27	0.71
23-Jun	61.20	1.06	3.32	28.40	0.83	0.72
24-Jun	63.60	3.49	3.33	27.33	2.74	0.72
25-Jun	44.40	2.89	3.30	44.53	9.14	0.60
26-Jun	51.87	0.35	3.30	34.27	2.70	0.75
27-Jun	42.67	2.13	3.33	33.07	1.54	0.64
28-Jun	42.93	6.63	3.29	21.47	0.48	0.61
29-Jun	107.15	6.47	3.22	42.27	4.22	0.61
30-Jun	42.99	2.70	3.14	19.43	0.41	0.63
1-Jul	49.31	3.81	3.16	29.20	0.50	0.64
2-Jul	141.03	18.57	3.16	31.84	2.24	0.63
3-Jul	41.26	0.70	3.11	27.82	0.30	0.62
4-Jul	36.67	0.61	3.09	27.01	0.80	0.61
5-Jul	35.86	0.91	3.15	23.68	0.41	0.63
6-Jul	48.28	4.14	3.15	20.00	2.60	0.63
7-Jul	31.84	1.28	3.16	16.90	0.40	0.63
8-Jul	28.97	1.63	3.10	17.13	0.41	0.61
9-Jul	26.78	1.44	3.12	38.16	3.06	0.61
10-Jul	28.16	0.41	3.16	21.84	2.85	0.63
11-Jul	33.91	2.22	3.13	18.05	0.75	0.62
12-Jul	41.61	0.30	3.13	16.78	0.41	0.62
13-Jul	139.64	1.98	3.09	59.71	4.02	0.72

Appendix D - Daily stream TR data including instantaneous sample concentrations and estimated daily loads

Table D.1: Total residue (TR) data from Kidd and Neachen creeks for 2018. TR in $mg \cdot L^{-1}$ is the instantaneous concentrations of each day's water sample. Estimated TR loads were calculated using the smearing method. Neachen was not sampled until April 28, 2018.

	Kidd		Neachen	
Date	TR $mg \cdot L^{-1}$	Est. TR load $tonnes \cdot day^{-1}$	TR $mg \cdot L^{-1}$	Est. TR load $tonnes \cdot day^{-1}$
7-Apr	124.6	10.80	-	-
8-Apr	179.5	10.62	-	-
9-Apr	151.4	9.83	-	-
10-Apr	112.0	9.58	-	-
11-Apr	104.0	9.35	-	-
12-Apr	161.5	10.06	-	-
13-Apr	120.5	9.76	-	-
14-Apr	111.7	9.66	-	-
15-Apr	109.1	9.77	-	-
16-Apr	258.2	11.58	-	-
17-Apr	157.0	10.53	-	-
18-Apr	134.2	9.85	-	-
19-Apr	219.2	9.40	-	-
20-Apr	112.3	9.30	-	-
21-Apr	110.8	8.98	-	-
22-Apr	127.0	9.19	-	-
23-Apr	113.5	9.45	-	-
24-Apr	112.0	9.17	-	-
25-Apr	121.1	8.12	-	-
26-Apr	112.3	8.01	-	-
27-Apr	105.7	6.75	-	-
28-Apr	113.2	6.96	92.31	2.98
29-Apr	109.3	7.16	70.13	3.03
30-Apr	107.9	7.62	88.77	3.13
1-May	119.5	7.30	59.90	3.04
2-May	115.4	7.49	80.52	3.10
3-May	123.9	7.77	102.56	3.17
4-May	121.1	7.77	98.28	3.19
5-May	108.3	7.71	71.79	3.15
6-May	109.9	7.66	93.51	2.99
7-May	80.0	7.83	114.44	3.21
8-May	97.2	8.13	98.73	3.08
9-May	100.5	10.04	107.69	2.94
10-May	112.8	11.57	68.42	2.93

Table D.1 Continued

	Kidd		Neachen	
Date	TR $mg \cdot L^{-1}$	Est. TR load $tonnes \cdot day^{-1}$	TR $mg \cdot L^{-1}$	Est. TR load $tonnes \cdot day^{-1}$
11-May	130.8	12.60	78.95	3.01
12-May	121.1	12.73	91.14	2.91
13-May	160.0	12.06	89.19	2.84
14-May	136.2	11.15	91.67	2.87
15-May	123.3	10.41	109.33	2.71
16-May	117.8	9.98	102.63	2.70
17-May	128.9	9.81	107.04	2.77
18-May	222.6	9.55	196.23	2.88
19-May	115.6	8.75	125.00	2.86
20-May	123.9	7.57	102.50	2.85
21-May	125.7	6.76	115.00	2.86
22-May	127.8	6.33	98.80	2.83
23-May	110.1	5.88	92.96	2.83
24-May	117.1	6.40	89.33	2.83
25-May	107.2	6.11	100.00	2.82
26-May	112.3	6.40	88.61	2.81
27-May	128.7	7.03	76.92	2.79
28-May	124.7	6.64	81.01	2.79
29-May	97.6	6.21	96.20	2.79
30-May	242.1	5.93	180.33	2.65
31-May	104.0	5.77	90.91	2.51
1-Jun	93.3	5.83	88.31	2.99
2-Jun	106.8	5.90	89.74	3.11
3-Jun	106.9	5.97	88.24	2.74
4-Jun	93.3	6.04	75.95	2.70
5-Jun	116.2	6.10	86.08	2.74
6-Jun	66.7	6.17	77.72	2.69
7-Jun	116.0	6.24	79.60	2.60
8-Jun	125.0	6.31	93.51	2.70
9-Jun	122.7	6.38	93.75	2.66
10-Jun	109.6	6.45	93.33	2.81
11-Jun	123.3	6.52	85.71	2.90
12-Jun	116.8	6.59	84.62	2.92
13-Jun	112.9	6.65	90.91	2.55
14-Jun	126.0	6.72	73.75	2.71

Table D.1 Continued

	Kidd		Neachen	
Date	TR $mg \cdot L^{-1}$	Est. TR load $tonnes \cdot day^{-1}$	TR $mg \cdot L^{-1}$	Est. TR load $tonnes \cdot day^{-1}$
15-Jun	240.1	6.71	202.50	2.61
16-Jun	126.7	6.74	81.01	2.74
17-Jun	117.6	6.69	120.00	2.79
18-Jun	103.2	6.72	98.73	2.86
19-Jun	115.9	6.71	101.99	3.00
20-Jun	123.5	6.74	80.00	2.90
21-Jun	120.1	6.78	97.99	2.85
22-Jun	124.6	6.74	91.67	2.86
23-Jun	122.2	6.72	82.87	2.89
24-Jun	124.0	6.72	108.94	2.87
25-Jun	114.3	6.68	130.00	2.68
26-Jun	134.3	6.68	108.75	2.93
27-Jun	113.3	6.72	92.31	2.75
28-Jun	110.5	6.67	93.15	2.69
29-Jun	226.4	6.55	199.06	2.59
30-Jun	117.8	6.44	106.33	2.73
1-Jul	115.5	6.47	106.17	2.74
2-Jul	144.4	6.48	88.10	2.74
3-Jul	125.3	6.38	101.27	2.71
4-Jul	111.4	6.36	87.50	2.69
5-Jul	118.8	6.45	87.80	2.73
6-Jul	114.3	6.46	94.53	2.73
7-Jul	111.9	6.47	86.96	2.73
8-Jul	85.2	6.38	102.34	2.70
9-Jul	104.3	6.40	130.43	2.71
10-Jul	110.2	6.48	96.20	2.74
11-Jul	128.6	6.42	93.83	2.72
12-Jul	131.4	6.42	101.99	2.72
13-Jul	-	6.36	-	2.70

Appendix E - Calculation of seasonal total phosphorus (TP) and total residue (TR) loads using the smearing method (Duan 1983)

The following method for the smearing approach (Duan 1983; Collin 1995; Helsel and Hirsch 2002) comes from previous work completed by MS students in the UI Limnology Laboratory (Rajkovich 2014; LaCroix 2015). LaCroix corrected the printed equation in 2015 and care should be taken to use it in place of the version printed in Rajkovich (2014). The correct equation is:

$$Load = exp[\beta_0 + \beta_1 \ln(Q)] \times \frac{\sum_{i=1}^{n} \exp(e_i)}{n}$$

Where Q is discharge ($m^3 \cdot sec^{-1}$), e_i are the residuals of the regression of the natural log of instantaneous load ($mass \cdot sec^{-1}$) by $\ln(Q)$, n is the number of residuals, β_1 is the slope of the regression, and β_0 is the intercept. β_1 and β_0 are sub-catchment-specific fitted parameters (Table E.1). This method calculates daily loads interpolated from instantaneous loads, which are the product of the day's sample concentration (mass of TP or TR per liter) multiplied by the instantaneous discharge at the time of sample collection ($L \cdot sec^{-1}$). Continuous discharge is calculated using the parameters of the stream's stage-discharge relationship as outlined in Appendix A.

TP (Figures E.1 and E.2) and TR (Figures E.3 and E.4) were plotted as a function of discharge to estimate their linear relationship for each stream. The fitted parameters (Table E.2) of this relationship were applied to continuous discharge data to calculate 15-minute interval TP and TR loads. Interval loads were summed per day and finally by season the season dated April 28 to July 13, 2018.

Literature Cited

Cohn, T. A. 1995. Recent advances in statistical methods for the estimation of sediment and nutrient transport in rivers, U.S. National Report to the International Union Geodesy and Geophysics 1991–1994, Reviews of Geophysics, Supplement., **33**: 1117–1123.

Duan, N. 1983. Smearing estimate: A nonparametric retransformation method. Source J. Am. Stat. Assoc. **78**: 605-610.

Helsel, D. R., and R. M. Hirsch. 2002. Statistical methods in water resources, *In* Techniques of Water-Resources Investigations of the United States Geological Survey: Book 4, Hydrologic Analysis and Interpretation.

LaCroix, T. 2015. A nutrient mass balance of Fernan Lake, Idaho, and directions for future research. MS thesis, University of Idaho, Moscow, ID, USA.

Rajkovich, H. 2014. Research in the Willow Creek watershed: Estimates of sediment and phosphorus loads from sub-catchments; gauging public response to a constructed wetland; and a quantitative assessment of a conceptual constructed wetland. MS thesis, University of Idaho, Mosscow, ID, USA.

Table E.1: Fitted parameters, bias-correction factor and R^2 values used in the Smearing Method (Duan 1983) calculation of cumulative total phosphorus load (tonnes).

Location	β_0	β_1	Bias-correction factor	R^2
Kidd	11.31	1.84	1.07	0.44
Neachen	10.83	1.54	1.05	0.22

Table E.2: Fitted parameters, bias-correction factor and R^2 values used in the Smearing Method (Duan 1983) calculation of cumulative total residue load (tonnes).

Location	β_0	B_1	Bias-correction factor	R^2
Kidd	11.84	1.34	1.024	0.54
Neachen	11.11	0.60	1.025	0.09

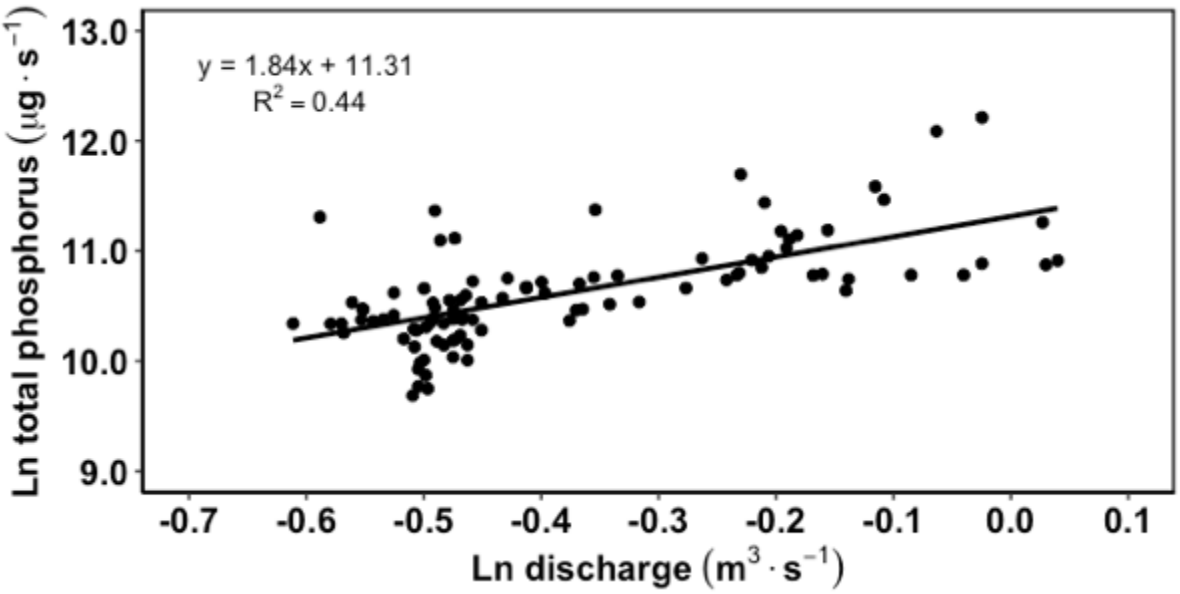

Figure E.1: Natural log of total phosphorus as a function of Ln discharge for Kidd Creek at Coeur d'Alene, Lake during the study period which occurred from April 7, 2018 to July 13, 2018.

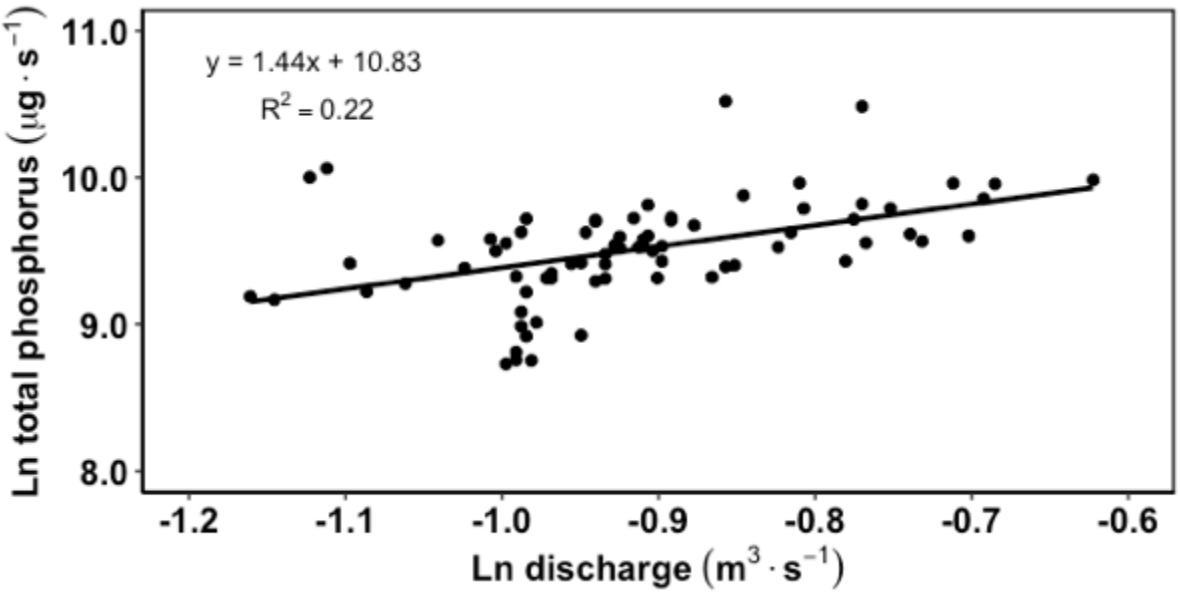

Figure E.2: Natural log of total phosphorus as a function of Ln discharge for Neachen Creek at Coeur d'Alene, Lake during the study period which occurred from April 28, 2018 to July 13, 2018.

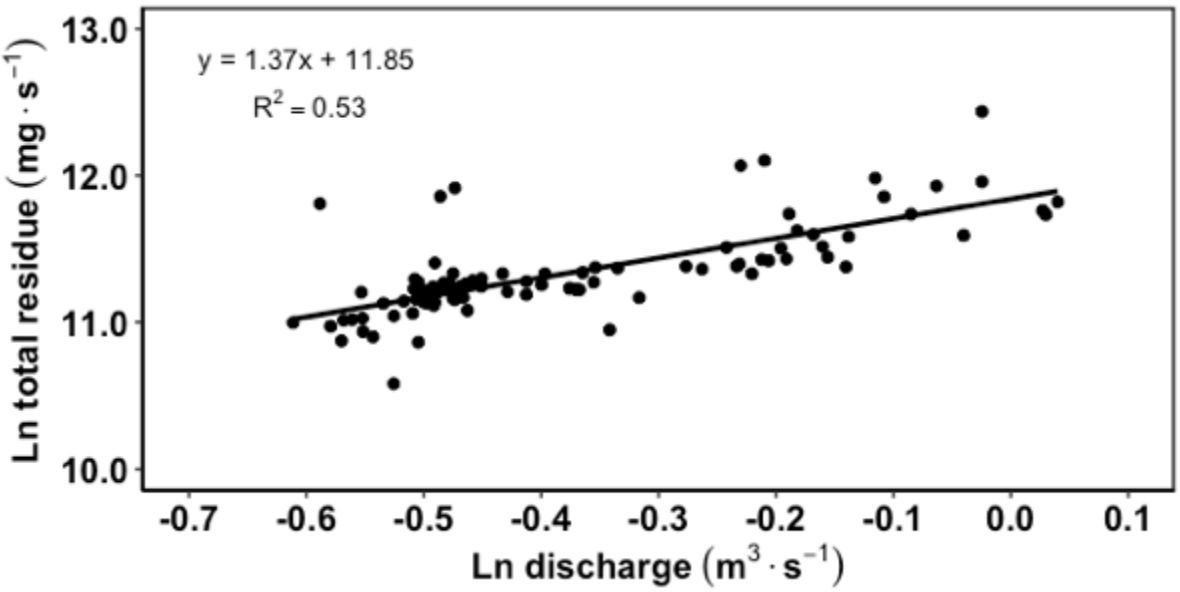

Figure E.3: Natural log of total residue as a function of Ln discharge for Kidd Creek at Coeur d'Alene, Lake during the study period which occurred from April 7, 2018 to July 13, 2018.

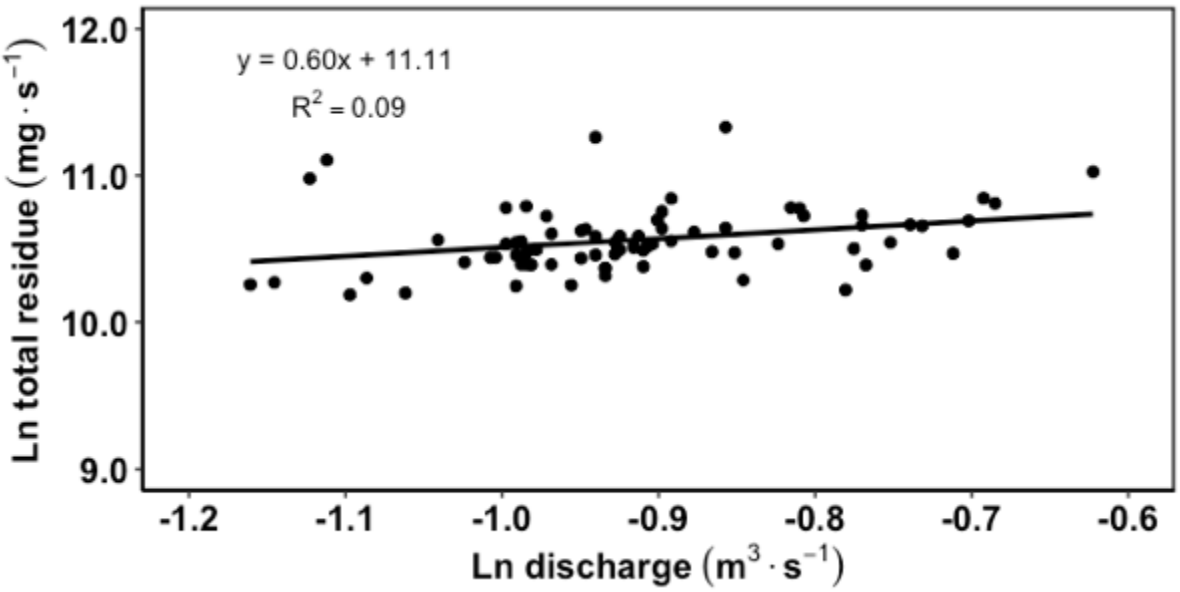

Figure E.4: Natural log of total residue as a function of Ln discharge for Neachen Creek at Coeur d'Alene, Lake during the study period which occurred from April 28, 2018 to July 13, 2018.

Appendix F - LakeLine Article

The following document is the PDF version of the printed LakeLine article contained in Chapter 4: Total phosphorus chemistry. The full-print version was included as an appendix because formatting and presentation are important factors in the process of displaying scientific material for a mixed audience. The full citation is "Notte, R. 2018 Lessons Learned: A "who done it?" investigation in search of mistakes in laboratory methods, the solution, and resulting data. LakeLine **38**: 38-40." Permission for publication of the full-print article in this thesis was given by Amy Smagula, editor of LakeLine, through email correspondence (Figure F.1).

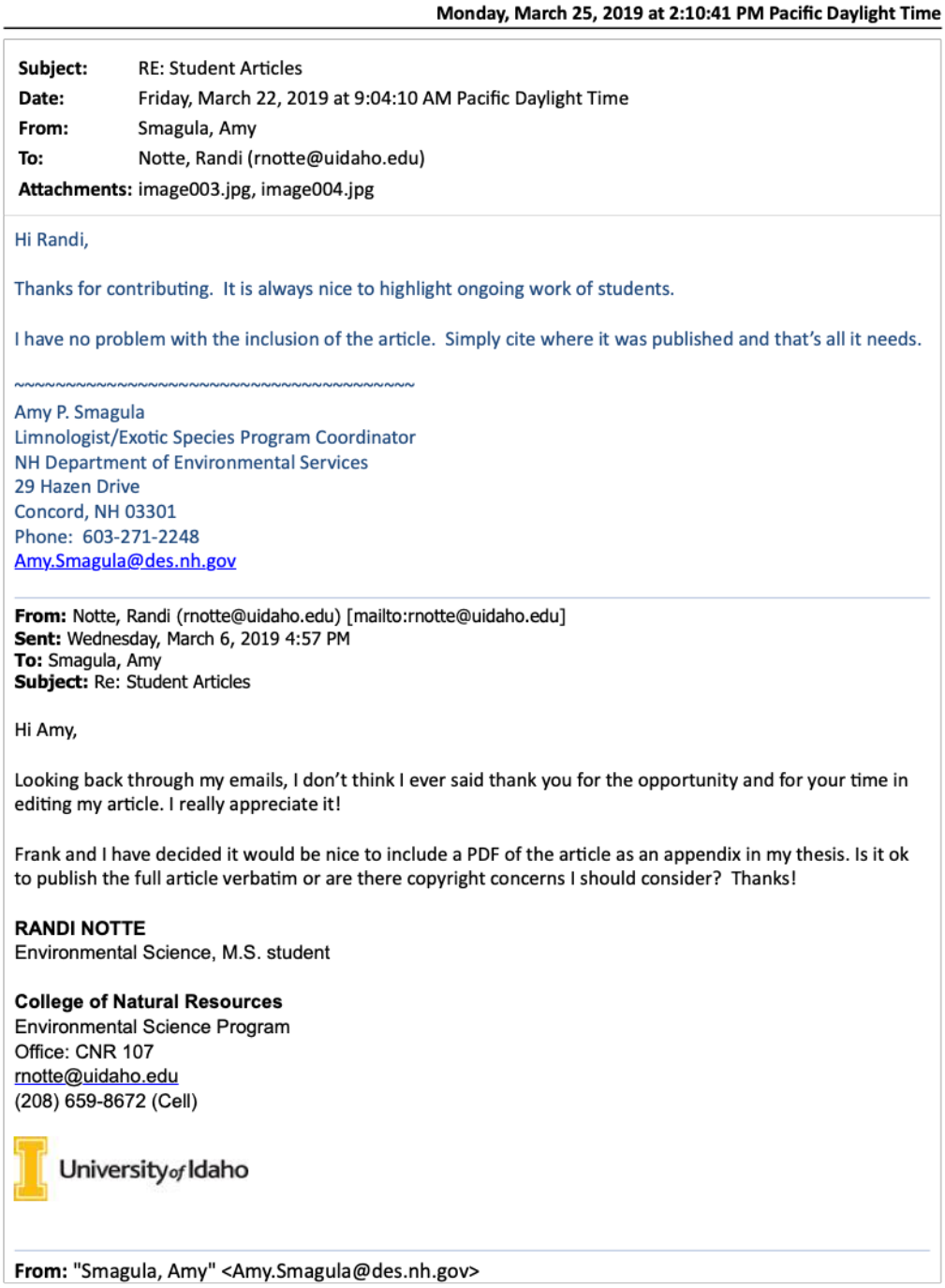

Monday, March 25, 2019 at 2:10:41 PM Pacific Daylight Time

Subject: RE: Student Articles
Date: Friday, March 22, 2019 at 9:04:10 AM Pacific Daylight Time
From: Smagula, Amy
To: Notte, Randi (rnotte@uidaho.edu)
Attachments: image003.jpg, image004.jpg

Hi Randi,

Thanks for contributing. It is always nice to highlight ongoing work of students.

I have no problem with the inclusion of the article. Simply cite where it was published and that's all it needs.

~~~~~~

Amy P. Smagula
Limnologist/Exotic Species Program Coordinator
NH Department of Environmental Services
29 Hazen Drive
Concord, NH 03301
Phone: 603-271-2248
Amy.Smagula@des.nh.gov

From: Notte, Randi (rnotte@uidaho.edu) [mailto:rnotte@uidaho.edu]
Sent: Wednesday, March 6, 2019 4:57 PM
To: Smagula, Amy
Subject: Re: Student Articles

Hi Amy,

Looking back through my emails, I don't think I ever said thank you for the opportunity and for your time in editing my article. I really appreciate it!

Frank and I have decided it would be nice to include a PDF of the article as an appendix in my thesis. Is it ok to publish the full article verbatim or are there copyright concerns I should consider? Thanks!

RANDI NOTTE
Environmental Science, M.S. student

College of Natural Resources
Environmental Science Program
Office: CNR 107
rnotte@uidaho.edu
(208) 659-8672 (Cell)

University of Idaho

From: "Smagula, Amy" <Amy.Smagula@des.nh.gov>

Page 1 of 6

Figure F.1: Copyright letter from publisher releasing article for full-print inclusion in this thesis document.
~~~~~~

Randi Notte

Student Corner

Lessons Learned: A "who done it?" investigation in search of mistakes in laboratory methods, the solution, and resulting data

Crime scene

"It's physically and theoretically impossible," I cautiously explained to my thesis committee member, "but the weekly results are like this consistently. What am I doing wrong?"

I knew that something had gone sideways in my laboratory analysis, but I never guessed that only one month into my graduate studies I had identified a chemistry conundrum that would follow me through the first year of my program. So like a criminal investigator supported by the chief of police and a high-ranking forensic scientist (read: my Master's Thesis advisor and chemistry-lead committee member), I set out to find and correct the error before the end of the field season.

Opening the investigation

As with every serious investigation, just as in scientific pursuits, it is critical to establish the storyline and lay out the facts. Beginning in June 2017, the Coeur d'Alene Lake Management periphyton project was established to develop and implement a periphyton monitoring method to observe potential changes in trophic status within littoral zones in the lake (Figure 1). Along with periphyton biomass samples from artificial substrates, weekly sampling for various water quality parameters included pH, temperature, conductivity, chlorophyll-*a*, total nitrogen, and the ever-fateful total and ortho-phosphorus samples (TP and OP samples, respectively).

Collected at 4 meters near the substrate surface, TP and OP samples were dispensed from the same Kemmerer sampler into their respective, acid-washed and native-rinsed 125 ml bottles. In the case of OP samples, water was filtered through a pre-rinsed 0.45 um nitrocellulose filter within 15 minutes of collection prior to bottling according to common methods (SM 4500-P; Eton et al. 2005). TP samples were preserved with sulfuric acid until digestion and OP was unpreserved but processed within 48 hours.

Laboratory methods were equally locked into place and well-worn. Generations of previous graduate students in the University of Idaho Limnology Lab had followed these lab methods for the colorimetric determination of TP and OP, although none before me had encountered my fatal error.

Despite using routine methods, week after week the near-bottom water samples from Coeur d'Alene Lake were returning OP concentrations two to five times higher than TP samples from the same location. This, of course, is impossible. OP is a fraction of TP, and should never be higher than TP. Immediately, a list was made of possible explanations including contamination, faulty filters, and minimum detection limits on the machines, etc. With a list made, the scientific process of elimination began. Contamination tests were executed on every piece of equipment

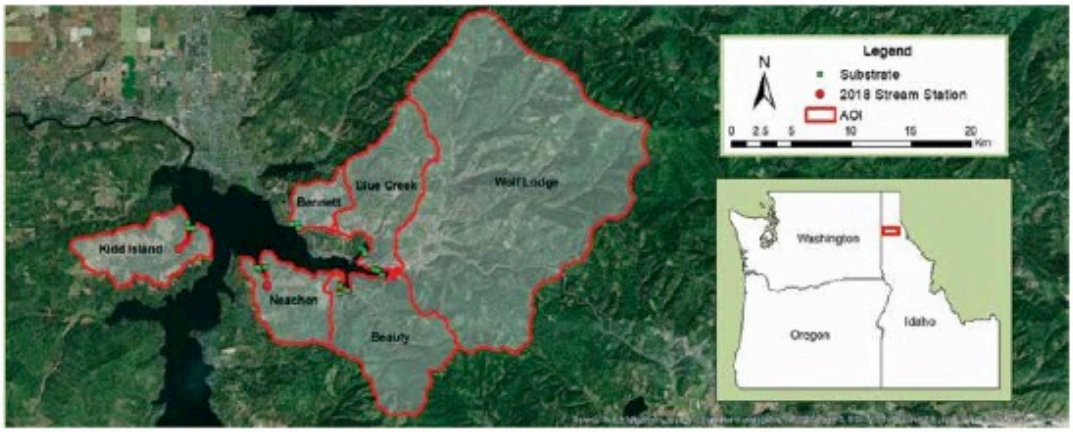

Figure 1. Site Map Water chemistry samples collected from substrate locations. Bay watersheds indicated as polygons.

Figure F.2: LakeLine article from Notte, R. 2018. *LakeLine* **38**: 38-41.

and reagent present in the field or lab. Laboratory machinery was interrogated for reliability, minimum detection and reporting limits calculated and percent recovery determined. Filters, those used by the group as well as other comparable brands, were tested on samples collected specifically for the investigation. All together, these tests yielded no reliable leads.

Trail growing cold

With little headway gained in that line of questioning, minute variables of the colorimetry method were tested. Although others before me had used non-digested standards for spectrophotometer calibration, I determined that slight changes in TP were indeed occurring with digested standards compared to non-digested standards, a method that more closely matched the sample handling methods. However, this distinction only occurred at higher concentrations than those seen in my low-level lake samples, making it a suspect without probable cause, incapable of altering my results significantly.

So, new experiments were devised to compare to historical TP and OP data available from Coeur d'Alene Lake. I moved along to question an expert witness, the technician from the local lab that had analyzed phosphorus samples from previous lake management projects at our site. The interview was promising but yielded few results. Detail after detail checked out and all my steps seemed to be in order, despite the technician's perfect record and my dismal one.

By fall, the case was growing as cold as the lake, signaling the end of my field season and my window to bring justice to the dataset. A year had passed and everyone in my greater academic circle had been consulted, if not begged, for information. It seemed time to close the case file, to move on without the data and draw conclusions about water-column nutrients some other way.

New evidence

Spring came, with fresh pursuits and new cases on my academic docket. They brought with them new expert witnesses, one ultimately providing the detail that would resurrect my cold case and solve it for good. The issue of sample digestion and handling was raised while training on an automated TP method in a new lab. Groups of grad students with varying phosphorous colorimetry methods were forced to amass a lab-wide, officially accepted method and through the discussions, an idea was born. "The calibration standards! Have the standards been treated *exactly* like the lake samples?"

Like a witness casually interviewed at the scene by first responders, calibration standard handling procedures had always appeared harmless and had been taken for granted. Preservation of samples, a step unique to TP but unemployed in OP samples, had been evaluated early on. Preserved samples in split tests had shown reduced TP concentrations when preserved, but not to a level of significance necessary for a trial judge's (or thesis advisor's) sentencing. However by my own fault, both preserved and non-preserved samples had been analyzed according to un-preserved standards in that test, the fatal mistake. Simple lab tests of the theory produced the smoking gun.

Case closed

All along, TP concentrations had been suppressed while I ran preserved samples on an un-preserved standard curve – the acidity between the samples and calibrants was wildly different and falsified the relationship between concentration and measured absorbance. The suppression had caused TP values to fall below the OP values, those samples which had not been affected by the preservation mix-up because they had never been preserved to begin with.

Effectively, a year's worth of stress had come down to the slope of a calibration line (Figure 2). Unpreserved standards had a steeper slope in the regression between calibrant concentration and machine-read absorbance values, meaning that for the same sample, the unpreserved standard curve calculated a lower TP concentration than a preserved standard curve would.

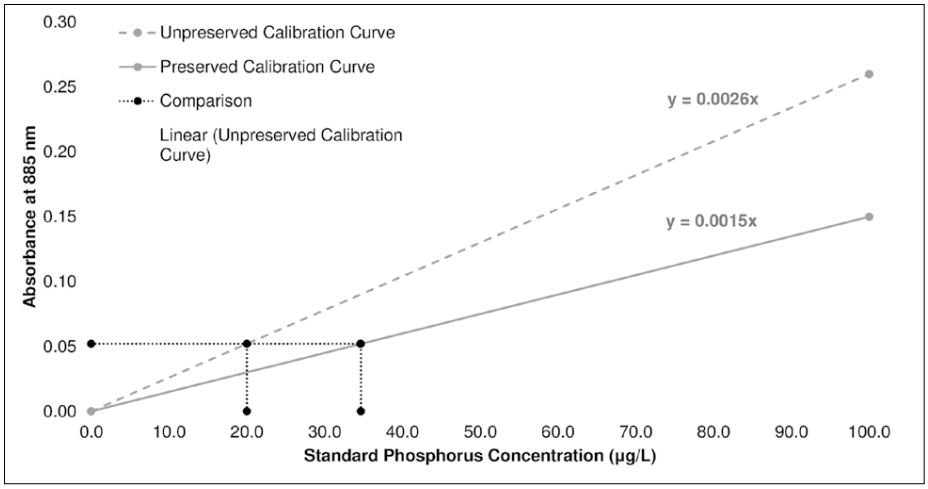

Figure 2. Effects of standard preservation on calculated phosphorus concentration When absorbance is held constant, total phosphorus concentration is lower (suppressed) when calculated on an unpreserved standard curve.

At long last, I had my answer. With so much time invested in this fatal mistake, I had to ask myself,

Figure F.2 Continued

"How did this happen?" Simply, no other students following the Limnology Lab methods had ever preserved their TP samples, yet I had insisted on the practice based on recommendations from others. Despite the confusion there was ultimately clarity, my lessons learned: In a mystery novel, never overlook the seemingly harmless bystander. And in science, your data is only as accurate as your calibration.

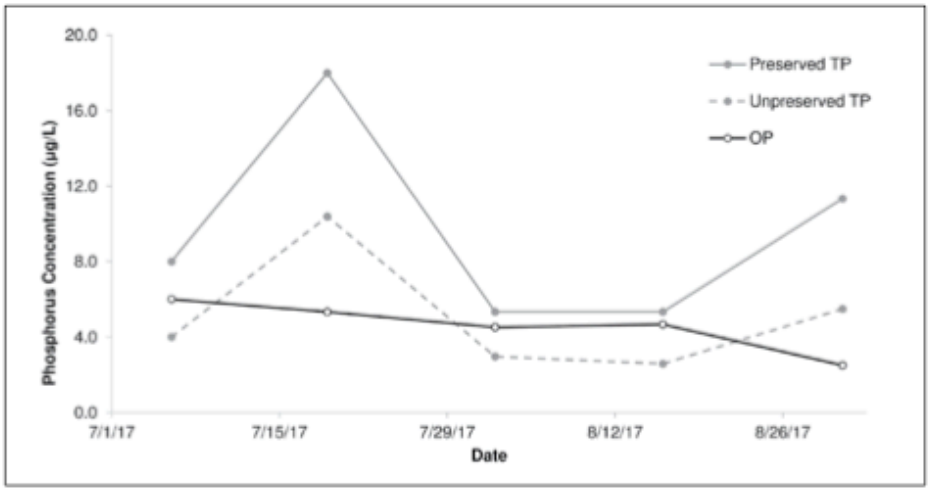

Figure 3. Corrected TP values Nutrient concentrations given for an example site over the course of the 2017 field season.

Moving forward

After the trial, it was time to reconcile my new-found knowledge to my victimized dataset. Fortunately, lab experiments showed a linear calibration relationship using preserved standards, allowing for the back-calculation of the first season's TP values. Better yet, corrected TP was greater than OP in all cases except when indistinguishable by the equipment reporting limit (4.90 mg/L). In conclusion, I'd like to draw the jury's attention to the final evidentiary exhibit, Figure 3, where data from a selected site displays the results of TP back-calculation. Although unpreserved TP values hang victimized below OP for most of the summer, corrected preserved concentrations rise above, resolved.

References

Eaton, A.D., L.S. Clesceri, E.W. Rice, A.E. Greenburge, and M.A.H. Franson. (SM 4500-P). 2005. *Standard Methods for the Examination of Water and Wastewater*. 21st ed. American Public Health Association, American Water Works Association, Water Environment Federation.

Randi Notte earned her B.S. in environmental science from Northern Arizona University in 2016. She now studies as a Master's student in environmental science at the University of Idaho, conducting research on Coeur d'Alene Lake where she focuses on littoral periphyton response to nutrient loading.

Figure F.2 Continued

Appendix G - (Casefile 1) Quality assurance/quality control investigations

Quality assurance (QA) protocols and tests are used to ensure data quality during sample collection and handling. Although similar, quality control (QC) measures differ in that they are used during the analysis process to control for methodological variables that may affect the accuracy or precision of the analysis. For example, protocols and tests to minimize the risk of equipment contamination are considered QA. Including calibration-check standards between regular water samples during total phosphorus (TP) analysis is an example of quality control. During the course of the periphyton study, an unidentified chemistry problem arose causing ortho-phosphate (OP) samples to have higher concentrations than co-collected TP samples, which is impossible. The following tests and QA/QC measures were enacted for corrective action.

Equipment contamination

Given the sensitivity of the method used for the low concentrations of P in the water samples from Coeur d'Alene Lake, in this study, it was important to rule out potential sources of contamination as quickly as possible. Laboratory contamination tests were run first to isolate equipment without introducing the aspect of potential field contamination. Field tests were added as a critical quality assurance protocol starting on July 14, 2017 and were executed weekly.

Methods

Laboratory testing occurred on July 11, 2017 at the UI Limnology Lab. Common equipment used for sample collection and processing were randomly selected for contamination testing. Four of each of the following products were tested in this trial: nitrocellulose filters (MilliporeSigma™ HAWP04700), plastic filter holders, plastic 60 ml syringes (BD®), 120 ml plastic sample bottles, and 10 ml pipette tips (FINNTIP® virgin polypropylene, Fisher Cat. No. 9402151). Filters and pipette tips were all new, while the other items were previously used and acid-washed (0.1 N HCl) according to lab protocols. One of each item was grouped into a "unit" and used to process distilled deionized water referred to as "blank water", from the Barnstead NANOpure LMX13 deionizer in room

216D. The machine sensor displayed 18.2 MΩ-cm, which is satisfactory for deionization standards.

Processing occurred as follows. Blank water was dispensed into a cleaned, acid-washed 1000 ml glass beaker. A filter, filter holder, and syringe were assembled using blank-rinsed forceps and gloved hands. According to SM.4500-P B.1, blank water was then syringed through the filter unit to pre-rinse the filter (Eaton et al. 2005). This rinse water was used to pre-rinse the 120 ml sample bottle twice, mimicking field methods. Next, new blank water was syringed from the 1000 ml beaker and 120 ml of sample was dispensed from the filter unit into the pre-rinsed sample bottle. The bottle was capped and shaken for eight seconds, then a new pipette tip was used to transfer 20 ml of sample into each of three glass test tubes containing 2 g of potassium persulfate. Samples were capped, shaken, digested, and tested according to normal lab protocols for total phosphorus analysis.

In addition, to examine potential contamination in glassware, four 150 ml glass beakers were randomly selected from the acid-washed glassware cabinet outside of room 216D. Blank water (120 ml) was pipetted into each beaker, swirled, and then transferred into glass test tubes for processing along with the other samples.

Field contamination test methods are borrowed from the IDEQ's regular monitoring methods and QA/QC plan (Woods and Beckwith 1997; Wood and Beckwith 2008). On a weekly basis in 2017, the final sample of the day was run as a "field blank" whereby 20 L of Type II distilled water was processed according to sampling procedures, including sample collection (USGS 2006). In this way, blank water came into contact with the Kemmerer sampler, churn splitter, and the filtering equipment listed above. These samples were processed in-batch with regular lake samples and the results over two seasons are included below. After contamination was suspected as a potential cause of the chemistry problem, field blanks were conducted during every 2017 sampling event starting on July 14th, for a total of seven out of ten trips. Field blanks were also conducted twice out of eight trips in 2018 on July 12th and August 10th.

Results and Verdict

Of the four units tested, two had concentrations of 1.38 and 1.58 $\mu g \cdot L^{-1}$, which is greater than the MDL (1.23 $\mu g \cdot L^{-1}$) but less than the reporting limit of 2.47 $\mu g \cdot L^{-1}$. Although some samples were found to have non-zero blank water concentrations, this equipment was

rejected as the source of error because the discrepancy between OP and TP samples was typically at least 3-5 $\mu g \cdot L^{-1}$, which was several micrograms higher than the minor variation found in this trial. No beakers had average TP concentrations greater than the MDL. Low level laboratory contamination plus field contamination was considered as a possibility, however, the probability of contamination in both sectors for every sample was impossible.

None of the field blank samples collected in 2017 or 2018 (n = 9) had TP concentrations higher than the MDL (1.23 $\mu g \cdot L^{-1}$). One triplicate sample on August 10, 2018 was 1.30 $\mu g \cdot L^{-1}$, but the triplicate sample average was 0.58$\mu g \cdot L^{-1}$ (See Table G.1 for field blank results). These field and laboratory tests for contamination strengthened the conclusion that contamination was not the source of the issue.

Filter efficacy

Filtration of lake water samples through a 0.45 µm membrane filter is included in all three commonly used determination methods by the U.S. Environmental Protection Agency, Standard Methods, and Silver Valley Labs (EPA, SM, and SVL). However, brand, diameter, and filter unit type are not specified. After discussion with DEQ employees, it came to light that other brands of filters were used during monitoring by IDEQ. One model (MDI Membrane FLTR MDI NYLN 25mm 0.45 µm) was used by Total Maximum Daily Load (TMDL) teams in North Idaho and screws directly into a threaded syringe. In collaboration with DEQ, we predicted that filter type could have influenced the ortho-phosphate concentration in the samples due to either contamination, effective pore size, clogging rate, or degree of cell lysis due to differences in pressure needed to force water through the filter. The screw-on filters clogged quickly requiring them to be replaced during filtering of single samples, hence the selection of the larger diameter nitrocellulose filters used in the UI protocol.

Methods

Due to limited supplies, I was only able to test three screw-on filters. One sample was collected at Bennet Bay Site 1 and the other at Beauty Bay Site 2. On July 27, 2017, 6.2 L lake water were collected from a depth of 4 m and homogenized in a churn splitter after which it was filtered using two different filters (MDI Membrane FLTR MDI NYLN 25mm 0.45 µm, and MilliporeSigma™ HAWP04700) and dispensed into individually labelled and

pre-rinsed acid-washed collection bottles. Pre-rinsing included flushing 100 ml of water through the filter and into the sample bottles. Care was taken to only filter 100 ml of sample water through the screw-on filter to avoid premature clogging. Samples were stored, processed, and analyzed with the rest of the water samples from the field day. To determine if concentrations of OP differed by filter type, OP concentrations were first compared using an F-test to determine variance equality, followed by a one-sided t-test.

Results and Verdict

The mean OP concentration for the nitrocellulose filter used in the UI protocol was 7.50 $\mu g \cdot L^{-1} \pm$ 0.38 $\mu g \cdot L^{-1}$(mean±SE), while the IDEQ screw-on filters yielded a concentration of 9.03 $\mu g \cdot L^{-1} \pm$ 0.32 $\mu g \cdot L^{-1}$. The variance was homogeneous (F-test, F= 19.16, d.f.= 3, P = 0.37), but the means differed (One-tailed t-test, T = -2.92, d.f. = 5, P = 0.02). The concentration at Bennett Bay Site 1 with the UI nitrocellulose filtered sample was 10.00 $\mu g \cdot L^{-1}$OP. This sample was not run in triplicate and therefore lacks a standard error calculation. The DEQ screw-on filtered sample had a concentration of 5.81 $\mu g \cdot L^{-1}$OP (± 0.67 $\mu g \cdot L^{-1}$ SE) at Beauty Bay Site 2. In this case, the findings were reversed with the UI filter yielding higher TP.

These results were inconclusive because of the conflicting concentration differences. Filter preference stayed with the UI nitrocellulose filters because they were less likely to clog. The IDEQ's filters clogged easily and often necessitated heavy force on the syringe to complete filtration of a sample. Doing so introduced the possibility of filter rupture, allowing passage of particles, or the rupture of cells, which could add additional P to the filtrate. Overall, filter type was rejected as the cause of the chemistry problem.

Machine minimum detection and reporting limits

For this study it was important to determine the minimum detection and reporting limits (MDL and RL, respectively) of the spectrophotometer, and therefore the method in general at the UI, because determining low concentrations of P in samples requires careful attention to details. However, because low-level samples had not been encountered or analyzed by previous generations of graduate students in the UI Limnology Lab, they had not been addressed in the standard methods used for OP and TP. Professional and EPA certified labs include specialty requirements in their standard operating procedures for low-level

samples. For example, Silver Valley Laboratories, Inc. (SVL) completes low-level samples by analyzing duplicate split samples run in triplicate (n = 6) (SVL 2014, see SVL methods line 8.2). The test was executed according to the EPA's Definition and Procedure for the Determination of the Method Detection Limit, Revision 2 using the methods to compute the MDL based on spiked samples (USEPA 2016).

Methods

The MDL test was conducted in the UI Limnology Lab on August 3, 2017 on the Thermo-Scientific AquaMate VIS visible-light spectrophotometer with a 5 cm glass cuvette using stock standards used regularly for P analysis. Care was taken to ensure that standards were not older than six months, the storage life of standards used in the UI Limnology Lab (SVL 2014, see SVL methods line 6.8). Twenty ml of each standard were transferred to clean, acid-washed glass test tubes and digested in the presence of 0.2 g of potassium persulfate at 207 kPa (30 PSI) for 20 minutes. One of each calibration standard (0.0, 2.0, 5.0, 10.0, 20.0, and 100.0 $\mu g \cdot L^{-1}$ P), seven 0.0 $\mu g \cdot L^{-1}$ P blank water standards, and seven 2.0 $\mu g \cdot L^{-1}$ P standards (further referred to as "0 standards" and "2 standards") were included.

Two $\mu g \cdot L^{-1}$ was selected as the baseline sample based on SVL instructions to choose a sample concentration as low as presumed detectable by the method, but no lower. SVL's MDL is 1.0 µg·L-1 , so I chose 2.0 $\mu g \cdot L^{-1}$ as my target because I had less experience with the method. Choosing a 2.0 $\mu g \cdot L^{-1}$ standard does not restrict the MDL to ≥ 2.0 $\mu g \cdot L^{-1}$ but allows the test to better approximate the test values.

After calibrating normally using the digested standards, 0 standards and 2 standards were tested alternately starting with a 0 standard. SVL warned to color only the number of samples that could be read on the spectrophotometer in less than 20 minutes after the addition of the mixed reagent, according to previous SVL lab trials of the method. In this MDL test, eight samples were colored and read, then the final six were colored and read. Next, the standard deviation of the 2 standards (EPA: "spiked samples") was calculated. Finally, the MDL was calculated in $\mu g \cdot L^{-1}$ using the following formula (EPA 1978):

$$MDL_s = t_{(n-1,\ 1-\alpha=0.99)} S_s$$

Where:

t = the student's t-value for a one-sided 99th percentile t-statistic (see Table G.2 below, copied from EPA Addendum Table 1, EPA 1978),

S_s = the standard deviation of the spiked samples (µg·L)

Results and Verdict

The MDL and RL for the OP and TP determination by spectrophotometry for the UI Limnology Lab was calculated as:

$$MDL_s = 3.143 \times 0.40\ \mu g/L = 1.27\ \mu g/L \text{ and,}$$

$$RL_s = 2(MDL_s) = 2.54\ \mu g/L$$

These limits were considered sufficient for the low-level conditions expected to occur in samples from Coeur d'Alene Lake. They also were lower than SVL employees predicted possible for a new technician running the methods for the first time. Reaching 1.0 µg·L^{-1} from 2.0 µg·L^{-1} required several years of refining, yet we were able to reach an MDL under 2.0 µg·L^{-1} in our first season. Should the MDL and RL have been higher than the OP and TP concentrations generated by the method in the lab, the data would not have been viable. However, OP and TP levels were typically above the reporting limit. In general, OP samples from Coeur d'Alene Lake are below SVL's reporting limit of 2.0 µg·L^{-1}, which was the initial indicator of the overall chemistry problem. Moving forward, quality control samples employed in OP and TP determination were compared to an MDL of 1.27 µg·L^{-1} and RL of 2.54 µg·L^{-1}.

Technician accuracy

One reasonable explanation for the overall chemistry problem could have been inaccuracy of the technician (me). Previous graduate students had succeeded with the method, so it was possible that I was completing the method erroneously in some way. To test this hypothesis, I ran split samples with another graduate student and compared results.

Methods

Nine samples were tested by each technician (Technician 1 = Sarah Burnet; Technician 2 = me) on July 2, 2018. The samples included four field-collected samples from Willow Creek Reservoir (WCR), OR, two standard ATP solutions (10.0 and 100.0 µg·L^{-1} P), one Continuing Calibration Blank (0.0 µg·L^{-1} P), and two Continuing Calibration Verification samples (15.0 and 100.0 µg·L^{-1} P). WCR samples were analyzed in triplicate, while the other samples were analyzed run in duplicate. Both technicians used the same stock calibration standards (0.0, 15.0, 30.0, 100.0, 200.0, and 400.0 µg·L^{-1} P).

Each technician independently completed the entire UI Limnology Lab method for the determination of total phosphorus by spectrophotometry. Samples and calibration standards were not preserved with sulfuric acid before analysis. WCR samples were pipetted from the same sample bottle. Other test standards (ATP solutions, blanks, and standards) were created by Technician 2 and used by both technicians. Following processing, results generated by each technician were compared using a one-sided paired t-test.

Results and Verdict

Concentrations for individual samples are listed in Table G.3. Results from the t-test show that there is no significant difference in concentrations generated between technicians (t-test, T = 1.06, d.f. = 8, P = 0.16). Because sample concentrations did not vary between technicians, it was concluded that user error was not the cause of the chemistry problem.

Percent sample recovery

Analytical chemistry methods often include percent recovery of the sample analyte as a quality control measure. A percent recovery experiment tests if a sufficient amount of analyte is detected in a sample during the analysis and should ideally be 100%. An important consideration in percent recovery is matrix interference, whereby constituents of the sample solution interfere with the accuracy of the analysis method. In the case of phosphorus determination by spectrophotometry, high turbidity, iron, arsenates, and hexavalent chromium are known to cause matrix interferences (SM4500-P E.1; APHA 2005). The following experiment was used to test the recovery of stock phosphorus *in situ*, fulfilling the quality control method for percent recovery described in SVL Analytical, EPA 365.3, and SM 4500-P E (EPA 1978; APHA 2005; SVL 2014).

Methods

Percent recovery was calculated once each for OP and TP during 2017 using matrix spikes. The sample from Blue Creek Bay Site 1 (Blu1) from September 13, 2017 was used to test the OP method, while the sample from Neachen Bay Site 2 (N2) from August 17, 2017 was used to test the TP method. The matrix spike method for percent recovery includes the addition of concentrated stock solution to a sample of unknown concentration. In this experiment, 1.5 ml of 100.0 $\mu g \cdot L^{-1}$ P stock solution was added to 18.5 ml of lake water sample. This combination is referred to as the "matrix spike sample." A regular, non-spiked

sample is run following the normal procedure and to determine the concentration of the unknown sample portion of the matrix spike sample. Both samples were processed according to normal handling procedure (i.e., TP samples were digested with persulfate) and then analyzed with the spectrophotometer. Finally, percent recovery was calculated with the following formulae (Dugan 2000):

$$\%\ Recovery = \frac{Observed\ Concentration}{Theoretical\ Concentration} \times\ 100$$

Where,

$$Theoretical\ Concentration = \frac{C_u V_u + C_s V_s}{V_u V_s}$$

And:

C_u = Concentration of unknown sample (µg·L^{-1})

V_u = Volume of the unknown sample in the matrix spiked sample (L)

C_s = Concentration of the spike (µg·L^{-1})

V_s = Volume of the spike (L) (equals total volume of matrix spiked sample)

For example, using the OP matrix spike from Blu1 on September 14, 2017; the matrix spike sample consisted of 18.5 ml of unknown concentration (Blu1) plus 1.5 ml of 100.0 µg·L^{-1} P stock solution. Upon completion, the unknown Blu1 concentration was 3.13 µg·L^{-1} P and the concentration of the matrix spike sample was 10.73 µg·L^{-1} P. The calculation of percent recovery was as follows:

$$Theoretical\ Concentration$$

$$= \frac{C_u V_u + C_s V_s}{V_u V_s}$$

$$= \frac{(3.13\ \mu g/L \times\ 0.0185\ L) + (100.0\ \mu g/L \times\ 0.0015\ L)}{(0.0185\ L + 0.0015\ L)}$$

$$= 10.395\ \mu g/L$$

So,

$$\%\ Recovery$$

$$= \frac{Observed\ Concentration}{Theoretical\ Concentration} \times\ 100$$

$$= \frac{10.73\ \mu g/L}{10.395\ \mu g/L} \times\ 100$$

$$= 103\%$$

Results and Verdict

According to SVL Analytical's phosphorus determination methods, percent recovery must be within 25% of the expected value (SVL 2014, see SVL method line 13.6). Both samples passed, with OP percent recovery at 103% and TP at 92%. For a summary table of parameters used to calculate percent recovery for both tests see Table G.4. Because each method passed quality control for percent recovery, the potential loss of phosphorus from samples during analysis was rejected as the cause of the overall chemistry problem.

Literature Cited

Dugan, M. 2000. Field Training Manual for Laboratory Analysts. [Online] http://home.windstream.net/mikeric/Chap1to9/Chap5QualityControls.htm (Accessed January 9, 2019).

Eaton, A. D., L. S. Clesceri, E. W. Rice, and M. A. Franson. 2005. Standard methods for the examination of water and wastewater. SM4500-P. American Public Health Association, 21st ed. American Public Health Association, American Water Works Association, Water Environment Federation.

EPA. 1978. Method 365.3: Phosphorous, all forms (colorimetric, ascorbic acid, two reagent). U.S. Environmental Protection Agency.

SVL Analytical. 2014. Total phosphorus (aqueous samples) by SM 4500 P E. Silver Valley Analytical, Inc. Version 16. 1–20.

USGS. 2006. Collection of water samples (ver. 2.0): U.S. Geological Survey techniques of water-resources investigations, book 9, chap. A4, *In* National Field Manual for the Collection of Water-Quality Data (NFM). Book 9.

Wood, M. S., and M. A. Beckwith. 2008. Coeur d'Alene Lake, Idaho: Insights gained from limnological studies of 1991–92 and 2004–06. USGS Sci. Investig. Rep. 2008-5168 52.

Woods, P. F., and M. A. Beckwith. 1997. Nutrient and trace-element enrichment of Coeur d'Alene Lake, Idaho. U.S. Geol. Surv. water-supply Pap. 2485 1–93.

Table G.1: Field blank total phosphorus concentrations for 2017 and 2018 contamination tests. Zero samples resulted in blank water concentrations greater than the 1.23 $\mu g \cdot L^{-1}$ minimum detection limit. Samples were analyzed in triplicate and concentrations are reported in $\mu g \cdot L^{-1}$. The sample mean and standard error are represented by $\bar{x}$ and SE, respectively.

Date	x_i	x_{ii}	x_{iii}	$\bar{x}$	SE
7/14/17	-0.04	-0.09	-2.20	-0.78	0.71
7/27/17	0.00	0.74	0.37	0.37	0.21
8/2/17	-1.11	-0.37	-1.11	-0.86	0.25
8/9/17	0.00	0.00	0.00	0.00	0.00
8/17/17	0.97	0.65	0.97	0.86	0.11
8/22/17	-0.94	0.00	0.00	-0.31	0.31
8/31/17	0.97	0.65	0.97	0.86	0.11
9/13/17	0.94	0.94	0.94	0.94	0.00
8/10/18	0.43	1.30	0.00	0.58	0.38
7/12/18	0.45	0.91	0.91	0.76	0.15

Table G.2: Student's t-values for the one-sided 99th percentile *t*-statistic (Copied from EPA method paper Addendum Table 1, EPA 1978)

Number of replicates (n)	Degrees of freedom (n-1)	$t_{(n-1, 0.99)}$
7	6	3.143
8	7	2.998
9	8	2.896
10	9	2.821
11	10	2.764
16	15	2.602
21	20	2.528
26	25	2.485
31	30	2.457
32	31	2.453
48	47	2.408
50	49	2.405
61	60	2.390
64	63	2.387
80	79	2.374
96	95	2.366
100	99	2.365

Table G.3: Technician accuracy test results. Values represent average total phosphorus concentration in $\mu g \cdot L^{-1}$. WCR stands for Willow Creek Reservoir. "0m" samples were collected at a depth of 0 m, "8m" at 8 m, and "15m" at 15 m. "1×" and "2×" represent dilution factors. ATP10 and ATP100 represent ATP solutions of 10.0 and 100.0 $\mu g \cdot L^{-1}$ P, respectively. CCB refers to a blank standard of 0.0 $\mu g \cdot L^{-1}$. CCV15 and CCV100 represent stock solutions of 15.0 and 100.0 $\mu g \cdot L^{-1}$. Samples with ± values were tested in triplicate and represent one standard error.

Sample	Technician 1	Technician 2
WCR 0m	37.65	37.59
WCR 8m	29.88 ± 0.004	27.41 ± 0.001
WCR 15m 1×	71.98 ± 0.004	79.26 ± 0.002
WCR 15m 2×	42.10 ± 0.009	40.37 ± 0.001
ATP10	7.96	11.67
ATP100	31.85	46.11
CCB	4.63	0.74
CCV15	22.04	14.26
CCV100	80.00	98.15

Table G.4: Parameters used to calculate percent recovery of phosphorus during TP and OP analysis. Refer to the methods of this test for description of formulae and variables.

Parameter	TP	Units	OP	Units
Sample	N2		Blu1	
C_u	3.70	$\mu g \cdot L^{-1}$	3.13	$\mu g \cdot L^{-1}$
V_u	0.0185	L	0.0185	L
C_s	100.0	$\mu g \cdot L^{-1}$	100.0	$\mu g \cdot L^{-1}$
V_s	0.0015	L	0.0015	L
Theoretical	10.923	$\mu g \cdot L^{-1}$	10.395	$\mu g \cdot L^{-1}$
Observed	10	$\mu g \cdot L^{-1}$	10.73	$\mu g \cdot L^{-1}$
Recovery	92	%	103	%

Appendix H - (Casefile 2) Analytical method investigations

Standard digestion and leverage

Calibration standards are used in colorimetry to predict the relationship between spectrophotometric absorbance and sample analyte concentration. In the case of the analysis of ortho- and total phosphorus, reagents in an acidic medium cause a complexation reaction that turns the sample solution blue, the shade of which is directly proportional to the phosphorus concentration in the sample. Selection of calibration standards is often standardized in laboratory standard operating procedures, as is the case in the UI Limnology Lab, EPA 365.3, and SVL methods. Because nutrient concentrations in Coeur d'Alene Lake are very low, the traditional UI lab standard concentrations were reduced from 0-400 $\mu g \cdot L^{-1}$ to 0-100 $\mu g \cdot L^{-1}$, increasing the number of standards below 100.0 $\mu g \cdot L^{-1}$. The operational standards used to analyze the samples from Coeur d'Alene Lake were 0.0, 2.0, 5.0, 10.0, 20.0 and 100.0 $\mu g \cdot L^{-1}$ P. Because the calibration curves are calculated as linear regressions, calibration standards with high concentrations could potentially leverage the regression, changing the slope of the line. A leverage test was conducted to test for this potential error.

Calibration standards should be treated in the same manner as analytical samples, however, UI Limnology Lab methods for TP did not instruct the user to digest standards with oxidizing reagent in the autoclave with the other samples. The effect of digestion was tested by creating standard curves with digested and non-digested samples.

Methods

To test if digested standards influenced the calculated nutrient concentrations, the slope of the calibration curves generated by digested and non-digested standard curves were compared using a *t*-test. After the problem was identified in early July 2017, standard curves were prepared both ways, using non-digested standards for the non-digested OP samples and digested standards for the digested TP samples. The *F*-test for equal variances and one-sided *t*-test comparison was conducted after six batches of samples were run. Significantly different means would indicate that standard digestion influenced the slope of the calibration line, and therefore the concentrations of nutrients analyzed would depend on the method. The test was repeated in 2018 to increase sample size.

An additional test was conducted to determine if the 100.0 $\mu g \cdot L^{-1}$ standard leveraged the slope of the calibration line. Two calibration lines were plotted for samples analyzed on September 14, 2017. The first line included all standards 0-100$\mu g \cdot L^{-1}$ and the second excluded the 100.0$\mu g \cdot L^{-1}$ standard. Slopes and resulting sample concentrations were compared to determine if inclusion of the 100 $\mu g \cdot L^{-1}$ standard influenced the results.

Results and verdict

The mean slope of non-digested calibration lines was $0.0030 \pm 4.5 \times 10^{-5}$ (n = 20), with a range of 0.0027 – 0.0032 (Figure H.1). For digested standards, the mean slope was $0.0027 \pm 4.3 \times 10^{-5}$ (n = 20), with a range of 0.0023 – 0.0031 (Figure H.2). Homogeneity of variance was confirmed (*F*-test, F= 1.24, d.f.= 19, $p < 0.01$) and the mean slope of non-digested standards is significantly higher than that on digested standards (one-sided *t*-test, *t*=4.88, d.f. = 46, $p < 0.001$).

For the leverage test, the slope of the full calibration line was 0.0032 (R^2=0.9999). The 0-20 $\mu g \cdot L^{-1}$ calibration line's slope was 0.033 (R^2=0.9984). OP concentrations were compared with an *F*-test for equal sample variance (F = 1.07, d.f. = 14, p = 0.45) and a two-sided *t*-test (F = 0.17, d.f. = 28, P = 0.87). TP concentrations were tested the same way, with a p-value of 0.45 for the *F*-test (df = 28) and a p-value of 0.87 for the *t*-test (n = 15). These results signify that neither OP nor TP mean concentrations differed depending on the calibration curve used. The 100.0 $\mu g \cdot L^{-1}$ standard did not leverage the slope of the calibration curve and was retained for the remainder of the Periphyton Study.

Oxidizing reagent choice

Standard Methods 4500-P B.5 governs persulfate digestion methods for total phosphorus analysis (Eaton et al. 2005). It states that potassium or ammonium persulfate ($K_2S_2O_8$ and $(NH_4)\ S_2O_8$, respectively) can be used as oxidizing reagents in the autoclave digestion method. Potassium persulfate is used in the UI Limnology Lab and SVL methods, but ammonium persulfate was investigated to determine whether reagent choice may have influenced OP and TP concentrations.

Methods

SM4500-P B.5 requires the addition of 0.5 g of potassium persulfate or 0.4 g of ammonium persulfate per 50 ml of sample solution. Smaller samples volumes (20 ml) are

used in the UI method, equating to 0.2 g of potassium persulfate or 0.16 g of ammonium persulfate per sample. Eight samples were analyzed using each oxidizing reagent, totaling 16 samples. The UI Limnology Lab method for TP determination was used for both splits, deviating only in oxidizing reagent. Calibration standards for each reagent method were also digested accordingly. TP concentrations were compared using an *F*-test for sample variance and a *t*-test to compare sample means. Percent recovery was calculated according to the methods in Appendix A.

Results and verdict

A water sample was collected from Mica Bay, ID and analyzed on November 13, 2017. The slope of the calibration lines was 0.0028 and 0.0029 for potassium and ammonium, respectively. Mean TP with potassium persulfate digestion was 32.86 ± 0.45 $\mu g \cdot L^{-1}$ P, and 32.54 ± 0.52 $\mu g \cdot L^{-1}$ P with ammonium persulfate. Variance were similar (*F*-test, F = 0.73, d.f. = 9, P = 0.32), as were the means (*t*-test, *t* = 0.47, d.f. = 18, P = 0.65). Percent recovery was 93% and 109%, for potassium and ammonium persulfate, respectively (Table H.1). The lack of significant difference in mean concentrations and high percent recovery (within ± 25%) indicated that reagent choice did not significantly affect the determination of total phosphorus in Coeur d'Alene Lake water.

Methods comparison

A review of phosphorus analysis methods comparing UI lab, SVL Analytical, and EPA method 365. 3 revealed that sample preservation with acid and subsequent neutralization was a component of both non-UI methods. In SVL's method, sample preservation to pH < 2.0 with concentrated sulfuric acid is required (see SVL method line 9.1), while EPA 365.3 states that preservation is optional (EPA 1978; SVL 2014). The following experiment of method comparison was the first to reveal that acid preservation of samples was the root of the overall chemistry problem. This experiment starts with the basics—comparing traditional UI Limnology Lab methods to SVL methods to determine if the methods produced similar TP concentrations for split samples.

To reduce the number of variables tested in this experiment, samples followed the *traditional* UI protocol of *not* preserving samples with sulfuric acid. The goal of the experiment was to answer the question, "does the traditional UI method produce comparable

results to the SVL method?" Failed lab splits with SVL had already revealed that my modified UI method using acid preservation did not produce similar results with SVL. Therefore, if the traditional UI method agreed with SVL, then the problem could be isolated as any difference between the traditional UI method and my modified one.

Methods

A grab sample of water was collected from Mica Bay, Coeur d'Alene Lake in December 2017. This sample was not preserved with sulfuric acid for either split sample. Seven environmental samples were portioned from the same grab sample. Quality control samples for both methods included matrix spikes, continuing calibration blanks, and verifications (10.0 and 20.0 $\mu g \cdot L^{-1}$ P). For the UI method, samples were analyzed according to the regular lab method, including use of oxidizing reagents, digestion, and analysis.

The SVL Analytical method was used on the other half of the samples (SVL 2014). Major differences in the SVL method from the UI method are: 1) the inclusion of 2.5 ml 1:1 sulfuric acid (H_2SO_4) in the digestion solution, 2) the use of ammonium persulfate $(NH_4)S_2O_8$ as the oxidizing reagent in the digestion solution, 3) addition of 0.625 ml of 10N sodium hydroxide (NaOH) before coloring, and 3) the preparation order of the mixed reagent used for coloring. Before digesting samples, I made the digestion solution (SVL method reagent 6.21) and color reagent (6.18) with the reagents listed in the SVL method Section 6 (SVL 2014). The digestion solution consisted of 1:1 sulfuric acid solution (6.14) and 3.2 g ammonium persulfate. The color reagent included 50 ml 5N sulfuric acid (6.3), potassium antimonyl tartrate solution (6.5), and ascorbic acid solution (6.6).

After transferring 20 ml of sample into acid-washed test tubes, 2.5 ml of digestion solution (6.21) was added to each test tube. Tubes were capped and shaken for ten seconds, unscrewed one-quarter turn, and autoclaved at 207 kPa (30 PSI.) for 20 minutes. After cooling, batches of samples were processed according to the number that could be colored and analyzed within 20 minutes of adding the mixed reagent, starting with calibration standards. Before coloring, 0.625 ml of 10N sodium hydroxide was added to each sample tube. Next, 0.56 ml of color reagent was added to samples, shaken, then analyzed using the spectrophotometer.

Following analysis, sample concentrations of total phosphorus were compared using an *F*-test for sample variance and a one-sided *t*-test with a hypothesized mean difference of

1.23 $\mu g \cdot L^{-1}$ P, the MDL of the UI method. A non-zero hypothesized difference tests whether the two means are more different than the given value, in this case testing whether the two mean concentrations were distinguishable by the method. Matrix spikes were analyzed to calculate percent recovery for each method.

Results and verdict

For the UI method, one environmental sample was discarded after pieces of the test tube cap were found floating in the cuvette during analysis. Particles appeared to influence the absorbance, which was abnormally high (9.64 $\mu g \cdot L^{-1}$ P) compared to the other samples. The mean TP concentration was 5.60 ± 0.20 $\mu g \cdot L^{-1}$ (n =6; ± SE). All seven samples were included in the mean calculation for the SVL method, yielding a mean concentration of 4.53 ± 0.23 $\mu g \cdot L^{-1}$ TP (n=7). The sample concentrations had equal variance (F = 6.88, d.f. = 6, P = 0.88), and there was no was no difference in sample means was greater than 1.23 $\mu g \cdot L^{-1}$ P (t-test, t = 0.54, d.f. = 6 and 7, p = 0.30). Matrix spikes passed quality control standards (±25%) with 105% for UI and 109% for SVL. See Table H.2 for parameters used to calculate percent recovery in this experiment.

These results show that using traditional UI methods without sample preservation with acid yielded the same results as the SVL Analytical methods. This indicates that UI methods are capable of matching SVL results in lab split samples. Therefore, any difference between the traditional UI method and those modified with acid preservation need to be evaluated as the cause of the overall chemistry problem. As the major discrepancy between the traditional and modified method was sample preservation, subsequent tests described in this chapter specifically address this issue.

Literature Cited

EPA. 1978. Method 365.3: Phosphorous, all forms (colorimetric, ascorbic acid, two reagent). U.S. Environmental Protection Agency.

SVL Analytical. 2014. Total phosphorus (aqueous samples) by SM 4500 P E. Silver Valley Analytical, Inc. Version 16. 1–20.

Table H.1: Parameters used for the calculation of percent recovery of phosphorus during the oxidation reagent choice experiment. Refer to the methods of this test for formulae and variable descriptions.

Parameter		Units		Units
Reagent	$K_2S_2O_8$		$(NH_4)S_2O_8$	
C_u	32.86	$\mu g \cdot L^{-1}$	32.54	$\mu g \cdot L^{-1}$
V_u	0.0185	L	0.0185	L
C_s	100	$\mu g \cdot L^{-1}$	100	$\mu g \cdot L^{-1}$
V_s	0.0015	L	0.0015	L
Theoretical	37.89	$\mu g \cdot L^{-1}$	37.60	$\mu g \cdot L^{-1}$
Observed	40.89	$\mu g \cdot L^{-1}$	34.64	$\mu g \cdot L^{-1}$
Recovery	93	%	109	%

Table H.2: Parameters used to calculate the percent recovery of phosphorus during the methods comparison experiment. Refer to the section “percent sample recovery” for formulae and variable descriptions.

Parameter		Units		Units
Method	UI lab		SVL	
C_u	6.17	$\mu g \cdot L^{-1}$	4.53	$\mu g \cdot L^{-1}$
V_u	0.016	L	0.016	L
C_s	100	$\mu g \cdot L^{-1}$	100	$\mu g \cdot L^{-1}$
V_s	0.004	L	0.004	L
Theoretical	24.94	$\mu g \cdot L^{-1}$	37.60	$\mu g \cdot L^{-1}$
Observed	23.75	$\mu g \cdot L^{-1}$	21.52	$\mu g \cdot L^{-1}$
Recovery	105	%	109	%

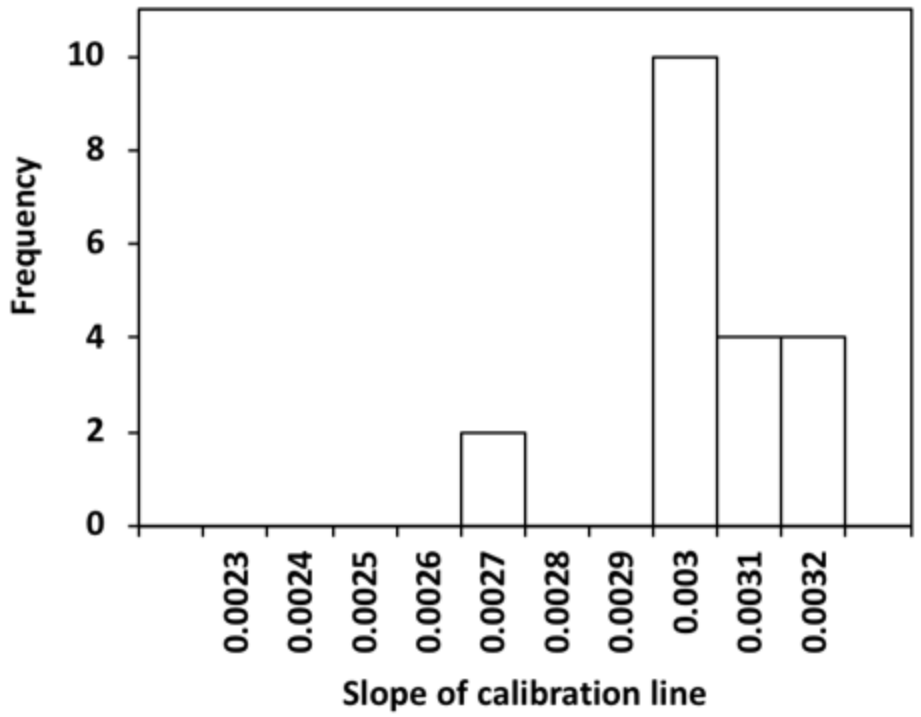

Figure H.1: Frequency distribution of calibration line slopes for non-digested standard curves.

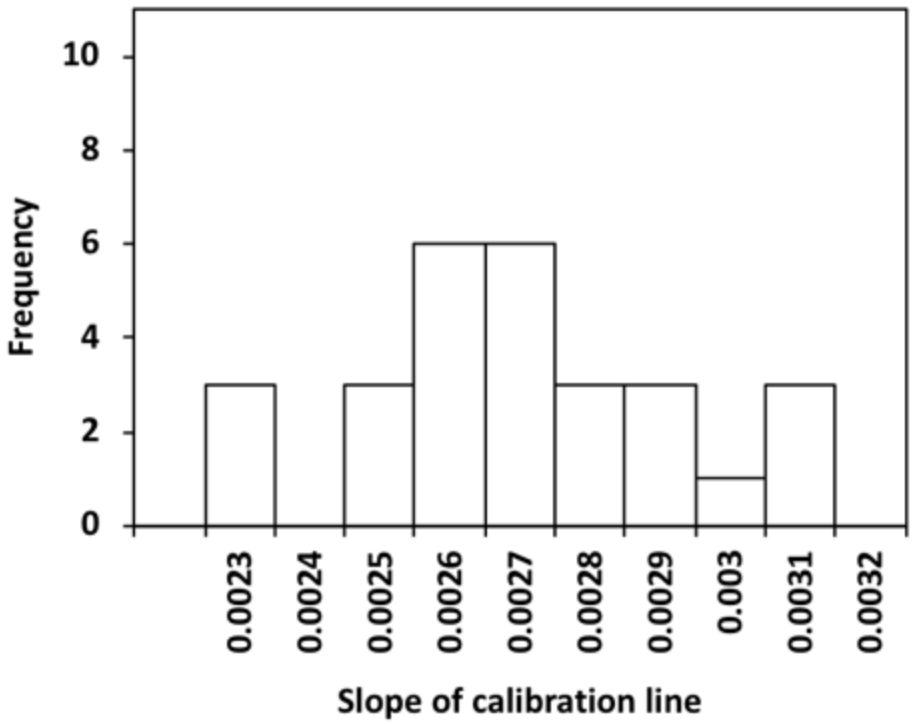

Figure H.2: Frequency distribution of calibration line slopes for digested standard curves (n = 20).

Appendix I - (Casefile 3) Field measures investigations

Sample collection depth

Early in my investigations I considered if depth of sample collection could be a reason for why OP values were higher than historic IDEQ data, because IDEQ samples for nutrient analysis were collected from multiple depths and homogenized into one integrated sample, while I only collected discrete samples from a depth near my substrates. Thus, I thought that perhaps collection of water from nearer the substrate could have resulted in higher OP values than samples collected from different depths throughout the water column. To test this hypothesis, I specifically analyzed water collected at discrete depths throughout the water column and homogenized versus water collected at one discrete depth on the same day at the same site.

Methods

To test the hypothesis that sampling method affected OP concentrations, discrete near-bottom samples were collected as well as an IDEQ-style integrated sample (4 depths) at the IDEQ monitoring site in the center of the bay on the same day. Discrete and integrated samples were collected at Kidd Island, Neachen, and Wolf Lodge bays on July 21 and August 17, 2017 and on August 22, 2017 in Beauty, Bennett, and Blue Creek bays. Both sample types were processed according to the modified UI Limnology Lab methods that included field-preservation with acid. I used a one-sided paired *t*-test to compare OP concentrations between discrete and integrated samples to determine if sampling method influence OP concentrations in samples.

Results and verdict

The mean OP concentration of discrete samples from depth was 5.11 ± 0.54 $\mu g \cdot L^{-1}$ ($n = 9$; mean ± one standard error) and 6.36 ± 0.51 $\mu g \cdot L^{-1}$ ($n = 9$) for integrated samples. These means differed (one-sided paired *t*-test, $t = -4.14$, d.f. =8, $P<0.01$). For TP, the mean concentration of discrete samples was 3.14 ± 0.41 $\mu g \cdot L^{-1}$ ($n = 9$) and 3.78 ± 0.32 $\mu g \cdot L^{-1}$ ($n = 9$) for integrated samples which did not differ (one-sided paired *t*-test, $t = -1.67$, d.f. =8, $P = 0.07$).

These results did not support the hypothesis that OP values were higher in my Periphyton Study samples compared to IDEQ samples based on sampling methodology. Instead they indicated that discrete samples like those taken in the Periphyton Study should have lower OP concentrations than the IDEQ's integrated samples. Therefore, sample collection method was rejected as a potential cause for the overall chemistry problem.

Appendix J - (Casefile 4) Case closed

The Standard Preservation Test was developed after it was realized that samples had been acidified but standards used for the calibration curves had not. This test concluded that calibration line slopes differ when acidified compared to no preservative, thus suppressing the calculated concentrations of TP in 2017 samples. These results were the final indication that the handling of standards was the mistake in the overall chemistry problem.

After standard solution preservation was identified as the cause of the overall chemistry problem, the next step in the case was to investigate if 2017 TP data could be back-corrected for inclusion in the dataset. The standard preservation test showed that preserved standards produced linear calibration curves with high R^2 values ranging from 0.9039 to 0.9998, with an average of 0.9881 (n = 9). The proposed back-correction method would apply the average slope of the tested preserved calibration lines to the absorbance values of 2017 TP samples. The Confirmation Test compares preserved and unpreserved standards to split samples from 2018 to confirm that the back-corrected method matches the "true values" produced by the unmodified UI Limnology Lab method.

Standard preservation test

Methods

To test if acidifying the calibration standards had an effect on calibration line slope, preserved and unpreserved standards were compared. On October 16, 2018, nine standard curves were prepared with sulfuric acid added to mimic sample preservation. Forty µl of concentrated sulfuric acid was added to 20 ml of standard solution in each test tube, then digested normally in the autoclave. Standards were the usual concentrations of 0, 2, 5, 10, 20, and 100 $\mu g \cdot L^{-1}$. Slopes of the calibration lines were calculated and compared to the slopes of calibration lines based on unpreserved standards run previously throughout the Periphyton Study. This list of unpreserved slopes includes all calibration lines (n = 28) run before the date of this test. After an *F*-test for sample variance reported unequal variance, a Mann Whitney test was executed in the statistical package R as a non-parametric alternative to a student's *t*-test. The Mann Whitney is a signed rank test that determines if sample medians differ from a known value; zero in this case (Hart 2001).

Results and verdict

The mean slope for preserved calibration lines was $0.0017 \pm 1.3\times10^{-4}$ (± standard error), while for unpreserved lines, the mean slope was $0.0027 \pm 4.3\times10^{-5}$. The *F*-test for sample variance rejected the null hypothesis of equal variance ($F = 3.15$, d.f. = 8, $p = 0.02$), which is why I followed up with a non-parametric Mann Whitney test. Results of this test indicated unequal median slopes (Mann-Whitney test, $U=3$. $P < 0.001$), meaning that the preservation of standards significantly influenced the slope of calibration curve.

The use of non-parametric tests in this case was decided after data transformations failed to generate samples of equal variance. Due to the low sample size of preserved standards (n = 9), careful attention was paid toward meeting the assumptions of any statistical tests employed. It should be noted that mean and median slopes were equal for both variables (means and medians of 0.0017 and 0.0026 for preserved and unpreserved, respectively).

This conclusion provided evidence that preservation had caused the overall chemistry issue. Although sample preservation had been tested previously (Appendix C), the equal treatment of samples and calibration standards had not been addressed. Subsequent tests were employed to quantify the effect of standard preservation so that preserved samples could be back-calculated.

Back-correction method confirmation test

Methods

Total phosphorus samples from 2018 were analyzed according to the modified UI Limnology Lab methods, whereby samples were preserved with sulfuric acid. Once standard preservation was identified as a concern, 2018 samples were re-run with preserved standard curves on October 16, 2018. The method presented here represents the back-correction method that was used on 2017 TP values. To confirm that this method was adequate, a subset (n = 15) of frozen unpreserved samples were analyzed on an unpreserved standard curve. Comparing these datasets tests if back-corrected concentrations are statistically different from the unmodified method.

Preserved and unpreserved samples in this test were considered splits because they were dispensed from the same sample collected with the Kemmerer sampler in the field.

Preserved samples received 0.25 ml of concentrated sulfuric acid and unpreserved samples were frozen within 24 hours of collection then thawed for analysis. The samples chosen for the unpreserved subset were selected randomly from the list of 2018 samples by assigning each sample a random number then selecting the smallest 15. Calculated concentrations from both sample methods were then tested using a one-sided paired *t*-test in R.

Results and verdict

Concentrations differed between methods (one-sided paired *t*-test, $t = -9.05$, d.f. = 14, $P<0.001$). However, likelihood estimations of hypothesized mean differences showed a breakpoint at 2.7 $\mu g \cdot L^{-1}$ TP. This means that TP concentrations are significantly different at this concentration, but not at a hypothesized difference of 2.8 $\mu g \cdot L^{-1}$. Because this level of difference is less than the reporting limit of 3.998 $\mu g \cdot L^{-1}$, the two datasets were considered "not different." In summary, back-corrected TP values are statistically different, but the estimated difference in means is such a low concentration that it can be ignored. 2017 TP concentrations can be acceptably back calculated by applying the slope of a preserved calibration line to absorbance values previously obtained from preserved samples.

Literature Cited

Hart, A. 2001. Mann-Whitney test is not just a test of medians: differences in spread can be important. BMJ **323**: 391–3.